



**Universidade de
Aveiro
Ano 2012/2013**

Departamento de Química

**Ana Vanessa
Silva Neves**

Desenvolvimento de um novo suplemento dietético de silício

This page intentionally left blank.



**Universidade de
Aveiro**
Ano 2012/2013

Departamento de Química

**Ana Vanessa
Silva Neves**

Development of a novel dietetic silicon supplement

This page intentionally left blank.



**Universidade de
Aveiro
Ano 2012/2013**

Departamento de Química

**Ana Vanessa
Silva Neves**

Desenvolvimento de um novo suplemento dietético de silício

Dissertação apresentada à Universidade de Aveiro para cumprimento dos requisitos necessários à obtenção do grau de Mestre em Bioquímica, ramo de Bioquímica Clínica, realizada sob a orientação científica do Doutor Nuno Faria, Investigador do Medical Research Council- Human Nutrition Research, do Doutor Brian Goodfellow, Professor Auxiliar do Departamento de Química da Universidade de Aveiro e do Doutor Jorge Saraiva, Investigador Auxiliar do Departamento de Química da Universidade de Aveiro.

This page intentionally left blank.

Dedico este trabalho aos meus pais.

This page intentionally left blank.

O júri

Prof. Doutor Pedro Miguel Dimas Neves Domingues
Professor Auxiliar do Departamento de Química da Universidade de Aveiro

Prof. Doutor Brian James Goodfellow
Professor Auxiliar do Departamento de Química da Universidade de Aveiro

Prof. Doutor Jorge Manuel Alexandre Saraiva
Investigador Auxiliar do Departamento de Química da Universidade de Aveiro

Doutor Nuno Jorge Rodrigues Faria
Investigador no Medical Research Council – Human Nutrition Research

Doutora Ana Luísa Daniel da Silva
Investigadora Auxiliar do Centro de Investigação em Materiais Cerâmicos e Compósitos (CICECO) da Universidade de Aveiro

This page intentionally left blank.

Agradecimentos

Agradeço a todos aqueles que de alguma forma me ajudaram, ao longo do meu percurso académico, a chegar a este momento.

Em especial queria agradecer aos meus pais, por me terem dado a oportunidade de ser uma das pessoas do mundo com um grau académico, sem nunca terem pedido nada em troca. Por terem tornado possível a minha vinda para Inglaterra, sem eles não teria acontecido, e não menos importante, por todo o amor, paciência e compreensão, que me ajudou a aguentar os momentos mais difíceis.

Agradeço ao Doutor Nuno Faria, por me ter aceite e orientado ao longo deste ano, e também aos meus orientadores na Universidade de Aveiro, Doutor Brian Goodfellow, e Doutor Jorge Saraiva, por todo o apoio.

Aos meus amigos, inclusive os mais recentes, agradeço todos os momentos de alegria proporcionados.

Por último, não posso deixar de mencionar e agradecer ao Rui Pedro Silva, pelo apoio dado a todos os níveis ao longo destes últimos anos, e por me ajudar a ser todos os dias uma pessoa melhor.

This page intentionally left blank.

Palavras-chave

Silício, suplementos, nanopartículas, nutrição

Resumo

Ao longo do tempo têm surgido alguns estudos que sugerem que o silício terá importância biológica, e que, sendo assim, se deveria ter em conta a quantidade que é ingerida e absorvida, a nível dietético. A única forma de silicato passível de ser absorvida no intestino é a forma monomérica, designada ácido ortossilícico, o qual existe apenas em certos fluídos, tais como, água mineral e cerveja. Assim, e apesar de ainda não existir um valor estabelecido para o consumo diário de silício, é de esperar que muitas pessoas estejam em défice, o que abriu o mercado para os suplementos dietéticos de silicato. Porém, muitos dos suplementos disponíveis têm certas lacunas, tais como, biodisponibilidade diminuta, ou concentrações de silício reduzidas.

O objectivo deste trabalho focou-se no desenvolvimento de um novo suplemento dietético de silício, através da síntese de nanopartículas, que apresentasse elevada biodisponibilidade, e que, de preferência, pudesse ser produzido no formato de cápsulas.

As nanopartículas foram sintetizadas a partir de uma solução de silicato, através de uma mudança rápida de pH, e tentou-se prevenir a polimerização através de ligandos de superfície. As suspensões foram caracterizadas através de DLS, Zeta, ICP-OES, e ATR-FTIR. A biodisponibilidade foi testada através de dois ensaios de dissolução distintos.

Os estabilizadores que apresentaram resultados mais promissores foram a sacarose e o PEG, e observou-se que a adição, na suspensão com sacarose, de etanol, aumentava ainda mais a estabilidade. Quando comparados, no que toca a biodisponibilidade, com Biosil, quase todos os materiais sintetizados apresentaram melhores resultados.

No geral, e tendo em conta todos os resultados, o PEG foi o composto que teve melhor performance como estabilizador, no entanto, ainda ficou aquém do período ideal de estabilidade para um suplemento.

This page intentionally left blank.

Key-words

Silicon, supplements, nanoparticles, nutrition.

Abstract

Over the years there have been some studies that suggest that silicon might have a biological role, and, therefore, that it should be taken into account how much of it is ingested, and absorbed, in our diet. The only form of silicate that is absorbed, in the intestinal lumen, is the orthosilicic acid, which only exists in certain fluids, like mineral water, and beer. Thus, and although there is still not an established value for a daily silicon intake, a lot of people do not get that much silicon from their diets, which opened the market space for silicate supplements. Some of those, however, have issues like low bioavailability, or low silicon concentration in the supplement itself.

The aim of this work was to develop a new silicon supplement, in the nanoparticulate range, with high bioavailability, that would, ideally, be manufactured in a liquid-filled capsule.

The silicate nanoparticles were synthesised from a soluble silicate suspension, through a pH driven process, and size was stabilised through the use of surface ligands. The suspensions were characterized using DLS, Zeta, ICP-OES, and ATR-FTIR. Bioavailability was assessed through two distinct dissolution assays.

The stabilizers that delivered the most promising results were sucrose and PEG, and further addition of ethanol, to the sucrose stabilised suspension, improved the stability even further. When compared, in terms of bioavailability to Biosil, most of the synthesised materials performed better.

Overall, and taking into account all the results, PEG was the compound that best performed as stabilizer, however, it is still far from the ideal stability time for the manufacturing of a supplement.

This page intentionally left blank.

Index

Tables Index	iii
Figure Index	v
Acronyms List	ix
Introduction	2
1.1. Silicon	2
1.1.1. Silicon Biochemistry	3
1.1.2. Silicon in the Organism	9
1.1.3. Silicon Intake	12
1.1.4. Silicon Supplements	14
1.2. Nanoparticles	16
1.2.1. Properties	17
1.2.2. Applications	19
1.2.3. Absorption in the Organism	22
1.2.4. Toxicity	23
1.2.5. Silicon Nanoparticles	24
1.3. Techniques	25
1.3.1. Dynamic Light Scattering	26
1.3.2. Zeta Potential	28
1.3.3. ICP-OES	29
1.3.4. Spectrophotometry	31
1.3.5. ATR-FTIR	32
2. Materials and Methods	36
2.1. Materials	36
2.2. Methods	36
2.2.1. Synthesis	36
2.2.2. Determination of Particle Size and Zeta Potential	37
2.2.3. Characterization of Silicon Phase Distribution	37
2.2.4. ATR-FTIR Spectroscopy	38
2.2.4. Dissolution Assay	38
2.2.5. Molybdate Assay	39
3. Results and Discussion	42
3.1. Silicate Nanoparticles Synthesis	42

3.1.1. Sucrose	44
3.1.2. PEG	47
3.1.3. Sucrose and Ethanol	49
3.2. pH vs Stability	51
3.2. ATR-FTIR	52
3.3. Phase Distribution Over Time	55
3.3.1. Sucrose	56
3.3.2. PEG	58
3.3.3. Sucrose in UHP Water and Ethanol	60
3.4. Bioavailability Assays	62
3.4.1. Molybdate Assay	62
3.4.2. Dissolution Assay	64
4. Conclusion and Future Work	72
6. Bibliography	76
Appendix A – Compounds Tested As Stabilizers	89
Appendix B – ATR-FTIR Spectrums	91
Background – UHP Water	91
Background – Air	98
Background – Medium	103
Appendix C – Fraction Analysis of Silicate Suspensions (EtOH 40% v/v)	109
Appendix D – Dissolution Assay Results for Biosil	111
Appendix E – Overlay of the ICP and Molybdate Dissolution Assay Results	113

Tables Index

Table 1 - Reference values for serum silicon in adults.....	12
Table 2 – Different ratios of silicate:sucrose tested, and negative control (NC), at pH 3.5, and the days that each suspension remained stable.....	45
Table 3 - Different ratios of silicate:sucrose tested, and the negative control (NC), at pH 3.5, and the days that each suspension remained stable.....	46
Table 4 - Different ratios of silicate:PEG tested, and negative control (NC), at pH 3.5, and the days that each suspension remained stable.....	48
Table A. 1 – Table of all the compounds tested as possible stabilizers and respective system characteristics.....	87

This page intentionally left blank.

Figure Index

Figure 1 – Molecular representation of the SiO ₄ tetrahedron.	3
Figure 2 – Effects of pH in the colloidal silica-water system	5
Figure 3 - Schematic representation of a dehydrated, but fully hydroxylated, colloidal silica particle. The fourth oxygen coordinated with Si is above or below the plane of the paper.	6
Figure 4 – Bond formation between silica particles	7
Figure 5 – Silica gel versus precipitate, a) soluble silica, b) gel, c) flocculation and precipitation.	8
Figure 6 - Photo by Carlisle, on the study about silicon deprivation. Animal in the right was subjected to a diet deprived of silicon	12
Figure 7 – Scheme “Top-Down” and “Bottom-UP” approaches for the manufacturing of nanoparticles	17
Figure 8 – Scheme of surface alterations in nanoparticles.	18
Figure 9 – Schematic representation of some nanoparticles applications	20
Figure 10 – Scheme of different possibilities for particles translocation across the gastrointestinal tract 1) Endocytosis through regular epithelial cells, 2) M-cell-uptake (transcytosis) at the surface of intestinal lymphoid aggregates, 3) Persorption, 4) Putative paracellular uptake.	23
Figure 11 – Comparison between the rate of intensity fluctuations triggered by small and big particles	27
Figure 12 – Schematic representation of zeta potential.	29
Figure 13 – Steps involved in the analysis of aqueous samples by ICP-OES	30
Figure 14 – Schematic representation of ATR spectroscopy	33
Figure 15 - Particle size distribution (A) and zeta potential distribution (B) of the silicate suspensions (0.50 M) in UHP water, at pH 3.50.	43
Figure 16 – Average number of days that the silicate suspensions remained stable with the different stabilizers used (A) and their respective particle size (B), at pH 3.5	44
Figure 17 - Particle size distribution (A) and Zeta potential distribution (B) of sucrose stabilised (1.50 M) silicate suspensions (0.50 M) in UHP water, at pH 3.50	47
Figure 18 – Particle size distribution (A), particle size of the centrifuged fraction (B), and zeta potential (C) of the PEG stabilised (1.00 M) silicate suspension (0.50 M), at pH 3.5.	49
Figure 19 - Particle size distribution (A) and zeta potential distribution (B) of sucrose stabilised (1.50 M) silicate suspensions (0.50 M) in UHP water and 14% v/v EtOH, at pH 3.50	51
Figure 20 – Stability of silicate suspensions as a function of stabilizer and pH.	52

Figure 21 – Overlay of the non-stabilised silicate suspension ATR-FTIR spectra with the spectrums of a sucrose solution and a sucrose stabilised silicate suspension, all at pH 3.5.....	54
Figure 22 – Overlay of the non-stabilised silicate suspension ATR-FTIR spectra with the spectrums of a PEG solution and a PEG stabilised silicate suspension, all at pH 3.5.....	55
Figure 23 – Silicon phase distribution of the non-stabilised silicate suspensions, at pH 2.5 and 3.5.	56
Figure 24 - Silicon phase distribution overtime of the sucrose stabilised silicate suspensions, at pH 2.5 (A), and the respective particle size analysis (B).	57
Figure 25 - Silicon phase distribution overtime of the sucrose stabilised silicate suspensions, at pH 3.5 (A), and the respective particle size analysis (B).	58
Figure 26 - Silicon phase distribution overtime of the PEG stabilised silicate suspensions, at pH 2.5 (A), and the respective particle size analysis (B).	59
Figure 27 - Silicon phase distribution overtime of the PEG stabilised silicate suspensions, at pH 3.5 (A), and the respective particle size analysis (B).	60
Figure 28 - Silicon phase distribution overtime of the sucrose stabilised silicate suspensions (14% EtOH v/v), at pH 2.5 (A), and the respective particle size analysis (B).....	61
Figure 29 – Silicon phase distribution overtime of the sucrose stabilised silicate suspensions (14% EtOH v/v), at pH 3.5 (A) and the respective particle size analysis (B).....	62
Figure 30 – Soluble silicon content in the silicate suspensions with the different stabilizers at pH 2.5 (A) and pH 3.5 (B).	64
Figure 31 - Total silicon content in the mixture surrounding the dialysis bag, as a function of time, at pH 2.5	66
Figure 32 – Total silicon content in the mixture surrounding the dialysis bag, as a function of time at pH 3.5 (B).....	67
Figure 33 - Soluble silicon content in the mixture surrounding the dialysis bag, as a function of time, at pH 2.5.....	68
Figure 34 – Soluble silicon content in the mixture surrounding the dialysis bag, as a function of time, at pH 3.5.....	68
Figure 35 - Monomeric silicon concentration in the mixture surrounding the dialysis bag (acquired through the molybdate assay), as a function of time, at pH 2.5.	70
Figure 36 – Monomeric silicon content in the mixture surrounding the dialysis bag (acquired through the molybdate assay), as a function of time, at pH 3.5.	70
Figure B. 1 – ATR-FTIR spectra of the non-stabilised silicate suspension, at pH 3.5, using water as background.....	89
Figure B. 2 – ATR-FTIR spectra of a sucrose solution, at pH 3.5, using water as background.....	90

Figure B. 3 - ATR-FTIR spectra of a PEG solution, at pH 3.5, using water as background.....	91
Figure B. 4 – ATR-FTIR spectra of the sucrose stabilised silicate suspension, at pH 3.5, using water as background.....	92
Figure B. 5 – ATR-FTIR spectra of the PEG stabilised silicate suspension, at pH 3.5, using water as background.....	93
Figure B. 6 – Overlay of the ATR-FTIR spectrums of the non-stabilised silicate suspensions, the sucrose solution and the sucrose stabilised silicate suspension, all at pH 3.5, using water as background.....	94
Figure B. 7 – Overlay of the ATR-FTIR spectrums of the non-stabilised silicate suspensions, the PEG solution and the PEG stabilised silicate suspension, all at pH 3.5, using water as background.....	95
Figure B. 8 – ATR-FTIR spectra of the non-stabilised silicate suspension, at pH 3.5, using water as background.....	96
Figure B. 9 – ATR-FTIR spectra of a sucrose solution, at pH 3.5, using air as background.....	97
Figure B. 10 - ATR-FTIR spectra of a PEG solution, at pH 3.5, using air as background.....	98
Figure B. 11 – ATR-FTIR spectra of the sucrose stabilised silicate suspension, at pH 3.5, using air as background.....	99
Figure B. 12 – ATR-FTIR spectra of the PEG stabilised silicate suspension, at pH 3.5, using air as background.....	100
Figure B. 13 – ATR-FTIR spectra of the non-stabilised silicate suspension, at pH 3.5, using, as background, the same medium as the silicate suspensions, minus the silicate and stabilizer.....	101
Figure B. 14 – ATR-FTIR spectra of a sucrose solution, at pH 3.5, using, as background, the same medium as the silicate suspensions, minus the silicate and stabilizer.....	102
Figure B. 15 – ATR-FTIR spectra of a PEG solution, at pH 3.5, using, as background, the same medium as the silicate suspensions, minus the silicate and stabilizer.....	103
Figure B. 16 – ATR-FTIR spectra of the sucrose stabilised silicate suspension, at pH 3.5, using, as background, the same medium as the silicate suspensions, minus the silicate and stabilizer.....	104
Figure B. 17 – ATR-FTIR spectra of the PEG stabilised silicate suspension, at pH 3.5, using, as background, the same medium as the silicate suspensions, minus the silicate and stabilizer.....	105
Figure C. 1 – Silicon phase distribution overtime of the sucrose stabilised silicate suspensions (14% EtOH v/v), at pH 2.5.....	107
Figure C. 2 – Silicon phase distribution overtime of the sucrose stabilised silicate suspensions (14% EtOH v/v), at pH 3.5.....	107
Figure D. 1 – Total and soluble silicon fractions for different concentrations of Biosil tested, with the dissolution assay, those being, 70 mM (green), 35 mM (red) and 17.5 mM (blue).....	109

Figure E. 1 – Overlay of the results acquired in the dissolution assay, for Biosil, with ICP and the molybdate assay.....	111
Figure E. 2 – Overlay of the results acquired in the dissolution assay, for the non-stabilised silicate suspensions, at pH 2.5, with ICP and the molybdate assay.....	111
Figure E. 3 – Overlay of the results acquired in the dissolution assay, for the non-stabilised silicate suspensions, at pH 3.5, with ICP and the molybdate assay.....	112
Figure E. 4 – Overlay of the results acquired in the dissolution assay, for the sucrose stabilised silicate suspensions, at pH 2.5, with ICP and the molybdate assay.....	112
Figure E. 5 – Overlay of the results acquired in the dissolution assay, for the sucrose stabilised silicate suspensions, at pH 3.5, with ICP and the molybdate assay.....	113
Figure E. 6 – Overlay of the results acquired in the dissolution assay, for the PEG stabilised silicate suspensions, at pH 2.5, with ICP and the molybdate assay.....	113
Figure E. 7 – Overlay of the results acquired in the dissolution assay, for the PEG stabilised silicate suspensions, at pH 3.5, with ICP and the molybdate assay.....	114
Figure E. 8 – Overlay of the results acquired in the dissolution assay, for the sucrose stabilised silicate suspensions, with 14% EtOH (v/v), at pH 2.5, with ICP and the molybdate assay.....	114
Figure E. 9 – Overlay of the results acquired in the dissolution assay, for the sucrose stabilised silicate suspensions, with 14% EtOH (v/v), at pH 3.5, with ICP and the molybdate assay.....	115

Acronyms List

ATR-FTIR – Attenuated total reflectance-Fourier Transform Infrared

DLS –Dynamic Light Scattering

ICP-OES – Inductively Coupled Plasma - Optical Emission Spectrometry

IR – Infrared

LO – Longitudinal Optic

MMST – Monomethyl Silanetriol

NMR – Nuclear Magnetic Resonance

PEG – Polyethylene glycol

PLGA – Poly(lactic-co-glycolic acid)

ROS – Reactive Oxygen Species

SAXS – Small-angle X-ray Scattering

SGIF – Simulated Gastrointestinal Fluid

TO – Transverse Optic

UHP Water – Ultra High Purity Water

UV-Visible – Ultra Violet-Visible

This page intentionally left blank.

Introduction

Introduction

Silicon is the second most abundant element in the earth's crust [1], and yet there is much about this mineral that remains to be learned, including its biological role. Despite being one of the most abundant elements, for many years it was considered that silicon was nonessential in most living organisms [2]. However, Holzapfel [2] showed that silicon is present in trace amounts in most animals and thus, it might have some definite function. Over time studies have been carried out, focused on trying to understand the role of silicon in organisms [3-5], and the results suggest a beneficial, if not essential, role for the occurrence of healthy tissue, especially concerning skin, hair, nails and, specially, bone. Recently, several results positively correlated silicon intake with bone mineral density [4, 6, 7]. Thus, regular silicon supplementation could be beneficial in improving general health, but also in preventing certain conditions, such as osteoporosis.

Dietary supplement use is common among adults, according to the National Health and Nutrition Examination Surveys (NHANES) [8]. Although a "food first" approach is encouraged in most cases, in order to achieve nutrient adequacy, it is also recognized that most people have dietary intakes, that fall short in some respects, silicon being one of them. Thus, dietary supplements can make a contribution toward achieving nutritional goals [9, 10].

The study of molecular interactions between (bio)macromolecules and silica species is complicated due to several processes occurring in parallel, these being, condensation of silicic acid, catalysis of silanol condensation with polymer units, as well as association of silicic acid and its oligomers with polymer chains [11]. Despite the difficulties, there are already a few silicon supplements available in the market. However, most show very low bioavailability, and those that are highly bioavailable, have very low silicon concentrations [4].

1.1. Silicon

Silicon (Si) is a metalloid with an atomic weight of 28 [1]. The word silica is used to refer to naturally occurring materials, composed mainly of silicon dioxide (SiO₂). Silicon dioxide is the main component of the earth's crust, and when combined with magnesium,

aluminium, calcium and iron oxides, it forms the mineral silicates which are present in the soil and rocks [12]. The building block of this component and of the structures of silicates is SiO_4 , which is a tetrahedral molecule, comprised of four oxygen atoms with a silicon ion at the centre (Figure 1). All forms of silica have the silicon-oxygen bond, which is the most stable of all Si-X bonds. [13]. The silicates are formed in a way similar to the polyborates and polyphosphate, through the sharing of oxygen atoms. Two different groups of SiO_4 can only share one oxygen atom between them, but any or all four oxygen atoms, in a SiO_4 group, may be shared with adjacent groups [13].

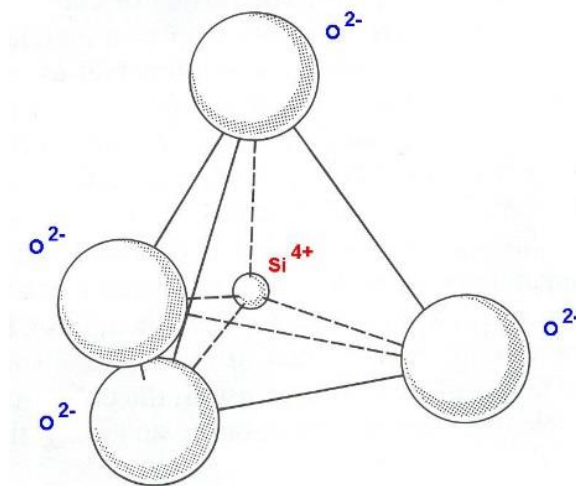


Figure 1 – Molecular representation of the SiO_4 tetrahedron [14].

1.1.1. Silicon Biochemistry

Silica (SiO_2) occurs in nature in several different forms: crystalline (quartz, cristobalite and tridymite) and amorphous [1]. When exposed to water, silicates release monomers, the soluble form of silica, designated orthosilicic acid or monosilicic acid, which is a weak acid and exists only in very dilute solutions [15]. This form of silica is essentially non-ionic in slightly acidic or neutral solutions, and it is not transported by electric current unless ionized in alkaline solution [2]. Also, it is not salted out of water nor can it be extracted by neutral organic solvents. Silica remains in the monomeric state for long periods of time at concentrations ranging from 2.5 to 5.0 mM, depending on the medium, under pH 10. However, at higher concentrations, it polymerizes quickly, initially forming polysilicic acids of low molecular weight, then larger polymeric species

recognizable as colloidal particles, and, finally, these particles link together into branched chains [2].

The polymerization of silica involves an ionic mechanism in which, when above pH 2, the rate of polymerization is proportional to the concentration of OH^- ions, and under pH 2, to the concentration of H^+ ions [2]. In the initial phase of polymerization, condensation quickly leads to the formation of ring structures, such as, cyclic tetramers, followed by the addition of monomers to these structures. Subsequent binding of the different cyclic structures results in bigger tridimensional molecules, which condense internally, for a more compact state, with the SiOH groups remaining on the outside [2]. The solubility of these particles depends on their size, that is, the radius of curvature of the surface. It also depends on their hydration state on the internal solid phase. Since not all particles in solution have the same size, and because smaller particles are more soluble than bigger ones, in the polymerization process, particles grow in average size and decrease in number, as the smaller particles dissolve and the silica is deposited upon the larger particles [2]. So, the basic step in gel formation is the collision of two silica particles, with sufficiently low surface charge, so that siloxane bonds are formed. Formation of this linkage requires the catalytic action of hydroxyl ions, and this is indicated by the fact that the rate of gel formation, in the pH range 3 to 5, increases with pH, and is proportional to the hydroxyl ion concentration [2]. Above pH 6, scarcity of hydroxyl ions is no longer the limiting factor for the gelling rate, instead, aggregation decreases because of fewer collisions between particles, due to their increasing charge [2]. In Figure 2 it is demonstrated the overall effect of pH on the stability of colloidal silica water systems, in the presence or absence of sodium salts. The salt decreases the ionic charge of the particles. At acidic pH this has little effect, both curves having approximately the same temporary stability, but in the neutral range a minimum of stability is achieved at a pH slightly higher when the salt is present [2].

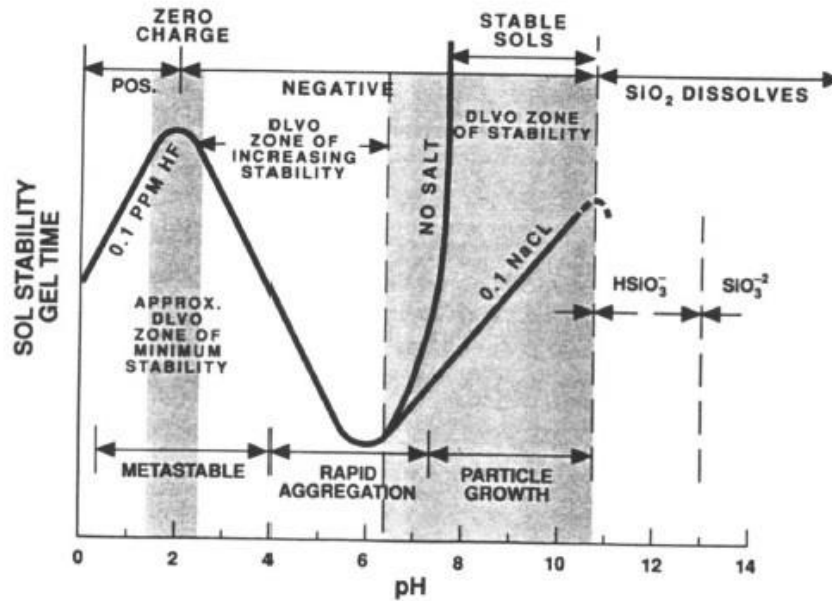


Figure 2 – Effects of pH in the colloidal silica-water system. The thick solid lines represent experimental results, while the shaded and white areas are approximate zones, corresponding to what would have been expected. [2]

So, two basic principles of particle growth, in an aqueous system, can be established. Particle growth at the expense of silicic acid molecules begins as soon as the solution is made, and that the formation of bigger particles is driven by silicic acid deposition, dissolving from smaller particles. This is a slower process and may be negligible at low pH, after the monomer has been used up [2].

As mentioned previously, polymerization leads to the formation of colloidal particles (Figure 3). That is, disperse systems in which the disperse phase is silica in the colloidal state. The colloidal state comprises particles with a size sufficiently small, $\leq 1 \mu\text{m}$, not to be affected by gravitational forces, but sufficiently large, $> 1 \text{ nm}$, to show marked deviations from the properties of true solutions [16]. A stable dispersion of solid colloidal particles in a liquid is a suspension in which the solid particles do not settle or agglomerate at a significant rate [16].

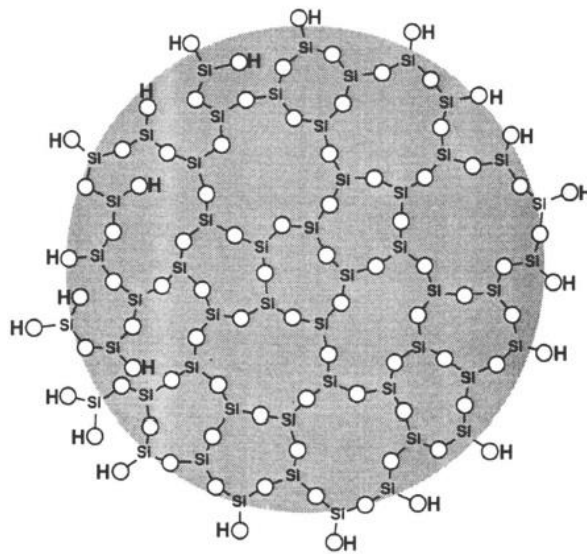


Figure 3 - Schematic representation of a dehydrated, but fully hydroxylated, colloidal silica particle. The fourth oxygen coordinated with Si is above or below the plane of the paper [12].

The conversion of a solution of spherical particles into a uniform gel, containing all the liquid present in the solution, is a process still not fully understood. When the particles collide, it is assumed that adhesion occurs, but in the case of silica particles, there is reason to believe that the bonding happens through the Si-O-Si linkage [2]. One of the reasons for this is that the same factors that promote polymerization of monomers and low molecular weight silicic acids, also promote the conversion of a solution of silica colloidal particles into a gel [2]. So, we can say that, when particles collide, there are neutral $\equiv\text{SiOH}$ and ionized $\equiv\text{SiO}^-$ groups in the particle surface, which condense to form Si-O-Si bonds, by the same mechanism involved in the polymerization of species of low molecular weight. Also, some researchers believe that the presence of silica monomers play a role in further cementing particles together (Figure 4) [2]. Indeed, it may even be possible that the presence of soluble silica species ($\text{Si}(\text{OH})_4$), at the point of contact between colliding particles, may play a role in promoting the formation of the initial bond [2].

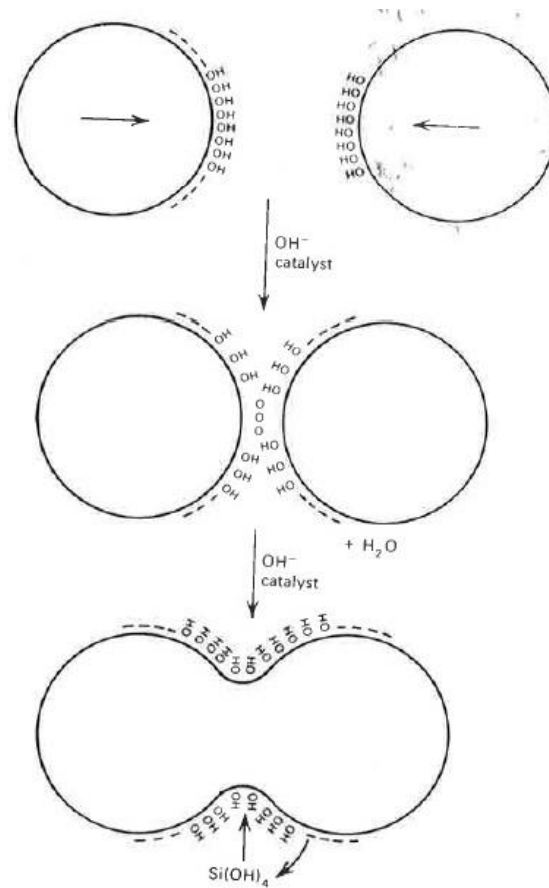


Figure 4 – Bond formation between silica particles [2].

Silica particles can aggregate in three different ways, by gelling, by coagulation and by flocculation (Figure 5) [17]. Every process involves colloidal particles or linking polymers, but there are basic differences between them. Gelling is when particles are linked together in branched chains that fill the whole volume of the solution, so that there is no increase in the concentration of silica in any macroscopic region in the medium. Instead, the overall medium becomes viscous, and then is solidified by a coherent network of particles that, by capillary action, retains the liquid [17]. Coagulation is when particles come together into relatively close-packed clumps, in which the silica is more concentrated than the original solution, so the coagulum settles as a relatively dense precipitate. Finally, flocculation is when the particles are linked together by bridges of the flocculating agent, that are sufficiently long so that the aggregated structure remains open and voluminous [17]. It is apparent that these differences will be noted mainly in dilute solutions containing only a few per cent of silica. In concentrated solutions one can distinguish gel formation,

but not between coagulation and flocculation. There is one last form of agglomeration, called coacervation in which silica particles are surrounded by an adsorbed layer of material. This makes the particles less hydrophilic, but does not form bridges between particles, thus resulting in a liquid phase immiscible with the aqueous phase [17].

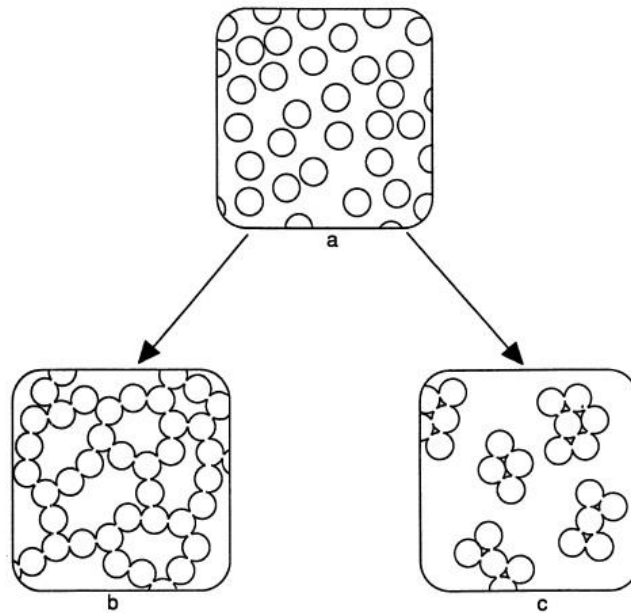


Figure 5 – Silica gel versus precipitate, a) soluble silica, b) gel, c) flocculation and precipitation [2]

As regards to stability it has also been defined three types, i) phase stability, which is analogous to the phase stability of ordinary solutions, ii) stability of disperse composition, that is stability with respect to change in the dispersion, and, lastly, iii) aggregative stability, the most characteristic for colloidal systems [17].

A concentrated silica solution can be stabilised against interparticle siloxane bonding in two possible ways. Either by an ionic charge on particles, so that they are kept apart by charge repulsion, or by an adsorbed, generally monomolecular, layer of inert material, which separates the silica surfaces to an extent that prevents direct contact of silanol groups, this has been referred to as “steric” stabilization [2]. Recently it was discovered that Si-O-C bonding is actually quite common in the aqueous environment, and that many aliphatic mono- and poly-hydroxy alcohols combine with silicates to produce alkoxy-substituted tetraoxosilicon complexes [18]. The complexing affinity is greater for smaller alcohols and increases with the number of attached hydroxy groups [18]. Also, in another study, Kinrade et al, reported that polyol chains which contain terminal carboxylic

acid groups, along with the requisite threo-plus-flanking hydroxyl group configuration, exhibit dramatically enhanced affinity for silicate complexation [19]. Bearing these characteristics in mind, the key for achieving a stable silicon solution, with a realistic concentration for use in the supplement field, might be a compound similar to those assessed in these studies.

1.1.2. Silicon in the Organism

Regarding the role of silicon in the body, it has been assumed for long that in higher life forms, the mineral does not play an essential role, however, there are several hints that point to the contrary [7, 20]. The typical adult intake of silicon is around 20-50 mg/d, thereby exceeding copper, zinc and iron, intakes, which are elements known to play important roles at the biological level [4, 7, 21]. It was also observed that connective tissue and its molecular constituents contain silicon levels significantly higher than soft tissues. In the 70s, in an animal study, Shwartz and Carlisle obtained convincing results of the significance of silicon in the organism [3, 22]. Both submitted animal groups to a diet without silicon, and they observed that this led to bone structure deformation in embryo development. Carlisle reported that silicon is required as a nucleating agent, probably in the form of calcium silicate. In turn, Shwartz reported that silicon is essential for the connective tissue, and is linked in mucopolysaccharides with bonds similar to ester, however these assertions are still subject to controversy [23].

Over time, several studies were carried out to try to better understand the biological relevance of silicon. There is still a lot to know, but there are already some mechanisms of action that have been proposed. Some studies obtained results which indicate that silicon may have an influence on DNA synthesis. It was observed that, in cultures of osteoblasts supplemented with silicon, thymidine incorporation was stimulated, along with cellular differentiation and turnover [24]. Moreover, microarray analysis revealed an overexpression of genes related to growth and cell cycle regulation in the same silicon supplemented osteoblast cultures [25].

There is also strong evidence that silicon is somehow involved in the synthesis and stabilisation of the extra cellular matrix [4]. Some results seem to indicate that silicon has an effect on the transcription of genes associated with type I collagen, as well as with

prolylhydroxylases, which are enzymes involved in the hydroxylation of proline [4, 26, 27]. Studies also suggest that silicic acid acts as a cofactor for these enzymes, since its activity was found to be modulated by silicon concentration. Also, inhibition of the enzymatic activity, with cis-hydroxyproline, eliminated the beneficial effect of silicon in the synthesis of collagen [26, 28]. Regarding stabilization, it has been suggested that silicon may function structurally as a cross link between the chains of pro-collagen, during the synthesis of collagen and/or within the overall extracellular matrix. Furthermore, the extracellular matrix formed, in the presence of silicon, contains collagen and elastin fibers more dense, better organized and distributed in a more homogenous form, compared to the extracellular matrix formed without silicon [29].

It is also suggested that silicon may be involved in the extracellular matrix mineralization process. Carlisle et al observed that silicon levels increased with primary mineralization but decreased with secondary mineralization, as calcium was being incorporated into the bone's mature mineral matrix [26]. Silicon supplementation in rats raised the calcium levels in their bone structure, while a diet devoid of silicon had the opposite effect [26, 30]. Also, silicon can affect the transport and mineralization of calcium in a direct way, by induction of the interaction of calcium with phosphate, or in an indirect way, through its effect on the extracellular matrix, by increasing synthesis or stabilization, and induction of osteoblast differentiation [25, 31, 32]. Lastly, Porter et al reported the formation of mature bone more crystalline when derived from a collagen matrix that formed in the presence of high levels of silicon [33].

Copper, zinc, calcium and magnesium are essential for bone and connective tissue health, and silicon supplementation is also reported to affect the metabolism of these minerals, raising their levels in the blood and tissues [26, 34]. However some reports suggest that silicon does not have any biological role, besides sequestering toxic aluminium ions [35]. Even if that were the case, it is important to note that aluminium is a potent neurotoxin, which interferes with calcium homeostasis and with enzymes in which magnesium is a cofactor, it also affects bone calcification and inhibits prolyl-hydroxylase activity [36, 37].

Despite several proposed hypotheses for the role of silicon in the body, most studies associate silicon with structural integrity of bone. Nutrition is an important factor for the bone structure, however, with the exception of calcium, little is known about the

effects of other nutrients and minerals. Ingestion of elements such as magnesium, potassium, fluorine, zinc, copper, boron and manganese, is positively associated with bone density, while the lack of these elements is associated with a decrease in bone density and increased fracture healing time [38, 39]. Interest in the role of silicon in this field has been increasing more recently. One study [7] positively correlated silicon ingestion with bone mineral density in the hip bone in men and pre-menopausal women, but not in post menopause, however, the author's gave a plausible biological explanation for this. From a biological perspective, the results obtained in this study indicate that the orthosilicic acid has a role in bone formation but not in resorption, and, in post menopause women, the bone mineral density is driven through resorptive processes [40, 41]. However, it is interesting that silicon ingestion had no effect at all in bone mineral density in post-menopausal women, suggesting that hormonal factors may override any potential effect silicon in the organism [7]. A contradiction observed in this study was the fact that the association between silicon ingestion and bone mineral density, in the lumbar spine, is much weaker than that observed between silicon ingestion and bone mineral density at the hip. Cancellous bone is usually more affected by metabolic factors than cortical bone, due to its higher rate of turnover [7]. However, if the effect of silicon is anabolic, this being, if the mineral promotes bone formation instead of inhibiting resorption, the same process that was observed for the parathyroid hormone in a prior study may be occurring. Here it was observed that the anabolic effects of the hormone were more prominent in cortical bone in comparison to cancellous bone [42]. A study in osteoporotic women, to whom was given a silicon supplement, supports this theory, in which a sharp increase in bone mineral density at the hip site, rather than in the lumbar spine was observed [43]. Thus, these results suggest that higher silicon intake is associated with higher bone mineral density, which is a marker of bone strength, and also, a potential interaction between silicon and oestrogen status [7].

Until now, no silicon deprivation studies have been conducted in humans, but, as described above, Carlisle [3] and Shwartz [22] observed, in laboratory animals, that silicon deprivation resulted in skeletal abnormalities and defects. In chicks, legs and beaks were paler, thinner, more flexible, and thus easily fractured (Figure 6) [3]. In rats were reported defects to the skull, including the eye sockets, as was disturbances and impairment to incisor enamel pigmentation [22]. Since then, no one was able to reproduce these dramatic

effects, but Seaborn and Nielsen reported decreases in bone mineral density, mineral content and collagen synthesis, and increases in collagen breakdown, thus confirming that silicon deprivation has a negative impact on bone [44].

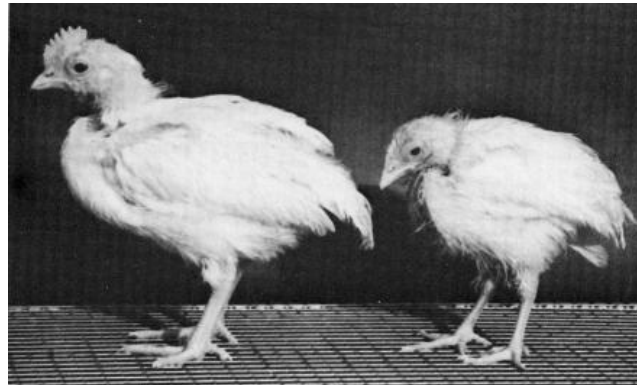


Figure 6 - Photo by Carlisle, on the study about silicon deprivation. Animal in the right was subjected to a diet deprived of silicon [3].

1.1.3. Silicon Intake

A daily minimum requirement for silicon has not been established, but was estimated at 10-25 mg/d on the basis of the 24h urinary excretion of silicon [26, 45], and, in studies that aimed to measure reference values for the level of silicon in the organism, it was found that these are age and sex dependent (Table 1) [46].

Table 1 - Reference values for serum silicon in adults [46].

	Age	[Silicon] $\mu\text{mol/L}$		Age	[Silicon] $\mu\text{mol/L}$
Male	18-59	9.50	Female	18-29	10.0
	60-74	8.50		45-59	9.23
	>74	7.70		>74	8.00

Given these values, it is important to try to understand the sources of dietary silicon, since the bioavailability of this element from solid foods is still not completely understood. The main entry source of silicon into the body is from the gastrointestinal tract, however, gastrointestinal absorption, metabolism and excretion of silicon is, also,

still poorly understood [4]. The absorption of silicon, however, is strongly influenced by the form of silica ingested, and this is related to the rate of production of soluble and absorbable species of silica in the gastrointestinal tract [21, 45, 47], being the monomer orthosilicic acid the most readily absorbed species. It is assumed that silicon in the orthosilicic acid form $[\text{Si}(\text{OH})_4]$ is available only in fluids, such as water and beer, but not in solids, in which is present as polymeric or phytolitic silica [48, 49]. However, since fluids only represent 20% to 30% of total silicon intake [50], and also because silica in solid foods can be hydrolysed to orthosilicic acid in the gastrointestinal tract [51, 52], studies that focus on the bioavailability of silicon from solid food are important. Jugdaohsingh et al found that the ingestion of silicon was ≥ 2 fold greater than the typical ingestion of iron, zinc, and also of two other elements with physiological importance [21]. Higher values were observed in diets rich in grains, cereals and plant-based food, when compared with animal products, such as meats and dairy [50, 53]. In this study it was also observed that the ingestion of silicon was about 20% to 33% higher in men than in women, and also that, in both genders, absorption decreases with age. The main reason for the difference observed between men and women is probably the greater intake of beer by males, this being the major dietary source of silicon for men [21]. It was also observed that, overall, an average of $40.9 \pm 36.3\%$ of the ingested silicon was excreted in urine in a 6 hour period, thus, confirming that silica from solid food is digested and absorbed in the gastrointestinal tract. The silicon in grains and derivatives such as rice, cereals, bread and pasta, is readily absorbed by the body, whereas, with the exception of green beans and raisins, the silicon present in fruit and vegetables is not as well absorbed [21].

Silicate additives are also present in foods and beverages, being added as inert additives or excipients, and are thought not to be absorbed. However, some studies have reported marked increases in serum silicon concentration or excretion of the mineral in urine, following ingestion of silicates, such as, zeolite, sodium aluminosilicate and magnesium trisilicate, suggesting that these are partly solubilised to orthosilicic acid in the gastrointestinal tract and absorbed [54, 55].

1.1.4. Silicon Supplements

There is a wide range of silicon supplements available, most of them being available in tablet or solution form. These show varying bioavailability, ranging from <1% to >50%, however, the majority of them show negligible to low bioavailability. It is important to note that, as mentioned above, the degree of polymerisation of silicon, is inversely proportional to its intestinal absorption [4, 47, 51, 56], or, in other words, monomeric silica, which is a small, neutrally charged molecule, is readily absorbed in the gastrointestinal lumen before absorption [47, 51]. The kinetics of dissociation or dissolution of the polymers or colloids will depend upon the degree of polymerization [2, 56].

The solubility limit of silica is about 2 to 3 mM at the intestinal peri-neutral pH [2]. In most supplements, however, silicon is present in higher concentrations, which means that larger and less absorbable polymers or colloids will form [57]. One exception to this is MMST – monomethyltrisilanol-, which is a silicon supplement presented as a solution, where a methyl group replaces one hydroxyl group of orthosilicic acid. This raises the solubility limit of silicon and maintains it in a small, monomeric and well-absorbed form [58]. Another silicon supplement that presents a rather high bioavailability, when compared to others, is Biosil. This choline stabilised orthosilicic acid is a concentrated solution of orthosilicic acid (2%) in a choline (47%) and glycerol (33%) matrix [4]. This is promoted as ‘biologically active silicon’, and although it presents polymerization to some extent, extensive polymerization and aggregation of silica particles are prevented by the presence of the high concentration of choline in the supplement [57]. The choline protects the silica by maintaining it in aqueous suspension, so that upon further dilution before ingestion, it will start to depolymerise to form orthosilicic acid [57]. This method is not as efficient as starting with monomeric silicate, but even though, it still achieves a depolymerisation rate high enough to have an amount of bioavailable Si(OH)_4 of 17% [57]. Another form of silicon supplement is called ‘colloidal silica’. Here is important to note that, what is referred by the manufacturers as ‘colloidal silica’ is, in fact, particulate silica, while, the choline-stabilised ‘orthosilicic acid’ for example, is in the colloidal form, or, in other words, nanoparticulate silica [57]. This ‘colloidal silica’, which is precipitated and completely polymerised silica, presents very low bioavailability, less than 2%, probably

because it is so aggregated. Also, the rate of hydrolysis in the gastrointestinal lumen is slow compared with the window of opportunity for absorption in the small bowel [57]. Other silicon supplements that can be found over the counter include Silicea, Silicol, Silica and Horsetail.

There have been some studies focusing on the effects of silicon supplementation [59-61], and until now results lead to the conclusion that they are beneficial for the organism. In a small intervention study, in which osteoporotic subjects were treated with silicon in the form of MMST, it was observed an increase in trabecular bone volume, compared to non-treated controls [62]. Also, in another study, femoral density was significantly increased after intramuscular administration of silicon, again in the MMST form, twice a week for four months [63]. In animals, supplementation with a choline-stabilised orthosilicic acid complex based supplement resulted in a higher collagen concentration in the skin [34], and in an increased femoral bone density [64]. Furthermore, Calomme et al. investigated the effect of the same choline-stabilised supplement on bone loss, in aged ovariectomized rats [6]. They observed that the increase in bone turnover in the animals tended to be reduced by the silicon supplementation. Also, the bone mineral density was significantly increased at two sites in the distal femur in the supplemented group, when compared with the controls [6]. Still with the same choline-stabilised supplement, another study obtained results that suggest that the combined treatment of silicon supplement with Ca/Vit D3 is safe, and has a potentially beneficial effect on bone turnover, especially on bone collagen, and possibly also on femoral bone mineral density, when compared to the treatment with Ca/Vit D3 alone [65]. Also, in a randomized, double blind and placebo controlled study, that aimed to see the effect of a silicon supplement on skin, nails and hair, in women with photo damaged skin, results illustrate a positive effect of oral supplementation [66]. After 20 weeks of oral supplementation, both skin microrelief and mechanical properties improved. Also brittleness of hair and nails was significantly lower, compared to the baseline, in the supplemented group.

Although there are already silicon supplements which present high bioavailability, like MMST, the absorption mechanism in the bowel is still poorly understood, there is still no experimental evidence demonstrating the conversion of monomethylsilanetriol to orthosilicic acid [67]. Also, due to the tendency of silicon to agglomerate, concentrations of solutions have to be relatively low, which impacts on the route of supplement

administration. Thus makes it impossible to take the supplement as just a capsule, as in this way, the consumer would not achieve the necessary dose, for the supplement to produce its beneficial effects. Instead, large quantities of supplement need to be ingested. For the choline-stabilised silicon supplement, the ratio of choline to silicon that is necessary to achieve stabilization is far higher than what would be ideal, and the pH of the final solution is very low, approximately pH 2 [68]. As mentioned above, the aim of this project is to try to develop a solution with small, stable, silicon nanoparticles, with realistic ratios of silicon:stabilizer, at a realistic pH. The nanoscale range would allow higher concentrations to be achieved, and further de-polymerization in the bowel would give the supplement high bioavailability.

1.2. Nanoparticles

Nanotechnology was introduced by Richard P. Feynman in 1959 [69] and, since then, there have been many developments in physics, chemistry, and biology that have demonstrated Feynman's ideas of manipulating matter at an extremely small scale, the nanoscale [70].

In a scientific context nano refers primarily to a specific magnitude order, more exactly 10^9 . In the nanotechnology context, the term nano refers almost exclusively to particle size, thus, nanoparticles are two dimension objects with a particle size from one to one hundred nanometers. This area of research is one of the fastest growing areas of science and technology, underpinned by the synthesis of nanomaterial with unusual and useful properties that differ from bulk materials [71]. In general, nanotechnology encompasses two main approaches, these being, the 'top down' and 'bottom up' approaches (Figure 7).

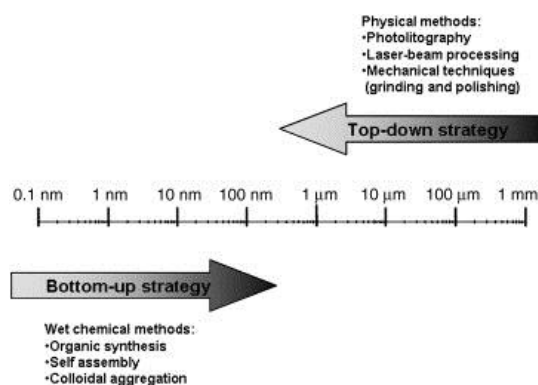


Figure 7 – Scheme “Top-Down” and “Bottom-UP” approaches for the manufacturing of nanoparticles [72]

Top-down strategy is defined as that in which nanoparticles are directly generated from bulk materials, while maintaining their original properties, via the generation of isolated atoms by using various distribution techniques [73]. The majority of the top down strategies involve physical methods, such as milling or attrition, repeated quenching and photolithography [74]. The bottom-up strategy, also called ‘molecular nanotechnology’ or molecular manufacturing [75], involves molecular components as starting materials linked with chemical reactions, nucleation and growth process, to promote the formation of more complex clusters [74]. However, size alone is not enough to make the distinction between nanoparticles, and other chemical molecules or polymers of a similar size. Nanostructures are fundamentally different forms of matter than simple chemicals. Their size and organization frequently take advantage of the quantum mechanical properties of these structures. Contrary to popular belief, nanoparticles are not just a product of modern technology, in fact, manufacturing of those structures has been going on in the biological world for many millions, or even billions of years, they are created by natural processes, such as volcano eruptions and fires. Indeed, our own bodies are full of self-assembling nanoparticle structures, like viruses for example [70].

1.2.1. Properties

Some properties associated with bulk materials, such as chemical composition and crystal structure, remain the same at the nanoscale, however, many properties of these materials change at the nanoparticle scale [76]. These differences arise from the small size

and large number of surface atoms of the particles [77]. Their surface-to-volume ratio is, actually, one of their most important features, and this ratio increases as the particle diameter decreases. A nanoparticle is composed of a few numbers of atoms, which means that a significant portion of the atoms are located at the particle surface [77]. A particle with a diameter of 10 nm has 20% of its atoms positioned at the particle surface, while with a particle with 5 nm this percentage rises to 40%, and with a particle of 1 nm almost all of its constituting atoms are at the surface [77]. The atoms at the surface, unlike those located at the core, suffer less influence of neighbouring atoms, presenting unsaturated bonds, which are responsible for the high reactivity of the particle. Indeed, if the surface of the nanoparticles is not protected with a molecule, a capping agent, interactions between particles will generally occur in such a way as to reduce this high surface energy and this, generally, results in aggregation. Capping agents can be organic molecules, polymers, or biological molecules, and they generally work by either charge or steric stabilisation mechanisms, which prevent further aggregation (Figure 8) [78].

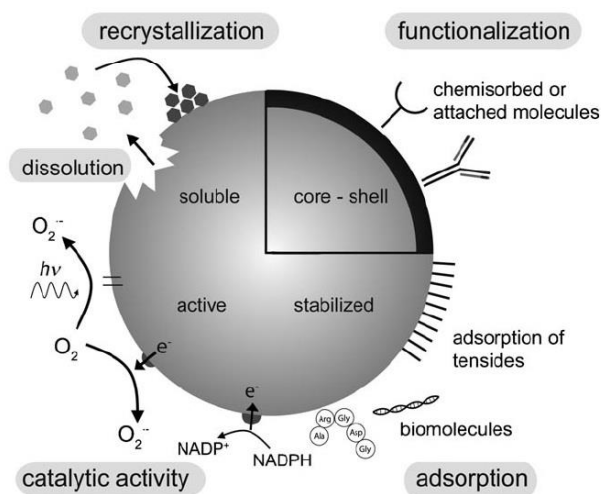


Figure 8 – Scheme of surface alterations in nanoparticles [79].

The model nanoparticle has three distinct features, these being, a defined structure, monodispersity, and large surface area, however, the feature that is most often cited is particle size. There are three different types of diameter to measure, primary particle size, hydrodynamic diameter, and aerodynamic diameter [80, 81]. By altering the nanoparticle

size, it is not only possible to modify their reactivity, but also their optical characteristics, such as transparency, absorption, luminescence and scattering.

The composition of a nanomaterial also defines its function and properties. In nanotechnology, each nanomaterial has a specific and very unique application, and, although some properties are shared among nanomaterials, there is always an optimal structure for the desired purpose [82]. So, nanoparticles may have different chemical compositions, they can be composed of metals, semiconductor materials, such as metal oxides (inorganic nanoparticles), carbon or carbon containing compounds, such as polymers (organic nanoparticles) [83]. Nanoparticles can also be single particles, aggregates or agglomerates. The aggregates are loose, reversible attachments, formed through strong attractive interactions, in solution this process can be reverted, and the aggregates may be dissolved into single particles. The agglomerates are, in turn, irreversible accumulations of particles and cannot be scattered back into single particles [83].

There is an increasing need for stable suspensions when it comes to the aggregation of nanoparticles, in both aqueous and non-aqueous systems. So, for the production of nanoparticles, the main objective is not simply to obtain nanoscale materials, as for most real world applications, other experimental conditions need to be tightly controlled. Manufactured nanoparticles need to have at least the following characteristics, these being, identical particles in terms of size, shape and morphology, chemical composition and crystal structure must be the same, and last but not least, they must also have monodispersity [84].

1.2.2. Applications

As mentioned before, nanomaterials present unusual and useful properties, quite different from other materials at the micron scale, which has led to an increasing interest in this technology (Figure 9) [85], i.e., in industries such as chemical, pharmaceutical, ceramics and microelectronics, both in scientific and technological terms. The applications are vast and can range from pigments, nanocomposites, drug delivery and ceramic materials, up to the manufacture of semiconductor films.

reagents and drugs that are being used for the development of these compounds have still to be approved, these findings serve as important milestones towards clinical application [100].

Nanoparticles also have a wide range of applications in biological research. They can be used for biomolecule detection in DNA assays, immunoassays and cell bioimaging. Usually they are derivatized with different functional groups, such as nucleic acid-targeted oligonucleotide probes, antibodies and protein, to produce nanoprobes. One example is the gold nanoparticle-based probes, that have been used in the identification of pathogenic bacteria in DNA-microarray technology [101]. Alternatively, nanoparticles can be used as fluorophores in FISH – Fluorescence In Situ Hybridization. Quantum dots attached to a specific oligonucleotide probe or immunoglobulin G have been used to successfully detect human Y chromosome [102], and to locate cancer markers in cellular imaging [103]. Magnetic nanoparticles also have applications in biological research, such as sample separation, purification and concentration. Different capturing molecules, such as antibodies and oligonucleotides probes can be immobilized on the surface of magnetic nanoparticles [104].

Nanoparticles also have applications in manufacturing and materials, i.e., silicate nanoparticles can be used to provide a barrier to gasses or moisture in plastics films used for packaging, which could slow down the process of spoiling or drying out in food. Silver nanoparticles can be used in fabric to kill bacteria, making clothing odour resistant. Nanoparticles can also be used for water purification, being a green chemical approach in comparison to the methods used at the moment. Gold nanoparticles can actually adsorb different organophosphorous pesticides and, in addition, they exhibit antimicrobial activity against different bacteria and yeasts [105].

Regarding nutritional sciences, nanoparticles already have a wide range of applications, such as, modifying taste, colour, and texture of foods, detection of food pathogens and spoilage microorganisms, enhancing nutrition quality of foods. As well as, serving as a tool to study nutrient metabolism and physiology [106]. However, the predominant food-related use of nanoscience in the short term is in food contact materials, such as packaging [107]. In the longer term, nanoscale food research appears, instead, to be focused on controlled release of nanoscale-encapsulated food ingredients or nutrients [107].

1.2.3. Absorption in the Organism

Although the aim of this project is to produce silica nanoparticles that will dissolve, to release silicic acid, it is important to provide context on the delivery of nanoparticles in biological systems. In particular, during the last years, due to the many biological applications of nanoparticles, it has become increasingly important to understand their behaviour in biological systems, starting on how their uptake is processed [79]. Following the intake, translocation of particles, to and through the gastrointestinal mucosa, may occur through four different routes (Figure 10) [108]. The most common route of absorption of nanoparticles, and also the most documented, is the M-cell rich layer of Peyer's Patch pathway. Des Rieux et al observed, in a co-culture of an intestinal epithelial cell line, which had been differentiated so as to acquire M cell characteristics, an increasing of about a thousand fold in the transport of particles, with diameters varying from 200 to 500 nm [109]. M cells are differentiated and specialized epithelial cells, which have a predisposition to perform transcytoses of macromolecules and particles [110, 111]. They are, also, able to pass intact material from the lumen to abutting/interlocking mononuclear cells. These cells can be found in anatomic sites that are believed to be important immune-inductive sites, and also to represent a constitutive mechanism for the continued surveillance of luminal antigens and pathogens.

Another possibility for nanoparticle uptake is through endocytosis at the enterocyte level. Although the main function of these cells is absorbing and transporting nutrients, there are some data that suggest that enterocytes can also absorb compounds in the nano range, as happens with ferritin present in meat [109]. A third route for particle translocation will be persorption. Volkheimer noted that enterocytes shed from the villous tip and into the gut lumen, which leaves a gap in the epithelium and allows the translocation of larger sized particles such as starch and pollen [112, 113]. In a post study performed by Hillyer et al, it was observed that this process also allows the passage of nanoparticles [114]. Lastly, it is also possible, under certain conditions, that very small nanoparticles have access to the gastrointestinal tissue through tight junctions of the epithelial cell layer. However, this is still just a theoretical possibility, since epithelial junctions are extremely effective in preventing paracellular permeation, although their

integrity may be affected by diseases, epithelial cell metabolism, calcium chelators [115] and even particle endocytosis [116].

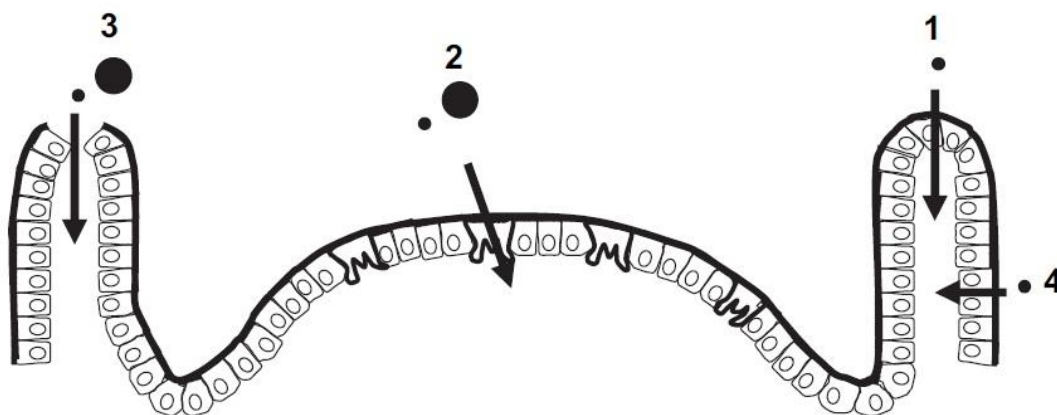


Figure 10 – Scheme of different possibilities for particles translocation across the gastrointestinal tract 1) Endocytosis through regular epithelial cells, 2) M-cell-uptake (transcytosis) at the surface of intestinal lymphoid aggregates, 3) Persorption, 4) Putative paracellular uptake [108].

1.2.4. Toxicity

In contrast to nanoparticle exposure through the use of consumer products, the new emerging biomedical applications of nanoparticles involve deliberate, direct ingestion or injection of nano materials into the body, thus toxicity has become a critical factor to consider, when evaluating their potential [117]. Nanotechnology has played an increasingly important role in the dietary supplements industry due to its efficiency in delivering bioactive compounds [118]. A wide variety of nanoparticles can be used in food supplements from solid nanoparticles, with various shapes, to nano-delivery systems. The benefit of using nanoparticles in food supplementation is mainly due to the ease of entry into the cells, and also, as mentioned, the increase in specific surface area. However, this easy entry into the body needs further study, because it can affect the detoxification capacity of the organism and facilitate the cross of the blood-brain barrier [118]. Another physicochemical factor of decisive influence is the solubility or biodegradation. Also, what type of cellular responses that can be induced by degraded nanoparticles, as they can accumulate within the cells and lead to intracellular changes, such as disruption of organelle integrity or gene alterations [117]. It is clear that degradable nanoparticles show distinctly different behaviour than persistent or inert ones. In most cases, soluble materials

rapidly release their constituents and can result in acute effects which, in most cases, are easy to detect [119, 120]. In contrast, persistent materials remain inside the organism for months to years. In this case, a clear prediction of risk is difficult, and proactive identification of harmful materials is challenging [79].

Nanoparticle functionalization can also be behind the toxic effects. Surface functionalization, as mentioned above, confers stability and interesting properties to nanoparticles, such as surface charges, hydrophilicity or hydrophobicity [121]. However, this addition of surface coatings confounds the bioactivity and potential toxicity of the functional groups on the nanoparticle surface, making it difficult to interpret the observed changes [122]. Surface charge also plays a role in toxicity with cationic surfaces being more toxic than anionic, and neutral surfaces being the most biocompatible [122]. This may be due to the affinity of cationic particles to the negatively charged cell membrane.

There are very few studies on immune and/or cellular reactions, in the gastrointestinal system, to nanoparticle intake, but there is, however, a common observation in non-gut systems that nanoparticles appear to enhance the formation of ROS (Reactive Oxygen Species), and can, through this route, exert a toxic effect in the body [108]. Ag nanoparticles were reported to exert significant cytotoxicity in rat liver cells, including depletion of intracellular glutathione levels, decrease of mitochondrial membrane potential and an increase in ROS levels [121].

1.2.5. Silicon Nanoparticles

Silicon nanomaterials are important and have been extensively studied and explored for a myriad of applications, ranging from electronics to biology [123, 124]. Silicon nanoparticles are very attractive because of their diverse properties such as, luminescence, size-dependent emission, band gap, biocompatibility, high sensitivity and reactive surface [125]. This creates great interest for industrial applications in the field of electronic and also for biological applications [126, 127]. Silica particles coated with organic modifiers are used in applications that include stationary chromatography phases [128], heterogeneous supported catalysts [129], consumer goods [130], aerospace and sensor industries [131]. Colloidal silica is of particular interest due to the ease of synthesis and precise control of the size and distribution of the particles [132].

The chemistry of silicon is based on covalent bonds and the methodologies used for growing silicon particles implies very different routes from those used in the case of metals, in other words, silicon obeys the rules of covalent chemistry, it is not dependent on quantum confinement effects. Hence, some researchers believe that covalent links between silicon atoms and surface functional groups, might be more inclined to directly influence the properties of the particles, rather than their size [133]. The silanol groups can be functionalized through different procedures. The hydroxyl group can react with various compounds to form amine, carboxyl, or thiol groups. Also, silica surface modification is not limited to chemically-mediated procedures, as passive of molecules, such as avidin, is also commonly used [134]. The versatility of silica in synthesis, as well as surface modifications, offers great advantage to the use of the mineral in a wide range of applications [134]. The versatility towards different surface modifications can be an advantage in the supplement field. The silica surface can be modified easily with many biomolecules for added biochemical functionality, in other words, to contain other compounds of interest to the organism, beyond the mineral itself [134].

1.3. Techniques

In this chapter it will be overviewed the techniques that will be used in this work. Since we are dealing with nanoparticles it is important to assess their size, charge, and overall stability overtime, as these parameters can affect their properties. One technique that allows the determination of particle size is DLS (Dynamic Light Scattering), and the charge can be acquired with zeta potential measurement. We will also use the molybdate assay to assess monomeric silicate concentration, and therefore we will use spectrophotometry. Silicon concentration in the produced dispersions is of great importance, and will be measured using ICP-OES – Inductively Coupled Plasma – Optical Emission Spectrometry. Also, structure of the nanoparticles will be assessed with ATR-FTIR. These techniques are relevant in the current work, and, therefore, they will be described in the next sections in some detail.

1.3.1. Dynamic Light Scattering

Particle size and shape can influence a large variety of important physical properties, manufacturing processability and quality attributes related to the production of health products, including, a) dissolution rate and bioavailability of active pharmaceutical ingredients [135], b) drug release rate for sustained and controlled release formulations [135], and c) *in vivo* particle distribution and deposition, absorption rate and clearance time, [135]. These properties ultimately affect the safety and efficacy of drugs [135].

DLS, also known as DLS-photo correlation spectroscopy or quasi-elastic light scattering, is a technique that can be used to determine the size distribution profile of small particles, in suspensions, or polymers in solution [136]. It may also be used to probe the behaviour of complex fluids and concentrated polymer solutions. This technique has led to major developments in the *in situ* measurement of the size of fine particles in the liquid phase [136, 137]. Since the advent of the laser in the 1960's, light scattering methodology has evolved fast, and there are five primary reasons for this, i) it is a non-invasive technique, ii) samples to be studied do not need to be prepared in any way, so there are few experimental artefacts, iii) it is relatively easy to use iv) it is fast and v) relatively inexpensive. Also, many different types of particles can be studied by light scattering, ranging from, ideal, hard sphere systems, to particle characterization in exhausts, biological systems, and study of dynamics and structures of food colloids [138]. DLS is ideal for investigation of colloidal suspensions, which are found in many foods. The technique is widely used as a convenient way of measuring particle sizes but also to study the dynamic behaviour of interacting colloids, and can follow processes such as aggregation and gelation [138].

DLS is based on the scattering of light by moving particles, i.e., it measures Brownian motion [138]. Brownian motion, is caused by the bombardment of solvent molecules that surround a particle, which also have movement due to their thermal energy [139]. When particles are illuminated by a laser, the scattered light intensity fluctuates at a rate which is dependent on particle size, since smaller particles are projected a greater distance by the solvent molecules, and also move faster. Thus, small, rapidly diffusing particles will give fast fluctuations, whereas larger particles will generate slow fluctuations (Figure 11) [139]. The intensity of the light arriving at the detector at any instant depends

on the interference pattern created by the scattered light from all of the particles in the scattering volume. If the particles are spherical and do not interact, their radius can be calculated from the diffusion coefficient by the Stokes-Einstein relationship [139].

$$d(H) = \frac{kT}{3\pi\eta D}$$

In this equation, $d(H)$ is the hydrodynamic diameter, k is the Boltzmann constant, T is temperature, η is the viscosity of the medium and D is the translational diffusion coefficient. If the particles are non-spherical, the radius of a sphere with the same D is calculated [139].

In a typical light scattering experiment, monochromatic light from a laser passes through a polarizer that defines the polarization of the incident ray, and then this is passed through a dilute, single scattering colloidal dispersion [139]. The scattered light then passes through an analyser which selects a polarization, and finally enters the detector.

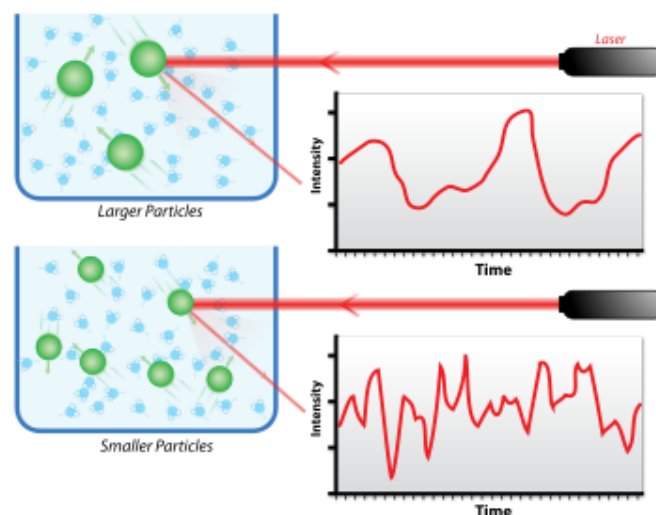


Figure 11 – Comparison between the rate of intensity fluctuations triggered by small and big particles [140].

Because the parameter obtained by DLS is the collective diffusion coefficient of the scatterers, involving the movement of the particles within their dispersing medium, there will be a layer of solvent molecules moving with the particle. Thus, DLS measures the apparent hydrodynamic radius of the scatterers [138]. One of the disadvantages of DLS method is that, in the case of samples with heterogeneous populations, the small particles may not be taken into account, due to the presence of much larger particles, even if the small ones are present in a bigger percentage. In the case of silicon nanoparticles, DLS is a

very useful technique to study sample stability overtime, since silicon, as it was discussed in previous chapters, has a tendency to agglomerate, and also, particle size, in the supplement context, will affect bioavailability, which is a very important factor.

1.3.2. Zeta Potential

The particles in a colloidal suspension or emulsion usually carry an electrical charge, which may be created in a number of ways. The surface of the particles may, sometimes, contain chemical groups that can ionize to produce a charged surface, or, even, the surfaces itself can, preferentially, adsorb either positive or negative ions. Whichever its on-going, the charge on the particle surface is an important characteristic, since it determines many of the properties of the system [141], and one way of assessing it, is through the zeta potential.

The zeta potential is the electrostatic potential on the surface of the particle (Figure 12). The liquid surrounding the particle exists as two parts, an inner region (Stern layer) where the ions are strongly bound, and an outer region where they are less firmly associated [142]. Within the diffuse layer there is a notational boundary inside which the ions and particles form a sable entity. When a particle moves, ions within the boundary move with it, while those beyond the boundary stay with the bulk dispersant, and it is the potential at this line that is acquired when measuring the zeta potential [142].

The magnitude of the zeta potential gives an indication of the stability of the colloidal system, due to the fact that if the particles have a large negative or positive zeta potential (± 30 mV) they will tend to repel each other, whereas if not, there will be no force to prevent the particles coming together and aggregating [141].

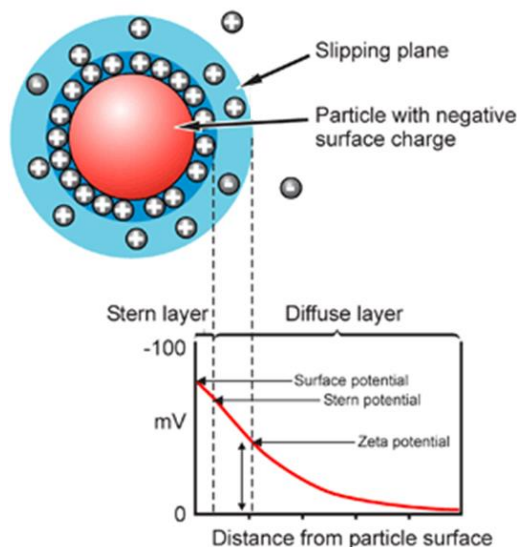


Figure 12 – Schematic representation of zeta potential [142].

1.3.3. ICP-OES

The determination of trace concentrations of silicon and silicon compounds like aluminosilicates or organic silicones, in biological and other organic samples, is still one of the most demanding tasks in analytical chemistry [143].

ICP-AES (Inductively Coupled Plasma-Atomic Emission Spectroscopy) also designated ICP-OES (Inductively Coupled Plasma-Optical Emission Spectroscopy), is an analytical technique used for the detection of trace metals. It is a type of emission spectroscopy that uses inductively coupled plasma to produce ions and excited atoms that produce electromagnetic radiation at wavelengths characteristic of the element being analysed [144].

One of the principles behind ICP-AES is atom emission of electromagnetic radiation as they relax from their excited state to the ground state. The radiation emitted can be easily detected when in the range of vacuum ultraviolet (VUV, 120-185 nm), ultraviolet (UV, 185-400 nm), visible (VIS, 400-700 nm), and also near infrared (NIR, 700-850 nm) [144]. Although some atoms emit electronic radiation in the infrared, microwave, and radiowave, range detection systems for these wavelengths are less sensitive. The main objective of analytical atomic spectroscopy is to identify elements and quantify their concentration in various media. The procedure consists of three basic steps, atom formation, excitation, and emission (Figure 13).

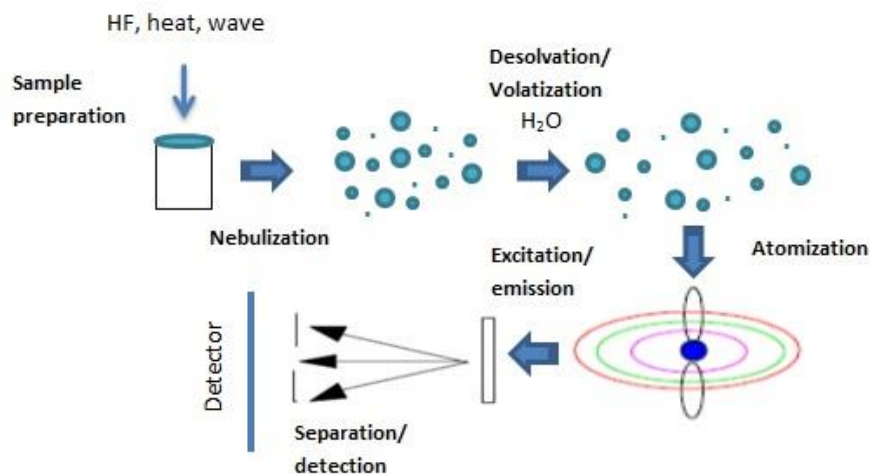


Figure 13 – Steps involved in the analysis of aqueous samples by ICP-OES [144].

ICP is just one of the many techniques available in analytical atomic spectroscopy. It uses plasma as a source of atomization and excitation, note that plasma is an electrically neutral, highly ionized, gas which consists of ions, electrons and atoms [144]. The energy that keeps the plasma is derived from a magnetic or electric field and most analytical plasmas use argon or helium, which makes combustion impossible. Plasmas are characterized by their temperature, and their electronic and ionic density, the analytical plasmas have temperatures ranging from 600 up to 8000 K [144]. Samples in all physical states have been successfully analysed using ICP, but the most commonly analysed samples are cations in solution. Note that when analysing solutions it is necessary to use a nebulizer, to convert the liquid into an aerosol consisting of particles with diameters ranging from 1 to 10 nm. ICP has some clear advantages in comparison to other radiation sources, as, it is a highly efficient atomization source, which means that every molecule should be dissociated provided that operating conditions are optimized for this purpose, the ionization efficiency is high, also the ICP exhibits excellent tolerance to high salt concentrations [144].

There are three common methods of separation or dispersion of light; gratings, prisms and Michelson interferometers. There are four types of detector system, PMTs (Photomultiplier Tubes), PDAs (Photo Diode Arrays), and CCD (Charge Coupled Devices) [144]. These methods of dispersion and detection are usually combined in one of four

configurations, which vary in sophistication; sequential, simultaneous with single point detection, simultaneous with one dimensional detection and simultaneous, with two dimensional detections. Sequential systems or monochromators allow the analysis of only one analytical line at a time [144]. More efficient systems, like polychromators, measure specific wavelengths at multiple positions simultaneously, this ability is a distinct advantage when compared to monochromators, however these systems lack flexibility, so just analytical lines and elements can be analysed [144].

Interferences in ICP-OES experiments can start at the sample preparation level and extend up to the operating conditions of the plasma. The most common type of interference involves two or more elements present in the matrix that emit radiation at the same wavelength as the compound being analysed [144]. These spectral interferences may be minimized by using high resolution systems, through the use of various analytical lines for the detection of a single element. Another type of interference involves the formation of undesirable species [144].

1.3.4. Spectrophotometry

Spectrophotometry is designed to measure the degree of absorption of light by a substance, in a definite and narrow wavelength range [145]. The absorption spectrum in the visible and ultraviolet regions of a substance in a solution is characteristic depending on its chemical structure [145]. A spectrophotometer is an instrument that measures the amount of photons (the intensity of light) absorbed after it passes through a sample solution. Depending on the range of wavelength of the light source, the spectrophotometer can be classified into two different types, these being, UV-visible, and IR [145].

One of the principles of spectrophotometry is that all substances absorb or transmit at specific characteristic wavelengths [146]. The light absorbed or transmitted must exactly match the energy required to cause electronic transition, this being, the passage of an electron from a quantum level to another, and only photons of certain wavelengths satisfy this energetic condition, thus, the absorption or transmission of certain specific wavelengths, characteristic to each substance, and posterior spectral analysis, may serve as the compound fingerprinting [146].

Once the intensity of light that passed through the sample is measured, it can be related to transmittance [145]. Transmittance is defined as the ratio between the amount of transmitted light and the amount of light that has been directed to the sample, while absorbance is defined as the negative logarithm of transmittance both relate according to the following formula:

$$A = -\log(T) = -\log\frac{P}{P_0}$$

Where A stands for absorbance, which is the amount of photons that are absorbed [145].

Absorbance can then be related to the concentration through the Beer-Lambert law:

$$A = \varepsilon * l * C$$

Where A stands, again, for absorbance, ε ($\text{L mol}^{-1} \text{ cm}^{-1}$) stands for molar absorptivity, l for cell size, and C for concentration.

1.3.5. ATR-FTIR

FT-IR stands for Fourier Transform InfraRed, the preferred method of infrared spectroscopy, which is a widely used technique that, for many years, has been an important tool for investigating chemical processes and structure. The combination of infrared spectroscopy, with the theories of reflection, has made advances in surface analysis possible. Specific IR reflectance techniques may be divided into the areas of specular reflectance, diffuse reflectance, and internal reflectance. The latter is often termed as ATR (Attenuated Total Reflectance) [147] and is the one used in the current work.

The concept of internal reflection spectroscopy originates from the fact that radiation propagating in an optically dense medium, of refractive index n_1 , undergoes total internal reflection at an interface of an adjacent medium, of lower optical density (refractive index $n_2 < n_1$) [147]. This phenomenon is called the evanescent wave, and was observed by Newton in the early 1700s. A schematic representation of a horizontal ATR-FTIR element is shown in Figure 14. IR radiation is internally reflected through a ZnSe crystal at an angle θ , producing an evanescent wave at each reflection that penetrates slightly past the crystal surface. At each internal reflection, the evanescent field interacts with any sample placed in contact with the ZnSe crystal. The depth that the evanescent field penetrates into

the sample at each reflection depends upon θ , as well as the IR wavelength in ZnSe, and the ratio of the refractive indices of the sample to ZnSe [147].

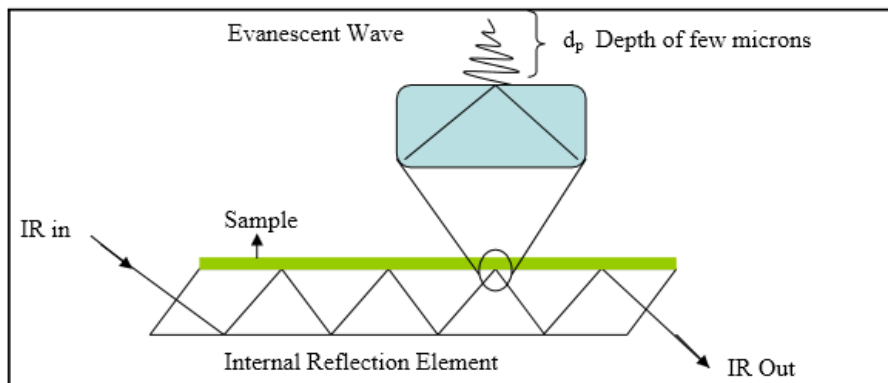


Figure 14 – Schematic representation of ATR spectroscopy [148].

One of the big advantages of ATR-FTIR is that is a sampling technique that enables samples to be examined directly in the solid or liquid state, as in the samples used in this work, without further preparation [148], being suggested as the best option to measure spectra for aqueous solution. Also, besides Raman spectroscopy, IR spectroscopy is the only other known, non-invasive, alternative of the Si^{29} NMR for studying small silicate nanoparticles, while being significantly faster, cheaper and more widespread than NMR [149].

This page intentionally left blank.

Materials and Methods

2. Materials and Methods

2.1. Materials

Water was ultra-high purity (UHP; 18 M Ω /cm) from an Elga water purifier. Sodium silicate solution ($\geq 10\%$ NaOH and $\geq 27\%$ SiO₂), sucrose (α -D-Glc-(1 \rightarrow 2)- β -D-Fru), poly(ethylene glycol) (average mol wt 200), Ethanol absolute ($\geq 99.8\%$ (GC)), sodium chloride ($\geq 99\%$), concentrated hydrochloric acid (37%), and sodium hydroxide ($\geq 98\%$), were all purchased from Sigma-Aldrich Co. Ammonium Molybdate ((NH₄)₆Mo₇O₂₄.4H₂O; AnalaR grade), Sulphuric Acid (2.5 mol/L (5 N); AnalaR; volumetric standard), were purchased from BDH Ltd. Pepsin from porcine gastric mucosa (4,220 units/mg protein) was from Sigma. Dialysis tubing cellulose membrane (43 mm; 12 400 nominal molecular-weight cut off) was purchased from Sigma-Aldrich Co.

2.2. Methods

2.2.1. Synthesis

In the synthesis of the following silicate solutions, which have an initial pH of approximately 11.0, when a drop in pH was needed, the acidic solution had to be added very fast, in order to avoid pH around 7.0, as gelling occurs rapidly in this range.

Non-stabilised silicate suspension

A silicate solution was prepared through dilution with UHP water (pH_i \approx 11), and its pH dropped to around pH 0.5 to 1.0 with 37% HCl. After this, pH was raised again, to the desired final pH, depending on the experiment, with NaOH. This solution had a [Si] of 0.5 M, and was used as negative control in all the experiments.

Sucrose stabilised Silicate suspension

A silicate 0.5 M solution was prepared through dilution with UHP water ($\text{pH}_i \approx 11$). Sucrose was then added to this solution, aiming for a final concentration of 1.5 M. The pH was dropped to around pH 0.5 to 1.0 with 37% HCl, and then raised again, to the desired final pH with NaOH.

PEG stabilised silicate suspension

This solution was done in the same way that of the silicate and sucrose, except PEG was added instead of sucrose, and a final concentration of 1.0 M was used.

Sucrose stabilised silicate suspension with 14% EtOH (v/v)

A 0.5 M silicate solution was prepared through dilution with UHP water ($\text{pH}_i \approx 11$). Sucrose was then added to this solution, aiming for a final concentration of 1.5 M. The pH was dropped to around pH 0.5 to 1.0 with 37% HCl. After the pH drop, ethanol was added to the solution, aiming for a final concentration of 14% (v/v). Then the pH was raised again, to the desired pH, with NaOH.

2.2.2. Determination of Particle Size and Zeta Potential

The samples were placed in an appropriated cuvette or cell, and then their particle size distribution (refractive index – 1.487; absorption – 0.010) or zeta potential ($F(\text{Ka})$ – 1.5), were determined by DLS in a Zetasizer, Malvern Instruments.

2.2.3. Characterization of Silicon Phase Distribution

First, for each solution, three aliquots were collected; i) total silicon, ii) silicon content in the supernatant, iii) and nanoparticulate silicon < 12 nm, which was ultrafiltered through a membrane of 1000 KDa. All aliquots were collected in duplicate. Before analysis by ICP-OES, each sample was diluted twice, first in UHP water and then in 5% HNO_3 . Silicon standards were prepared, with silicon concentration ranging between 0 and

100 ppm, through the dilution of a silicon stock standard, 1000 ppm (Fisher Scientific), with 5% HNO₃. The nanoparticulate fractions (i.e. < 12 nm, and > 12 nm), as well as the precipitated fraction of silicon, were determined, using inductively coupled plasma optical emission spectrometry (ICP-OES; JY 2000, Horiba), using a wavelength of 251.611 nm. Silicon fractions were calculated as per below:

$$\text{Nanoparticulate silicon } < 12\text{nm } (\%) = \frac{\text{Si}_{\text{UF}}}{\text{Si}_{\text{total}}} \times 100$$

$$\text{Precipitated silicon } (\%) = \frac{\text{Si}_{\text{total}} - \text{Si}_{\text{supernatant}}}{\text{Si}_{\text{total}}} \times 100$$

$$\text{Nanoparticulate silicon } > 12 \text{ nm } (\%) = 100 - \text{UF Si } (\%) - \text{Precipitated Si } (\%)$$

2.2.4. ATR-FTIR Spectroscopy

A Shimadzu IRPrestige-21 Fourier Transform Infrared spectrometer was used, equipped with a Specac MKII Golden Gate single reflection diamond ATR. Spectrums were all acquired with purge bellows. The samples spectrums were obtained using a droplet on the diamond ATR surface. All spectra were acquired in the transmittance mode from 4000 to 500 cm⁻¹ by accumulating 20 scans. The FTIR spectrometer has a wavenumber accuracy of 0.125 cm⁻¹. Transmittance spectrums were corrected against a spectrum of UHP water, obtained in the same instrumental conditions.

2.2.4. Dissolution Assay

The dissolution assay was adapted from a previously described method, used to compare the absorption of silicon from different foods and supplements. This is a two stage assay, aiming to mimic the process of digestion. In the current work, Biosil was used as the positive control, since in the referred study it had the highest bioavailability of the supplements studied. Prior to sample analysis, the silicon concentration of all solutions, including the positive control, was determined by ICP-OES, and after that the solutions were treated, so that their silicon concentrations matched. In this case, the Biosil was

diluted from approximately 19000 ppm to 13000 ppm. For the dissolution assay, 0.25 mL of each sample was transferred to a 10 mL polypropylene tube, and mixed thoroughly with 5 mL simulated gastrointestinal fluid (SGIF), and then preheated to 37 °C in a water bath. To prepare the SGIF, 0.24 g of NaCl were dissolved in 9.6 mL 1 M HCl and 110.4 mL of UHP water and, just before use 0.384 g of pepsin was added. The pre-heated samples were then placed in pre-washed (in UHP water) dialysis bags, which were then placed in a 50 mL tube containing 30 mL of pre-warmed to 37 °C SGIF. The 50 mL tubes were placed in a water bath at 37 °C, under agitation, for 24 hours. After two hours, the SGIF mixture surrounding the dialysis bag was adjusted to pH 7.0, with 1 M NaHCO₃, this way mimicking intestinal conditions. The surrounding mixture was sampled for ICP analysis at the following time intervals, 0 min, 15 min, 1h, 2h, 4h, 6h and 24 h. All samples were taken in duplicate for total silicon concentration analysis and for ultrafiltered fraction analysis, using 3 KDa filters, which corresponds to a particle size of approximately 1 nm, and diluted with 0.7% HNO₃.

2.2.5. Molybdate Assay

The molybdate assay was used in this work at two different times, on itself and associated with the dissolution assay, with some changes between experiments. In both, to prepare the colour solution, which has to be fresh, 0.6105 g of Ammonium Molybdate were dissolved in 85 mL of UHP water and 15 mL of 0.5N H₂SO₄.

For the assay in itself, the samples were first diluted for a final silicate concentration of 0.6 mM, after what, 1.0 mL was taken from each diluted sample at 0, 10, 20 and 30 minutes, and left to react with 2.0 mL of the colour solution for 10¹ minutes. After the 10 minutes its absorbance was read in a Perkin Elmer Lambda 25 UV/Vis spectrometer, at 400 nm, using a 1.0 cm quartz cell.

For the molybdate assay associated with the dissolution assay, 50 µL samples were taken, in quadruplicate, from the surrounding mixture, at the same time intervals as for the ICP analysis (0 min, 15 min, 1h, 2h, 4h, 6h and 24 h). The samples were placed into a 96 well plate, and then 200 µL of colour solution was added with a multi-channel pipette.

¹ It is important that the sample is not left to react with the colour solution for more than the 10 minutes. This is due to the fact that the molybdate in excess, after reacting with all the monomeric species, might induce cleavage of dimers, and even trimmers, subsequently reacting with the monomers generated, which will result in an inaccurate increase of signal.

After addition of the colour solution the plates were placed on an orbital shaker for 10 minutes, and, immediately after, the spectrophotometer analysis was done at 405 nm (Labsystem Multiskan RC Optical Plate Reader).

For both analysis, water was used as blank, and for calibration purposes a calibration curve was acquired, with the concentration of silicon in the standards ranging from 0.0 to 1.0 mM. The standards were prepared with the same silicon solution used for the preparation of ICP analysis standard, and the dilution was made in the former with water and, in the later with SGIF. Reacting

Results and Discussion

3. Results and Discussion

3.1. Silicate Nanoparticles Synthesis

The first part of this work consisted in the synthesis of nanoparticulated silicate materials, in which different systems were tested, so as to improve the silicate suspensions stability. For discussion purposes, out of all the compounds tested, only the ones that significantly improved stability, when compared to the silicate suspension with no stabilizer, will be assessed in detail. A complete list of all the chemical compounds tested can be found in Appendix A. The materials were also characterized by DLS, to obtain the size distribution of particles in suspension, by zeta, to obtain the electric potential, and by ICP, to determine the silicate phase distribution.

Solubility of amorphous silica, in water, at 25 C, under pH 10, range, approximately from 2.5 mM to 5.0 mM, depending on the medium conditions, higher than this, they start to form aggregates [2]. Silicate suspensions are very stable at alkaline pH's (\approx pH 10), and start to dissolve above pH 11 [2], however this is not a suitable characteristic for a dietetic supplement, as there could be potential safety issues, such as damage to the mucosa and a severe shift of the stomach pH [150]. Neutral pH's were not an option either, because silicate suspensions have their lowest stability point at this range (pH \approx 5 to pH \approx 8) [2], so the materials synthesised, at first, had a final pH of approximately 3.5, since this is a pH close to the range at which silicate suspensions are metastable, and also an acceptable pH to be ingested by humans [151]. In this work, the silicate suspensions were synthesised with a silicate concentration of 0.50 M, since this was the highest possible to be added, without making the suspension unstable, leading to rapid aggregation. At pH 3.5, the 0.50 M silicate suspensions were stable for an average of approximately 4 days, after this they became very viscous, and finally they form a hardened gel like material. Immediately after being synthesised, the particles in these suspensions were very small, with an average particle size of approximately 2.4 nm (Figure 15A). This was a desired characteristic, since the aim was that the nanoparticles in the supplement, or at least their majority, become soluble, once they reach the duodenum, and the smaller the nanoparticles, the easier this process happens [2]. The zeta potential of the silicate suspensions was also measured, being very close to 0 mv, tending to the

negative side, so the surface of the particles was not charged, thus being more prone to aggregation, since there was no repulsion factor. Therefore, at pH 3.5, the stability of the silicate nanoparticles is due, only, to the lack of hydroxyl ions, which is a catalyst for the siloxane bonding formation [2]. The zeta potential graph can be observed in Figure 15B, and although there is the hint of a peak near 0 mv, this is not sharp, so the results may not be very accurate. This might be due to the sample being too concentrated, resulting in a high content of nanoparticles, this way hindering their movement, which would affect the measurement of the surface electrostatic potential. Also, it could be due to the existence of different populations of nanoparticles with different charges, however if this was the case, agglomeration and gel formation should happen almost immediately. Nonetheless, according to the literature [12], in less concentrated silicate suspensions, the particles, in the pH range 1.5 to 2.5, are reported to have zero charge, starting to become negative at pH's higher than approximately 2.5, so the particles synthesised in this work seem to behave the same way.

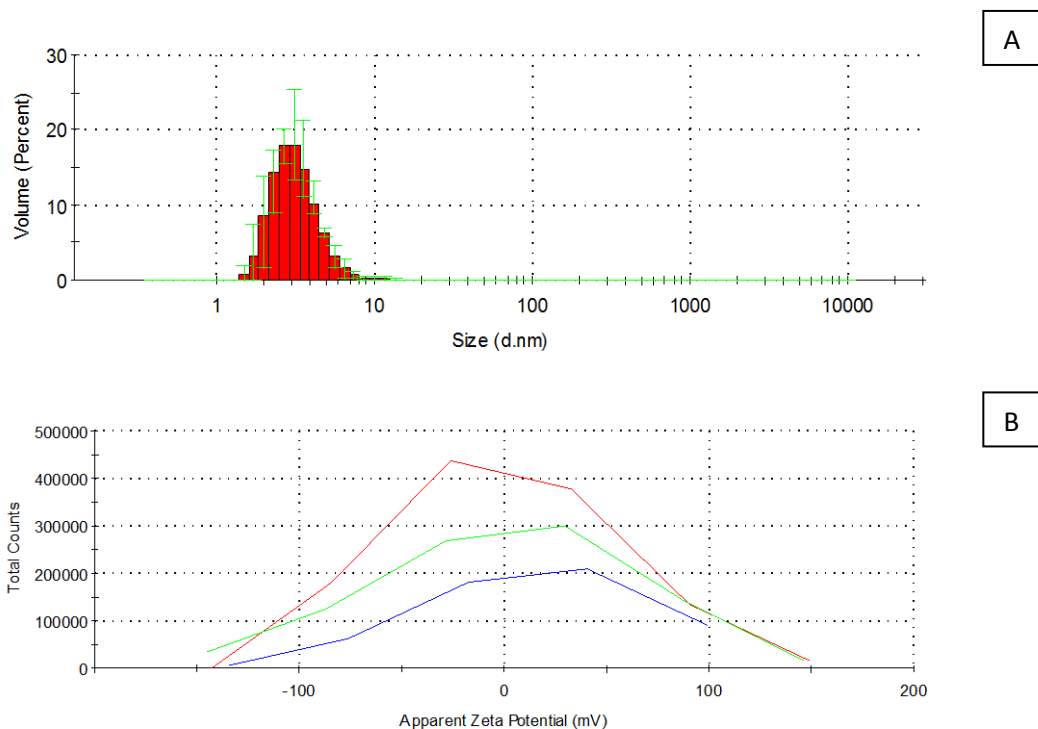


Figure 15 - Particle size distribution (A) and zeta potential distribution (B) of the silicate suspensions (0.50 M) in UHP water, at pH 3.50.

Even though the nanoparticles in these silicate suspensions were small, a shelf life of 4 days for a supplement is not acceptable, so the next step was to try to improve stability. This, as stated above, was done by testing different chemicals as possible stabilizers, and among all the compounds tested there were four systems that clearly enhanced the stability of the silicate suspensions, when compared to the negative control (Figure 16), those were sucrose and PEG in UHP water, and sucrose in a matrix of UHP water and ethanol. These suspensions will now be discussed in detail.

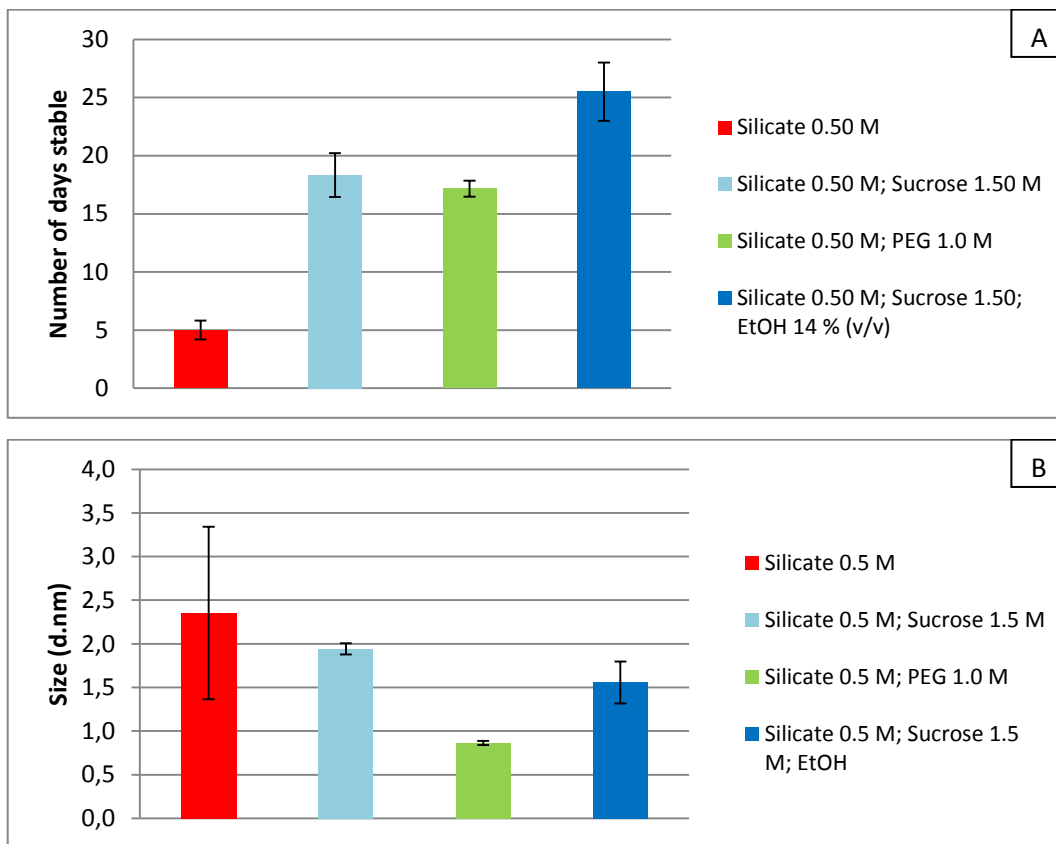


Figure 16 – Average number of days that the silicate suspensions remained stable with the different stabilizers used (A) and their respective particle size (B), at pH 3.5

3.1.1. Sucrose

Carbohydrates are the most abundant organic material in the biosphere, so there ought to be considerable opportunity for silicates and carbohydrates to interact [152]. Also, it is widely known the role of sugars as well established cements set retarders, which are mostly composed of silicates, being sucrose one of the most effective [153]. Although the

mechanisms by which they interact with the heterogeneous solid components in cement slurries, to influence the cement hydration, are not well understood, there are several theories that link the sugars with the silicate present in the mixture. There have also been some studies in the interaction of sugars with silicic acid in solution, and their effect in stability, and, although all the studies so far, at least to our knowledge, were made with slightly different conditions, from the ones in this work, i.e. strongly basic medium, the positive results made sucrose an obvious stabilizer possibility [152] [154].

During the synthesis of the sucrose stabilised silicate suspensions, the 0.50 M concentration of silicate was kept, at first, as in the non-stabilised suspensions, however, different ratios of silicate:sugar were tested, by altering the sucrose concentration (Table 2). It was observed that the best results were achieved with a concentration of 0.50 M of silicate and 1.50 M of sucrose, so this was. Sucrose stabilised silicate suspensions, at pH 3.5, were stable for an average of approximately 18 days, delivering the best result, out of all the suspensions in UHP water, at this particular pH. So it seems that a ratio of 1:3, silicate:sucrose, would be the minimum required to increase stability significantly, however, this is not ideal, since for the silicate concentrations being used, the amount of sucrose needed would make the sugar content of the supplement very high, turning it, in the worst case, depending on daily dose, not recommended for diabetics.

Table 2 – Different ratios of silicate:sucrose tested, and negative control (NC), at pH 3.5, and the days that each suspension remained stable.

		Compound	[Compound] (M)	pH	Stability (days)
	Silicate 0.5 M	Sucrose	0.50	3.50	8
			1.00		10
			1.50		17
NC	Silicate 0.5 M			3.50	4

Also, the same ratios were tested with higher concentrations of silicate (Table 3), in the attempt of increasing its content, however, this too fell short to the stability time achieved with 0.50 M silicate and 1.50 M sucrose. This might be due to the silicate concentration being too high, that despite the silicate and sucrose stoichiometry being the same, the aggregation rate is too fast for the sugar to exert the same effect.

Table 3 - Different ratios of silicate:sucrose tested, and the negative control (NC), at pH 3.5, and the days that each suspension remained stable.

		Compound	[Compound] (M)	pH	Stability (days)
	Silicate 1.0 M	Sucrose	1.0	3.50	3
			2.0		6
			3.0		7
NC	Silicate 1.0 M			3.50	7

The sucrose (1.50 M) stabilised silicate (0.50 M) suspensions were characterized for particle size and zeta potential (Figure 17). The particles had a particle size of approximately 2.0 nm, and, even though they were slightly smaller than the particles in the silicate suspensions with no stabilizer, the difference is not substantial. However, despite the fact that sucrose did not show a big improvement in the particle size, when compared to the negative control, 2 nm is a very good starting point. Also, similar to the negative control, the zeta potential of these suspensions was approximately 0 mV, however, this time, the graph showed a very sharp peak, which might be because the hydroxyl groups in the sucrose are stabilizing the charge of the nanoparticles. Also, this suggests that the sucrose is not stabilizing the silicate suspensions by changing the surface charge either positively or negatively, which would create electric repulsion between the particles, preventing aggregation. In a previous study, which assessed the formation of silicate complexes with sugars in aqueous solutions, although the system conditions were not the same, when sucrose was tested, it failed to react with silicic acid, which they found was consistent with sugars lacking an open hydroxyl group on an anomeric carbon [152]. However, in this same study, in terms of stability, only silicic acid solutions with sucrose and glycitols (inositols) were stable indefinitely. Sucrose might be stabilizing the silicate suspensions through steric hindrance, preventing collision between particles, though in the long term this does not seem like a suitable mechanism, since particles would eventually have contact with each other, leading necessarily to gel formation [152].

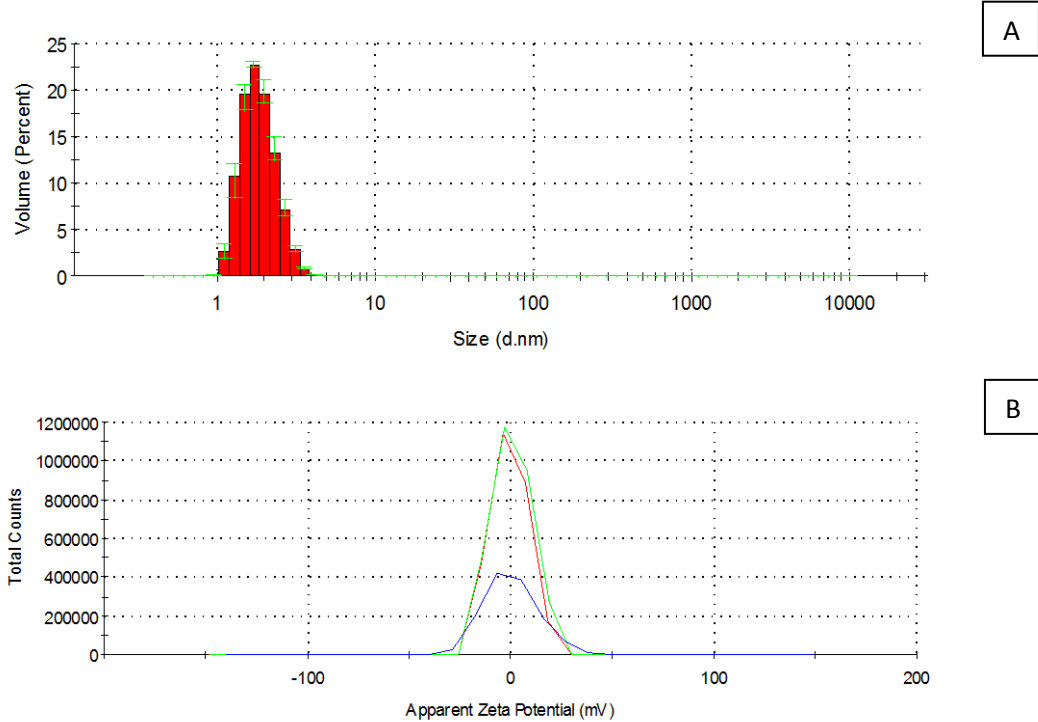


Figure 17 - Particle size distribution (A) and Zeta potential distribution (B) of sucrose stabilised (1.50 M) silicate suspensions (0.50 M) in UHP water, at pH 3.50

3.1.2. PEG

PEG is widely used for the synthesis of several functionalized nanoparticles, in some cases increasing their stability dramatically [155]. It has been reported that PEGylation can improve nanoparticles dispersity in aqueous solutions, and also that it is one of the most efficient ways to enhance their circulation, permeability and retention in biological systems [156]. A lot of studies have been done on PEGylated silica nanoparticles, and although they were mainly focused on mesoporous nanoparticles, and in general the conditions used were very different from those employed in this work, positive results have been reported [156]. Also, PEG would be a suitable stabilizer to use in a dietetic supplement since it is a typically biologically inert, non-immunogenic chemical [157].

As in the case of sucrose, different ratios of silicate:PEG were tested, while maintaining a silicate concentration of 0.50 M (Table 4). The ratio that delivered the best result was 1:2 (0.5 M of silicate and 1.0 M of PEG), those experiments were, however, restricted, since due to the solubility of PEG, it was not possible to test higher ratios while

keeping the 0.5 M of silicate. PEG stabilised silicate suspensions were stable for an average of approximately 17 days, at pH 3.5, very similar to sucrose and significantly better than the negative control, however, still far from the ideal goal for the manufacturing of a dietetic supplement.

Table 4 - Different ratios of silicate:PEG tested, and negative control (NC), at pH 3.5, and the days that each suspension remained stable.

		Compound	[Compound] (M)	pH	Stability (days)
	Silicate 0.5 M	PEG	0.5	3.50	11
			1.0		16
NC	Silicate 0.5 M			3.50	7

These suspensions were also characterized for particle size (Figure 18A), and the results showed a particle size around 900 nm, however, this result was not in concordance with the increase in stability achieved with PEG, since silicate particles this large would rapidly aggregate even further, and form a gel. The PEG stabilised silicate suspensions were then centrifuged and the particle size of the supernatant was measured, showing an average of approximately 0.86 nm (Figure 18B). This result indicates that there are very small nanoparticles in the suspension, despite the first result, which could be due to the excess of PEG forming bigger polymers, and thus preventing the machine of sizing such small particles. Next, the supernatant was analysed with ICP, to determine the fraction of silicon that corresponded to these small particles. The ICP results showed that out of the total amount of silicon in the sample, approximately 95% was in the supernatant, thus confirming that the bulk of the nanoparticles was indeed small. The zeta potential of the PEG stabilised silicate suspensions was also determined (Figure 18C), however, as in the non-stabilised silicate suspensions, it did not deliver a sharp peak, and the same result was achieved every time the DLS was repeated. This might be because, contrary to sucrose, PEG does not have a significant number of hydroxyl groups that could stabilize the charge of the nanoparticles. Some studies on silica nanoparticles report the formation of a PEG layer on the surface of the particle [158], however, if this is the case, something changed in the

long term, since eventually particle aggregation was observed. This might be due to several reasons, i.e., the polymer did not adsorb with sufficient strength to avoid displacement due to Brownian encounters, or slow dissolution of the surface layer of silica, to which the PEG chains are bound.

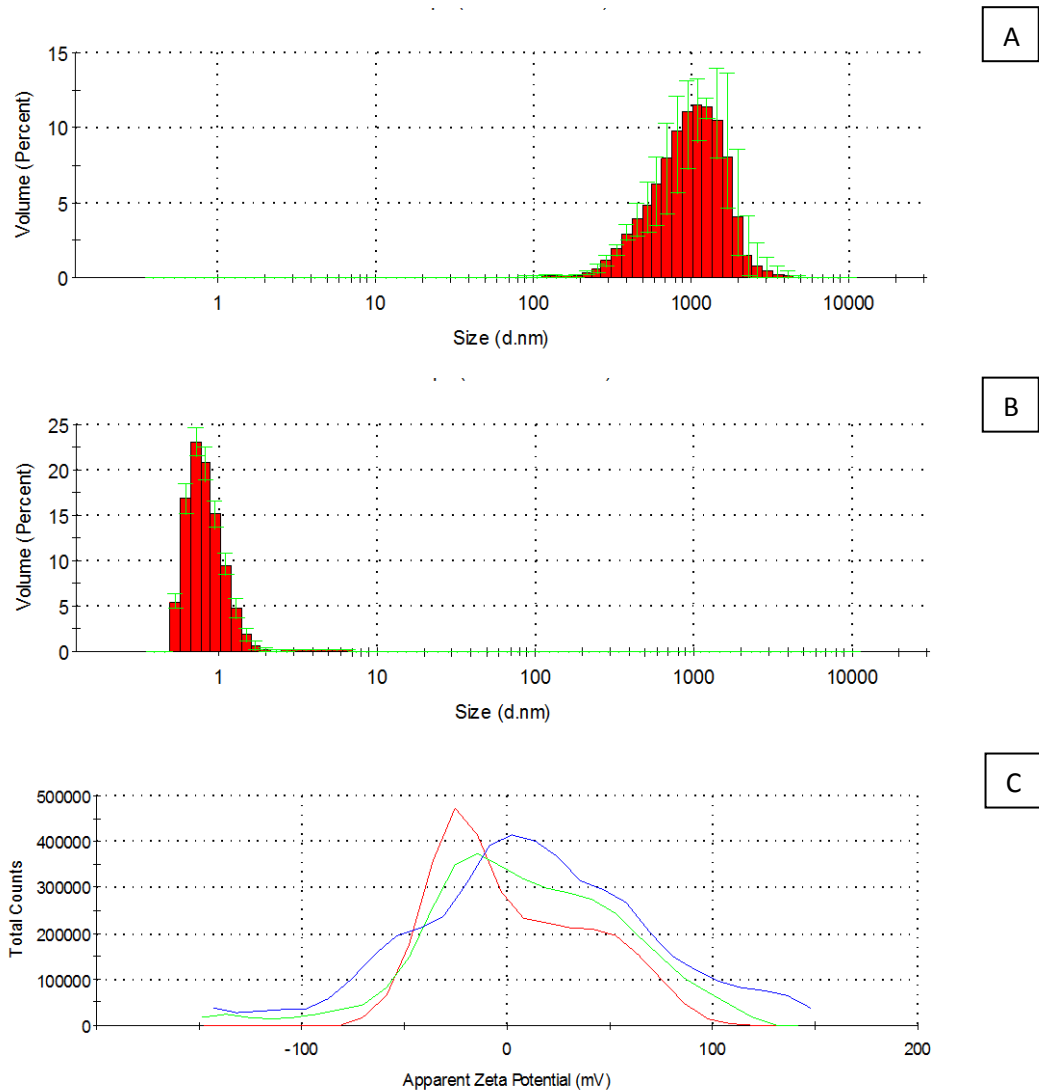


Figure 18 – Particle size distribution (A), particle size of the centrifuged fraction (B), and zeta potential (C) of the PEG stabilised (1.00 M) silicate suspension (0.50 M), at pH 3.5.

3.1.3. Sucrose and Ethanol

Another approach to improve stability of the silicate suspensions, besides using different stabilizers, would be altering the medium, which for the results discussed above

was UHP water. Fine particles dispersed in a polar matrix acquire surface charges due to ionization or dissociation of surface groups or adsorption of ions onto the surface [159]. They remain suspended in the dispersion for a long period of time due to the electrostatic repulsion between the charged surfaces [159]. It has been described in the literature that the solubility of very low concentrations of silica increases when in the presence of certain alcohols, like methanol [2]. However methanol has a high level of toxicity to humans, since it can break down into formic acid, which can cause permanent blindness, and, depending on the dose, it can be fatal, so it would not be suitable for a dietetic supplement [160]. As an alternative, ethanol was used instead, though, even ethanol, has to be used sensible, since the presence of high concentrations of alcohol in a dietetic supplement could be potentially off putting, and also, possible reactions of the organism would have to be assessed.

At first it was tested the effect of a high percentage of ethanol (40% v/v) in the stability of a silicate (0.50 M) suspension, in the absence, at pH 3.5. These suspensions were stable for 70 days and it was not possible to observe the formation of a gel, since the samples were being used at the same time for ICP analysis, and ran out before aggregation occurred. Still, 70 days is an impressive improvement when compared to the negative control, the silicate suspensions, which were stable for an average of 4 days, however, this amount of alcohol would not be suitable for the manufacturing of a dietetic supplement. Then it was tested the effect of a lower percentage of alcohol (14% v/v) in a sucrose (1.50 M) stabilised silicate (0.50 M) suspension, at pH 3.5. Those suspensions were stable for an average of 25 days, which is a slight improvement from the sucrose stabilised silicate suspensions, in UHP water, which were stable for an average of 18 days. Therefore, this clearly demonstrates that ethanol improves the silicate nanoparticles dispersion, and also, that this effect is directly proportional to the percentage of alcohol in the suspension. The later suspensions were analysed for particle size (Figure 19A) and the results show an average size of approximately 1.5 nm, with a much smaller population around 5.0 nm, slightly smaller than the particles in the sucrose stabilised silicate suspension in UHP water (approximately 2.0 nm), but the difference is not substantial, which suggest that the ethanol does not impact on the initial size of the particles. The zeta potential was also acquired (Figure 19B), and, similar to the sucrose stabilised suspension in UHP water, it is very close to 0.0 mV, so, unlike other particles in polar mediums [159], in this case the surface

of the nanoparticles did not acquire any charge, which would be beneficial, as this would improve stability.

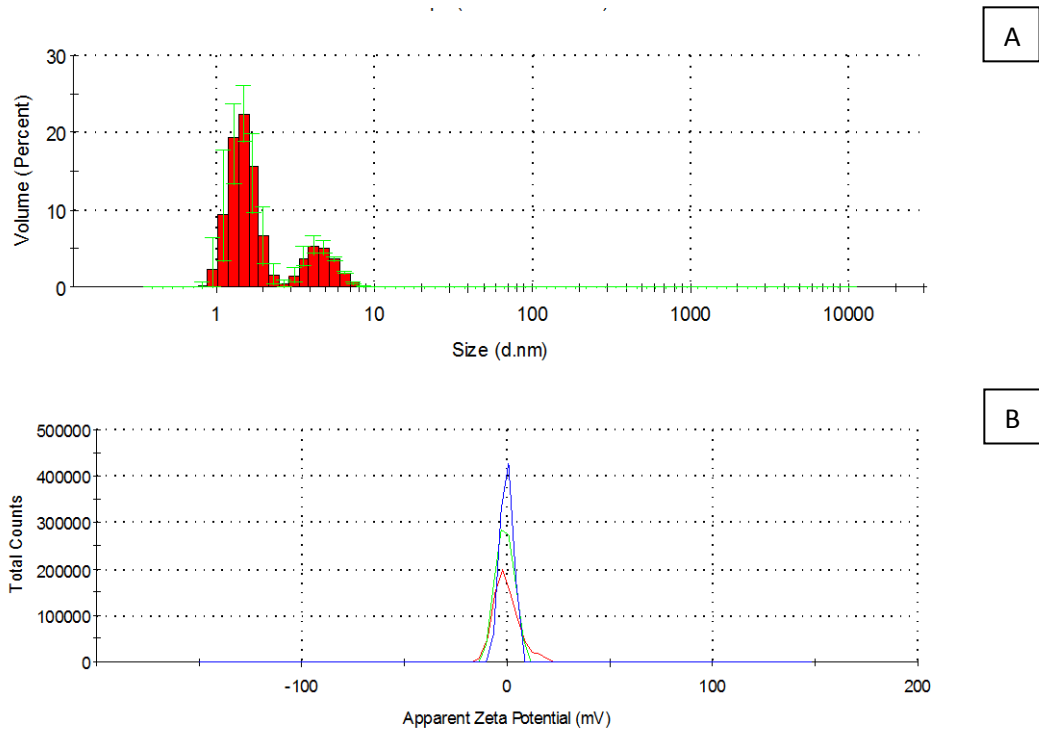


Figure 19 - Particle size distribution (A) and zeta potential distribution (B) of sucrose stabilised (1.50 M) silicate suspensions (0.50 M) in UHP water and 14% v/v EtOH, at pH 3.50

3.2. pH vs Stability

The pH range acceptable for human ingestion is quite broad [151], so, even though it was not possible to use the highly basic mediums at which silicates are very stable, it would be possible to use a pH slightly lower than 3.50, and closer to the pH range at which the silicate particles are metastable, according to the graph in Figure 2. The samples discussed above were tested from pH 1.0 to 3.5, with intervals of 0.5 and the results can be observed in Figure 20. Analysing the graph, all the samples demonstrated similar pattern and behaviour, reaching their peak of stability between pH 1.0 and 2.0, so, in concordance to the literature, which described the effect of pH in low concentrated silicate suspensions, the synthesised silicate suspensions are, also, clearly more stable at low pHs. Although at pH 3.5, the sucrose stabilised silicate suspension, in UHP water, delivered better results

than PEG, as the pH lowers the stability of the PEG stabilised suspension increases exponentially, even surpassing, at pH 2.5 and onwards, the stability of the suspensions in UHP water and ethanol. All of synthesised materials were better than the negative control, however, the PEGylated suspensions, and the sucrose stabilised suspensions in UHP water and ethanol, had a more significant improvement in stability, both reaching their maximum stability at approximately pH 1.5, being stable for 80 and 67 days respectively. Nonetheless, despite the peak in stability being observed around pH 1.5, this would be too acidic for human ingestion, so it is not desired for the manufacturing of a dietetic supplement. It would be of interest, though, to analyse more in depth the effect of a more acidic pH in the silicate suspensions properties. Therefore, pH 2.5 was chosen to serve as a comparison with pH 3.5, since, while it is still a quite acidic pH, it could possibly be implemented for the supplement. Another possibility would be manufacturing the supplement in a way, so that when to be ingested, it would be mixed with a solution that would raise its pH.

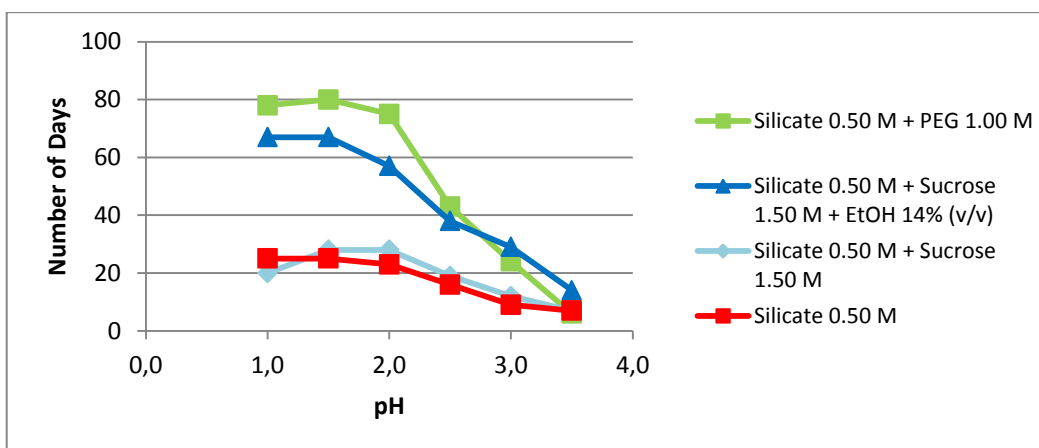


Figure 20 – Stability of silicate suspensions as a function of stabilizer and pH.

3.2. ATR-FTIR

In order to try to better understand the nature of the interactions between the stabilizers (sucrose and PEG) and the silicate particles, FTIR analysis was performed on the synthesised samples. Different backgrounds were tested for this step, those being, a mixture of UHP water, HCl and NaOH, UHP water only, and air, and although they all achieved quite similar results, the UHP water only was the background of choice.

Therefore, these are the spectrums that will be used for discussion purposes, and only the overlay is shown, however, all the singular spectrums achieved with water, and with the other backgrounds, can be seen in Appendix B.

The overlay of the ATR-FTIR transmittance spectrums of the non-stabilised silicate (0.5 M) suspension with both, a silicate (0.5 M) suspension stabilised with sucrose (1.5 M), and a sucrose (1.5 M) solution, all at pH 3.5, is shown in Figure 21. In Figure 22, an overlay is also shown for, the non-stabilised silicate suspension with a silicate (0.5 M) suspension stabilised with PEG (1.0 M), and a PEG solution (1.0 M), also at pH 3.5. In the spectra of the non-stabilised silicate suspension, the broad IR band at 1087 cm^{-1} , with a shoulder around 1190 cm^{-1} , is attributed to the TO and LO modes of the Si-O-Si asymmetric stretching vibrations. While the band at 975 cm^{-1} can be assigned to silanol groups [161].

Regarding sucrose, in the spectra of the sucrose solution alone, the sample has well resolved bands in the wavenumber range from 3000 to 2800 cm^{-1} , which may be attributed to the C-H stretching modes, and especially from 1500 to 800 cm^{-1} , in this case, the intense bands in the 1000 cm^{-1} region are due to the C-O and C-C stretch vibrations, and the broad band near 1400 cm^{-1} may be produced by the C-C-H and C-O-H deformation [162]. Additionally some negative bands, which correspond to the typical water absorption, were observed around 1600 , 3400 and 3650 cm^{-1} [163]. In the spectra of the synthesised silicate suspension stabilised with sucrose, the sucrose pattern completely dominates the outcome, and analysing the overlay of the three spectrums, it is not visible any new peak or significant change in the stabilised sample. This indicates that no bonds were formed, and although it was not expected to see the formation of strong bonds, such as covalent, it was possible that some sort of weak interaction would be occurring, however this did not verify. Therefore, the stabilizing effect of sucrose must be due exclusively to steric hindrance, preventing to some extent the silicate nanoparticles from becoming into contact with each other.

Regarding PEG, in the spectra of the PEG solution, the sample shows significant bands from 2960 to 2850 cm^{-1} , which are due to C-H stretch vibrations [164], and especially from 1500 to 880 cm^{-1} . The band from 1150 to 1000 cm^{-1} is usually assigned, in alcohols, to either the C-O stretching, or in-plane bending vibration of the C-O-H group, and in ethers to the stretching vibration of C-O-C, so all would add up to form this band,

and the region from 1450 to 1300 cm^{-1} can be assigned to scissoring and bending vibrations of C-H [164]. Similar to the spectra of the sucrose solution, some negative bands are present in the spectra of the PEG solution, and again they correspond to the typical water absorption. Analysing the spectra of the synthesised silicate suspension stabilised with PEG, and the respective overlay, it is possible to observe that the former is an addition of the non-stabilised silicate suspension spectra with the PEG solution spectra, being this particularly clear in the region from 1250 to 1150 cm^{-1} . This suggests that, similar to sucrose, there is no interaction between the silicate nanoparticles and the stabilizer, being, again, steric hindrance the most reasonable explanation for the increased stability. However, PEG provides a clear improvement when compared to the use of sucrose, especially at lower pHs, this might be because PEG, as a polymer, forms a net-like structure around the nanoparticles, due to inter and intra hydrogen bonds.

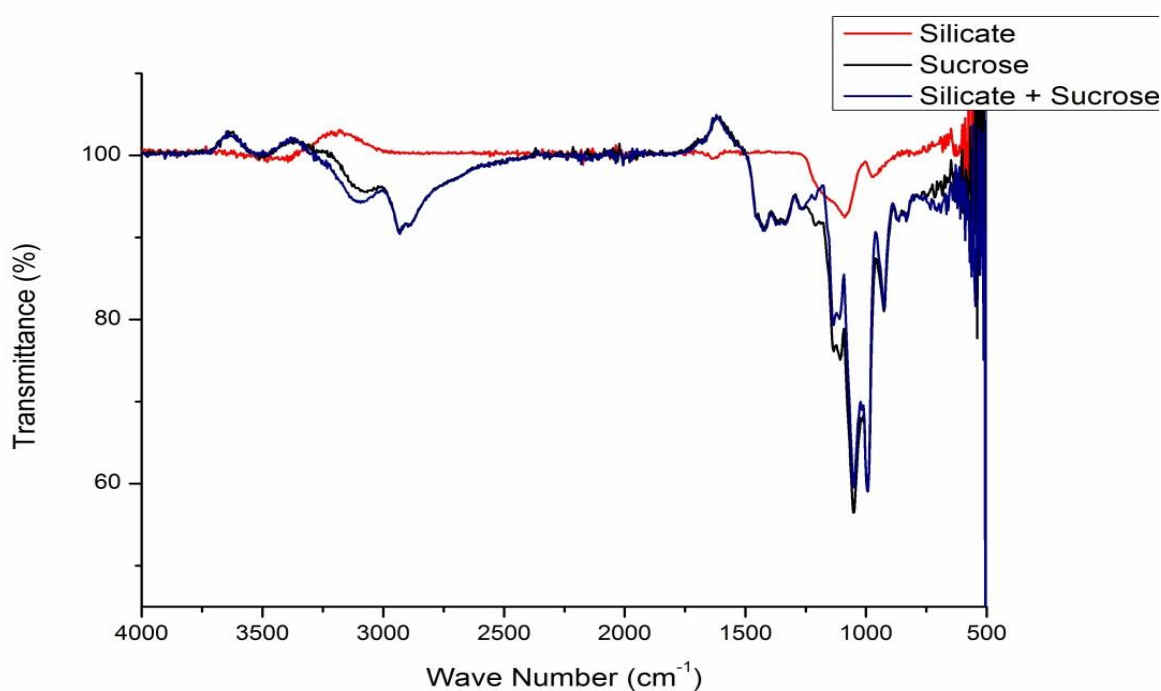


Figure 21 – Overlay of the non-stabilised silicate suspension ATR-FTIR spectra with the spectrums of a sucrose solution and a sucrose stabilised silicate suspension, all at pH 3.5.

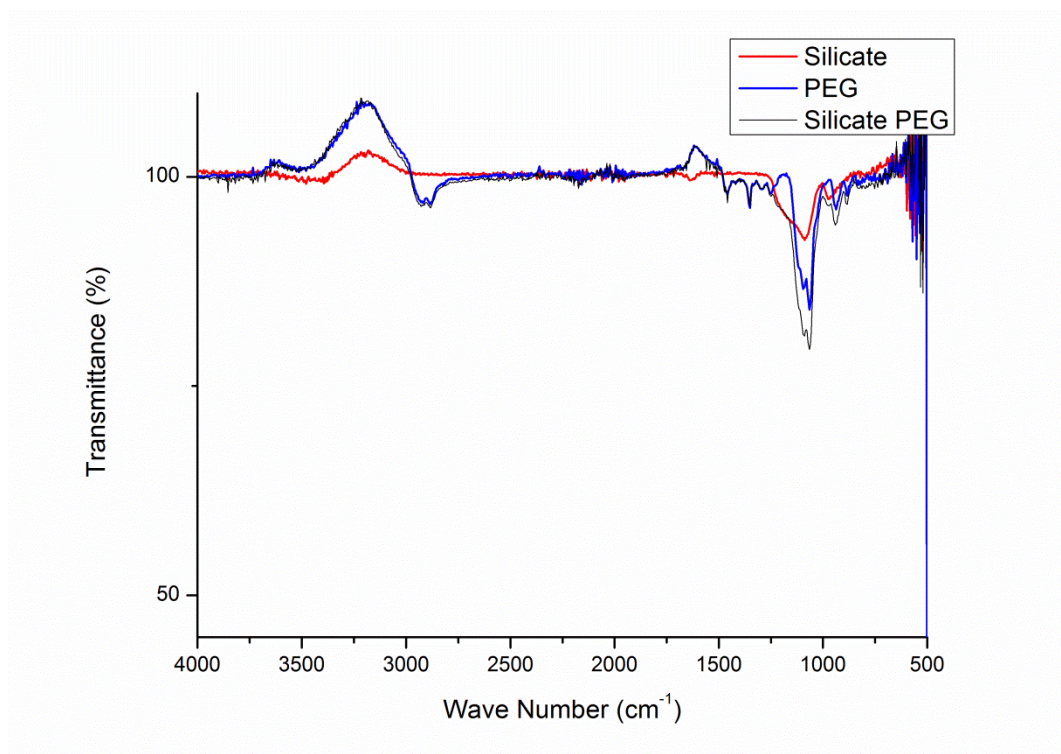


Figure 22 – Overlay of the non-stabilised silicate suspension ATR-FTIR spectra with the spectrums of a PEG solution and a PEG stabilised silicate suspension, all at pH 3.5.

3.3. Phase Distribution Over Time

The second part of the work involved the analysis of the fractions (nanoparticulate and precipitated) in the suspensions discussed in 3.1., and how they changed over time, so as to better understand the process of aggregation, and to assess which synthesised material provided an higher concentration of small nanoparticles. To study the nanoparticulate fraction, the first choice was to use 3 kDa filters, which corresponds to a particle size of approximately 1 nm, so any portion of material passing through the sieve could be considered soluble, allowing to estimate the nanoparticulate fraction in its whole. However, no significant amount of sample would come from the ultrafiltration, so 1000 kDa filters were used instead, which corresponds to a particle size around 12 nm. With these filters any material that goes through the sieve could potential not be only nanoparticulate, but also some soluble, still, it was assumed that it was all in the nanoparticulate range, due to the low solubility of silicates at these pHs. Particle size analysis was also performed through the time course, to assess if the changes in the particle

size were gradual or if there was a sudden increase at any time point. Also, all the materials were studied at pH 2.5 and 3.5, and for a maximum of 20 days if gelling did not occur.

Even though no temporal study was done in the silicate 0.5 M suspensions without stabilizer, since a gel was formed, on average, in 4 days, an ICP analysis was still performed, in samples at pH 2.5 and 3.5, to serve as comparison (Figure 23). Through the analysis of the graph, it is possible to see that the percentage of the nanoparticulate fraction, below 12 nm, is slightly higher at pH 2.5, 97.5% against 92.3% at pH 3.5, which was expected, since, as it was observed before, the suspensions are more disperse at lower pHs. However, the difference is minimal and both have a very high percentage of nano material < 12 nm, which is a positive result, as this would favour the dissolution in the gut of a big part of the nanoparticles, ingested as the supplement.

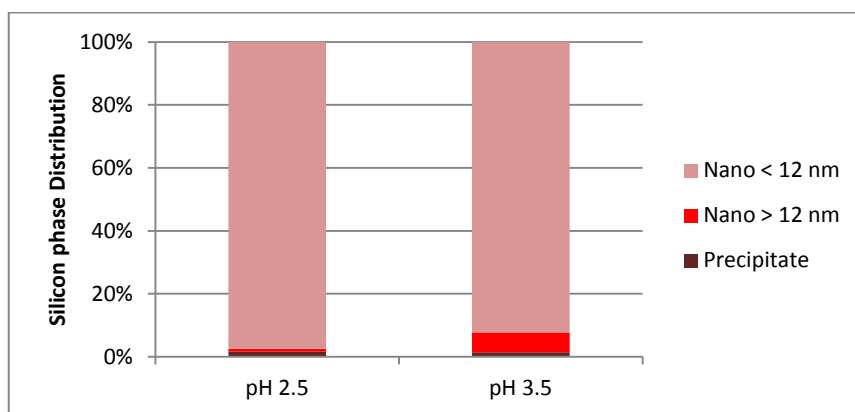


Figure 23 – Silicon phase distribution of the non-stabilised silicate suspensions, at pH 2.5 and 3.5.

3.3.1. Sucrose

As stated before, the sucrose stabilised silicate suspensions were stable for an average of 18 days, both at pH 2.5 and 3.5, therefore, the difference in pH did not seem to affect stability. However, observing the silicon phase distribution graphs, for both pHs, there is a slight improvement at pH 2.5 (Figure 24A), in which, after 5 days, the nanoparticulated fraction was still almost 80% of the suspension. Whereas at pH 3.5 (Figure 25A), according to the ICP results, there is no nanoparticles under 12 nm at the same time point. Regarding the precipitated fraction, it remained almost non-existent throughout the whole experiment, which suggests that the particles grow until a certain

size, and then create links between each other, like a net, increasing the viscosity until a gel is formed. In terms of the analysis with DLS (Figure 24B; 25B), the results show that, at both pHs, the size of the nanoparticles is always about 2.0 nm, which would be a very positive result, however it is not in concordance with the ICP results. This might be due, either to the correction that the instrument performs altering the results, or because, when doing the ultrafiltration, with the 12 kDa filters, for ICP analysis, the bigger particles clog the sieve, this way obstructing the passage of the smaller ones, already hindered due to the viscosity of the suspension.

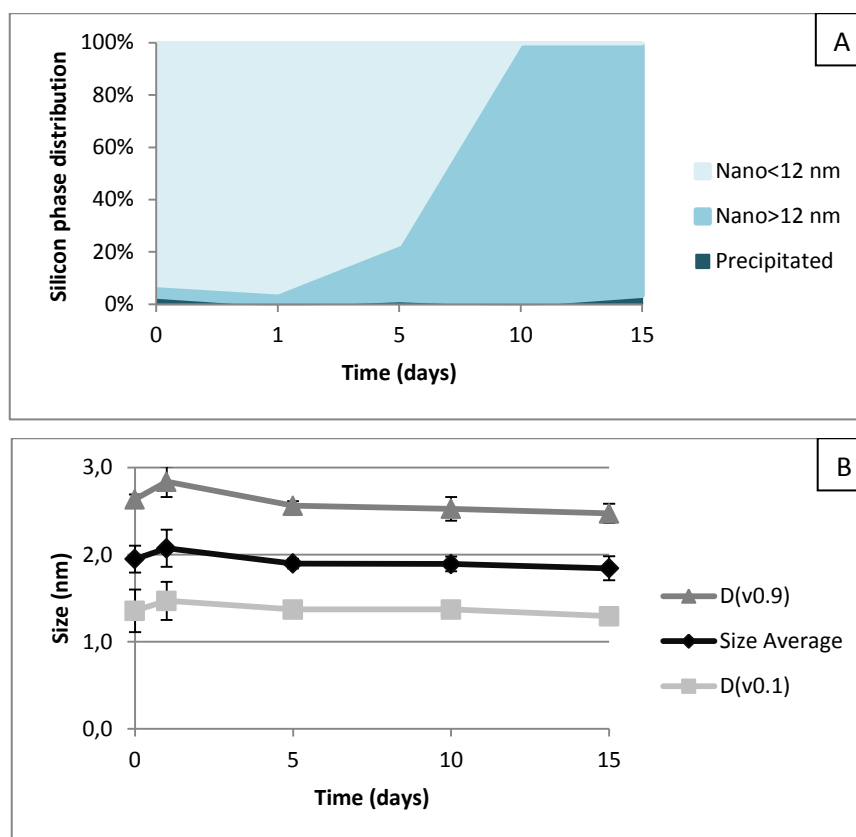


Figure 24 - Silicon phase distribution overtime of the sucrose stabilised silicate suspensions, at pH 2.5 (A), and the respective particle size analysis (B).

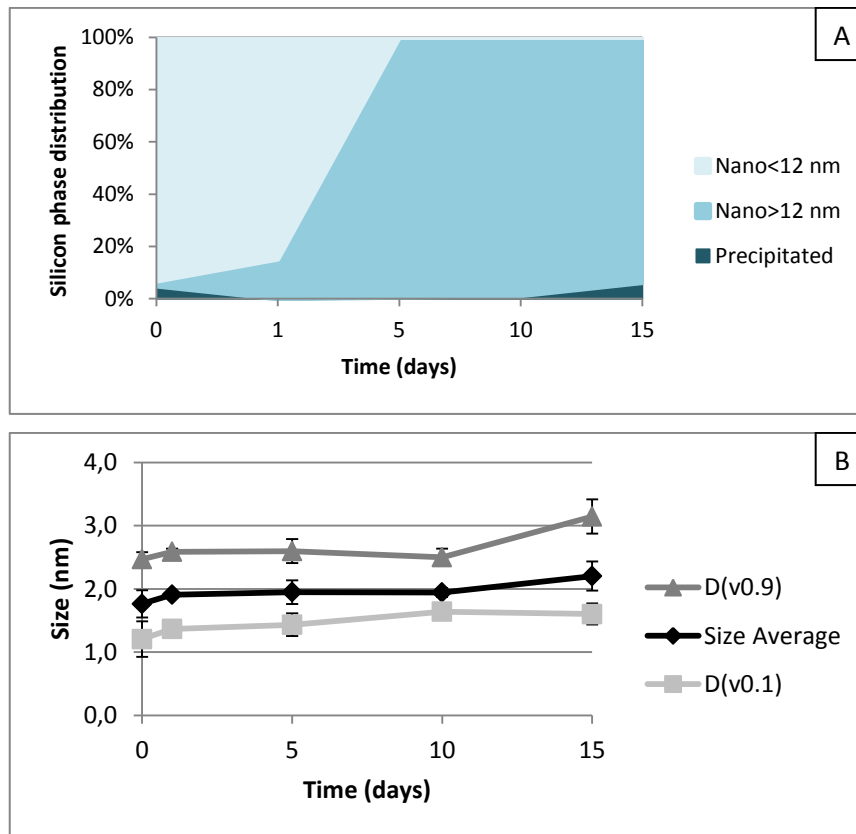


Figure 25 - Silicon phase distribution overtime of the sucrose stabilised silicate suspensions, at pH 3.5 (A), and the respective particle size analysis (B).

3.3.2. PEG

As seen in previous results, PEG stabilised silicate suspensions were clearly more stable at lower pHs than pH 3.5. Looking at the fraction analysis overtime, at pH 2.5 (Figure 26A) and 3.5 (Figure 27A), in the former, the percentage of nanoparticles under 12 nm is higher throughout the whole experiment, and it is worth mentioning that the suspension was still stable past the 20 days of analysis. The comparison of PEG and sucrose stabilised nanoparticles, at pH 2.5, showed that, immediately after synthesis, the use of sucrose resulted in a higher percentage of small nanoparticles, bordering 100%, however, those agglomerated much faster than when PEG was used. This suggests that, although in the PEG stabilised suspensions the content of really small nanoparticles is not as big as with sucrose, they remain more stable in the long term, not aggregating as fast. Similar to what was observed with sucrose as stabilizer, the precipitated fraction was

negligible, again supporting the hypothesis that the particles, instead of aggregating, form branched chains. Regarding size analysis, the DLS results show, for the suspensions at both pHs, an exponential particle growth, however, at pH 3.5 (Figure 27B), much bigger particles are formed, reaching approximately 150 nm after 15 days, while at pH 2.5 (Figure 26B), after 20 days, the particles were just on average 26 nm in diameter.

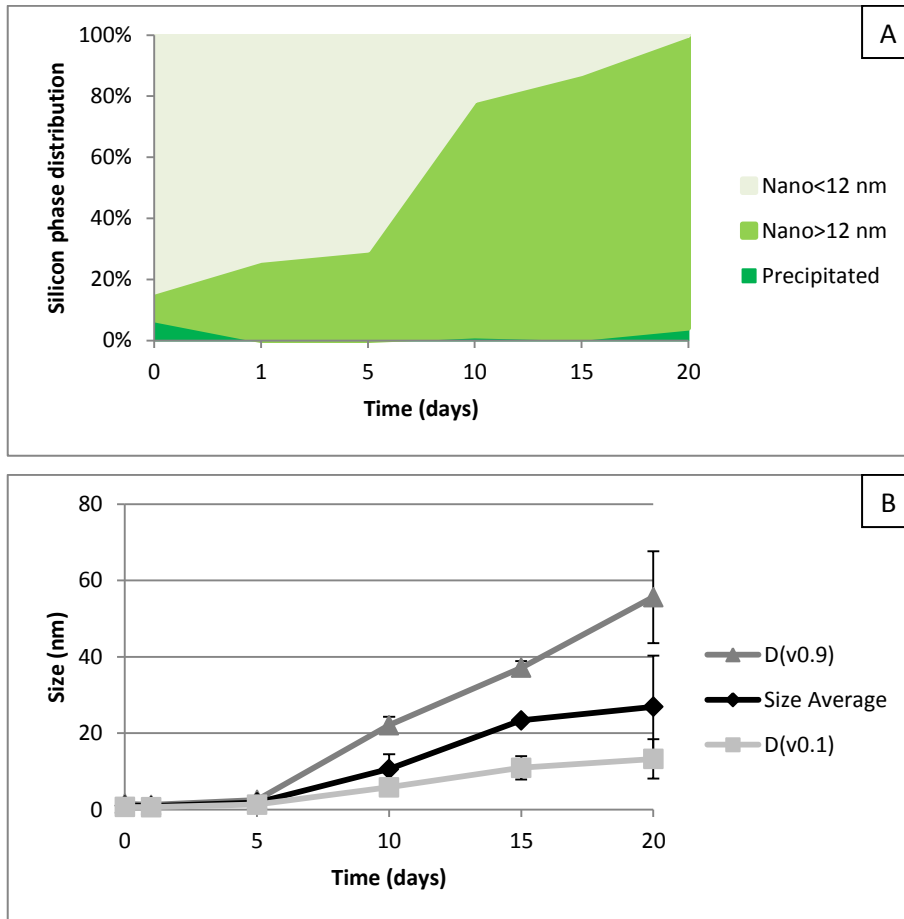


Figure 26 - Silicon phase distribution overtime of the PEG stabilised silicate suspensions, at pH 2.5 (A), and the respective particle size analysis (B).

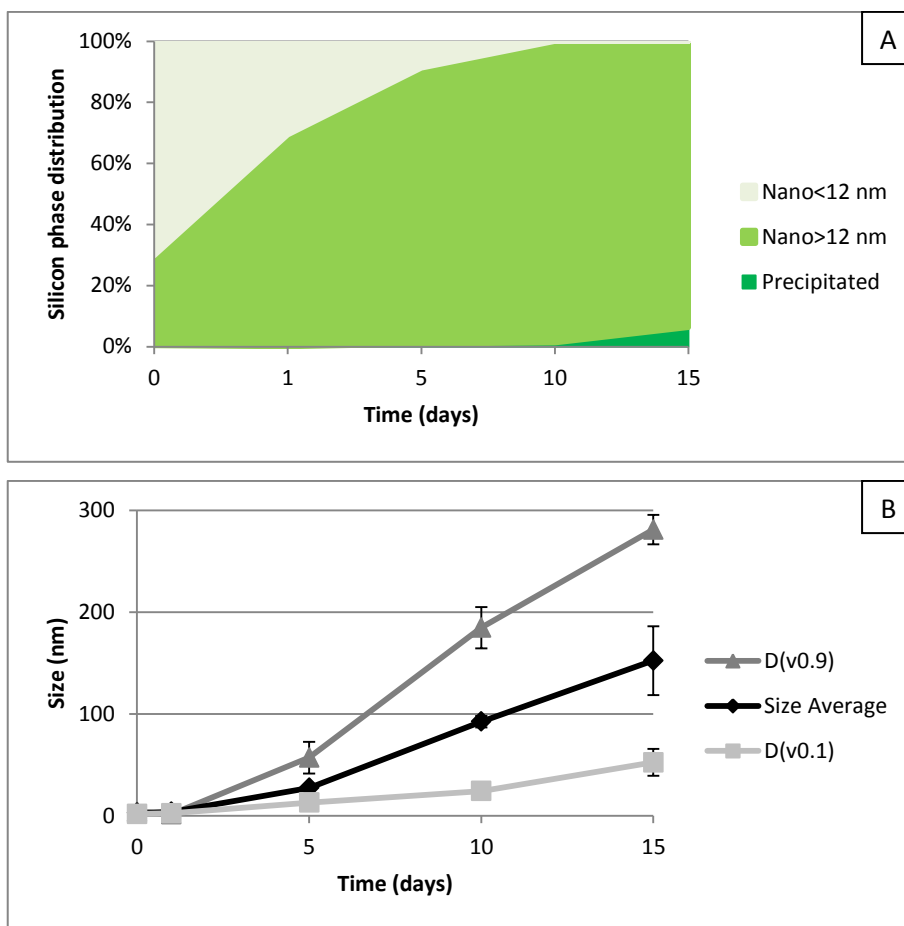


Figure 27 - Silicon phase distribution overtime of the PEG stabilised silicate suspensions, at pH 3.5 (A), and the respective particle size analysis (B).

3.3.3 Sucrose in UHP Water and Ethanol

As observed above, the addition of a small quantity of ethanol (14% EtOH v/v), to the sucrose stabilised silicate suspensions, clearly improved the stability, and the lower the pH, the more dramatic the improvement. This is definitely due to the presence of the ethanol, as in a previous experiment, where a much higher percentage of ethanol was used (40% EtOH v/v), and no stabilizer was added, the sample remained stable for more than 70 days, and the ICP analysis still showed a fraction of nanoparticulate under 12 nm around 100% after 30 days, as it can be seen in Appendix C. Looking at the graphs for the fraction analysis of the sucrose stabilised suspensions, in UHP water and ethanol, pH 2.5 (Figure 28A) and pH 3.5 (Figure 29A) delivered similar results, showing a dramatic increase in aggregation after 10 days. Also, the results for both pHs were similar to the results of the

sucrose stabilised suspensions at pH 2.5, so the addition of ethanol would allow to increase the synthesis pH without dramatically altering the outcome. Again, as in the other suspensions analysed with sucrose and PEG, the precipitated fraction was almost non-existent. Regarding the size analysis, that can be seen in Figure 28B for pH 2.5, and in Figure 29B for pH 3.5, the results were not conclusive and did not show any trend, which might be due to ethanol affecting the measurement, by altering the particles mobility in the medium. Also it is not in concordance with the ICP results, similar to the case of sucrose, since after 15 days the DLS show an average particle size of less than 4.0 nm, while, at the same time point, the ICP analysis do not show any fraction of nanoparticles under 12 nm.

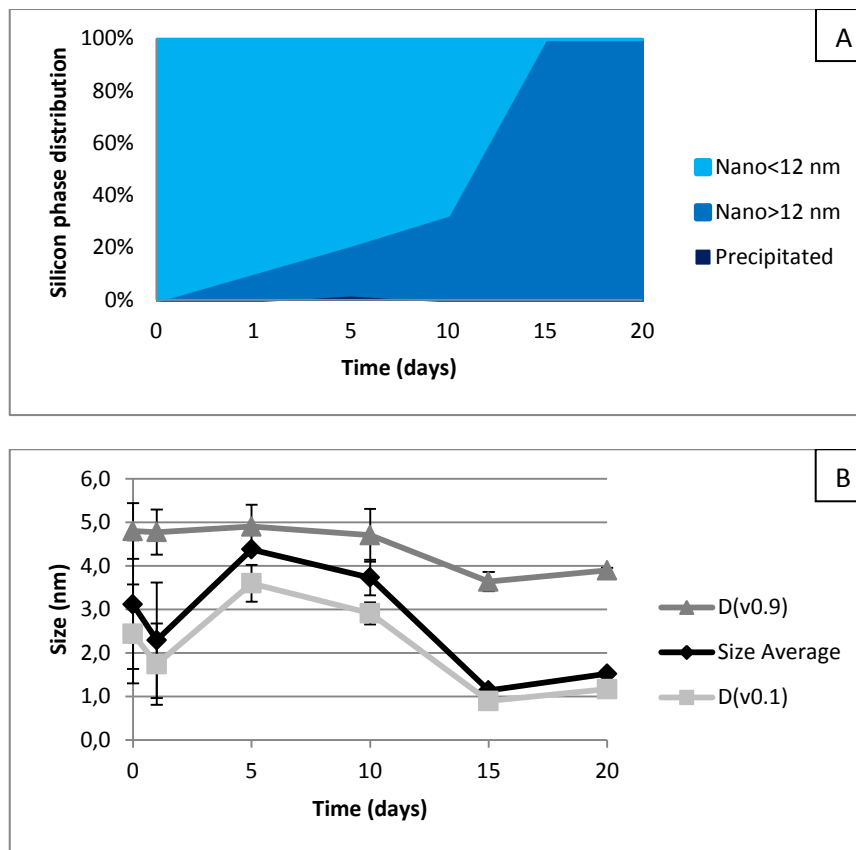


Figure 28 - Silicon phase distribution overtime of the sucrose stabilised silicate suspensions (14% EtOH v/v), at pH 2.5 (A), and the respective particle size analysis (B).

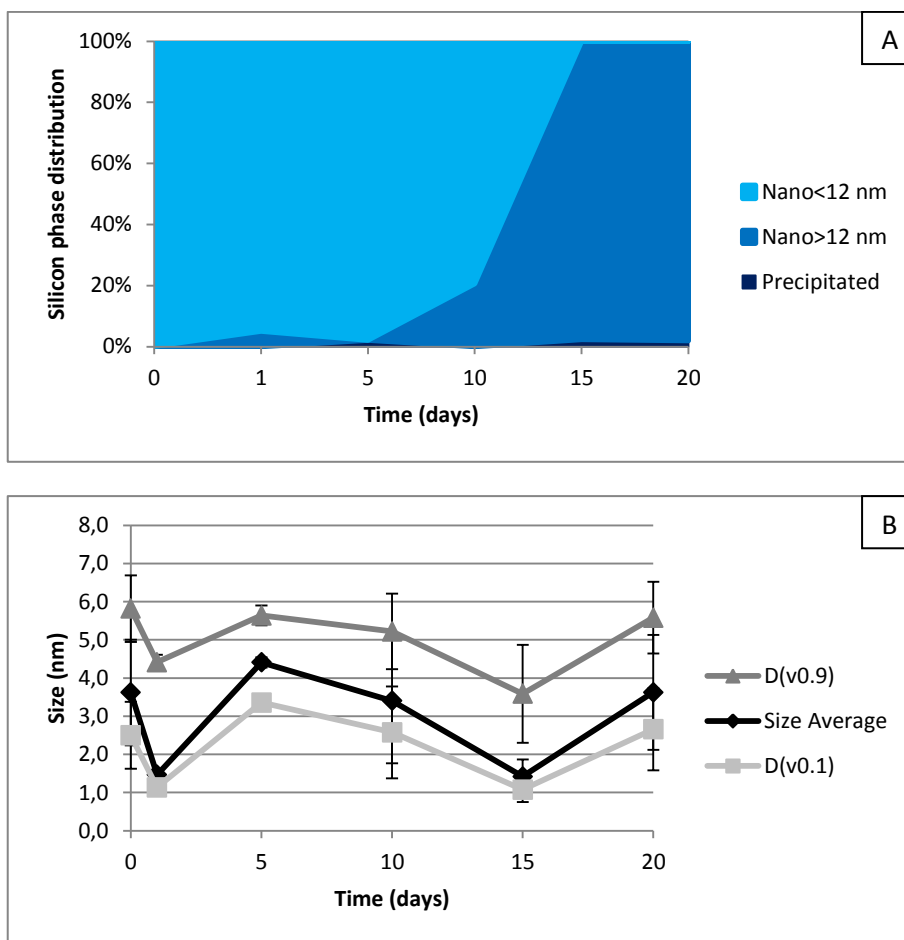


Figure 29 – Silicon phase distribution overtime of the sucrose stabilised silicate suspensions (14% EtOH v/v), at pH 3.5 (A) and the respective particle size analysis (B).

3.4. Bioavailability Assays

3.4.1. Molybdate Assay

The results from the fractions analysis over time were in general positive, since, while the suspensions were stable, they all showed high percentages of particles smaller than 12 nm. Those very small nanoparticles would in theory break into soluble silicon dioxide more easily, when diluted in the gut, which is the main goal, as the absorption in the nanoparticulate form could potential lead to toxicity issues, or the nanoparticles could not even be absorbed at all. So, the next logical step was to assess the dissolution matter, so as to try to better understand how these synthesised materials would possibly behave in biological systems.

It is well known that molybdate ions form polyanions in acidic medium, and that, in the presence of silicate ions, give rise to the formation of heteropolyoxyanions. Under acidic conditions silica reacts with the molybdate to form a yellow coloured acid, silicomolybdic acid, as it is represented in the following equations [165].

1. $SiO_2 + H_2O \rightarrow H_2SiO_3$
2. $H_2SiO_3 + 3 H_2O \rightarrow H_8SiO_6$
3. $H_8SiO_6 + 12(NH_4)_2MoO_4 + 12 H_2SO_4 \rightarrow H_8[Si(Mo_2O_7)_6] + 12 (NH_4)_2SO_4 + 12 H_2O$

This mechanism was used as the first attempt to test how the synthesised suspensions would behave when diluted, as would happen in the gut. An additional colour development, from yellow to blue, could have been used, through a reducing agent, as the heteropoly blue formed is more intense than the yellow colour of silicomolybdic acid, and, hence, a little more sensitive [165]. However, for the goal of this assay it was not needed to increase the detection limit, since the aim was only to analyse the pattern of dissolution.

The absorbance of the suspensions at 405 nm was analysed at 0, 10, 20, and 30 minutes, and the colour was allowed to develop for 10 minutes, after addition of the molybdate reagent. The results can be observed in Figure 30 for the silicate suspensions at pH 2.5 and 3.5. It is important to note that, the samples were diluted, prior to addition of the molybdate, from 0.5 M to 0.6 mM, which is a concentration below silica solubility, so the nanoparticles should dissolve. As stated in the introduction, the molybdate only reacts with soluble silica, so the concentrations on the graph do not stand for total silicon in the suspensions, only for the soluble fraction. Analysing the graph, for pH 3.5, it is possible to observe that, in all synthesised suspensions, the soluble fraction increases slightly with time, thus suggesting that dissolution is occurring and it would be reasonable to assume that the tendency would be to increase even further. At pH 3.5, the sucrose stabilised silicate suspension was the material that delivered the best result, with a maximum concentration of soluble silicon slightly above 0.15 mM. The results for the PEG stabilised silicate suspension, and for the sucrose stabilised suspension in UHP water and ethanol, were pretty much the same, the curves almost overlay perfectly. For those samples, the results were slightly worst at pH 3.5, with a maximum concentration of soluble silicon around 0.15 mM, however the same increasing pattern, as for sucrose, is observed. At pH

2.5 the increasing of soluble silicon is not as dramatic, and the best result was delivered by the silicate suspension stabilised with PEG, followed by the suspension stabilised with sucrose, in ethanol and UHP water, and finally, in contrast to pH 3.5, the silicate suspension, in UHP water, stabilised with sucrose. However, the most important thing to retain from this assay is that it suggests that, upon dilution, with all the synthesised materials, the silicate nanoparticles start to dissolve, which would be the ideal scenario for their behaviour *in vivo*.

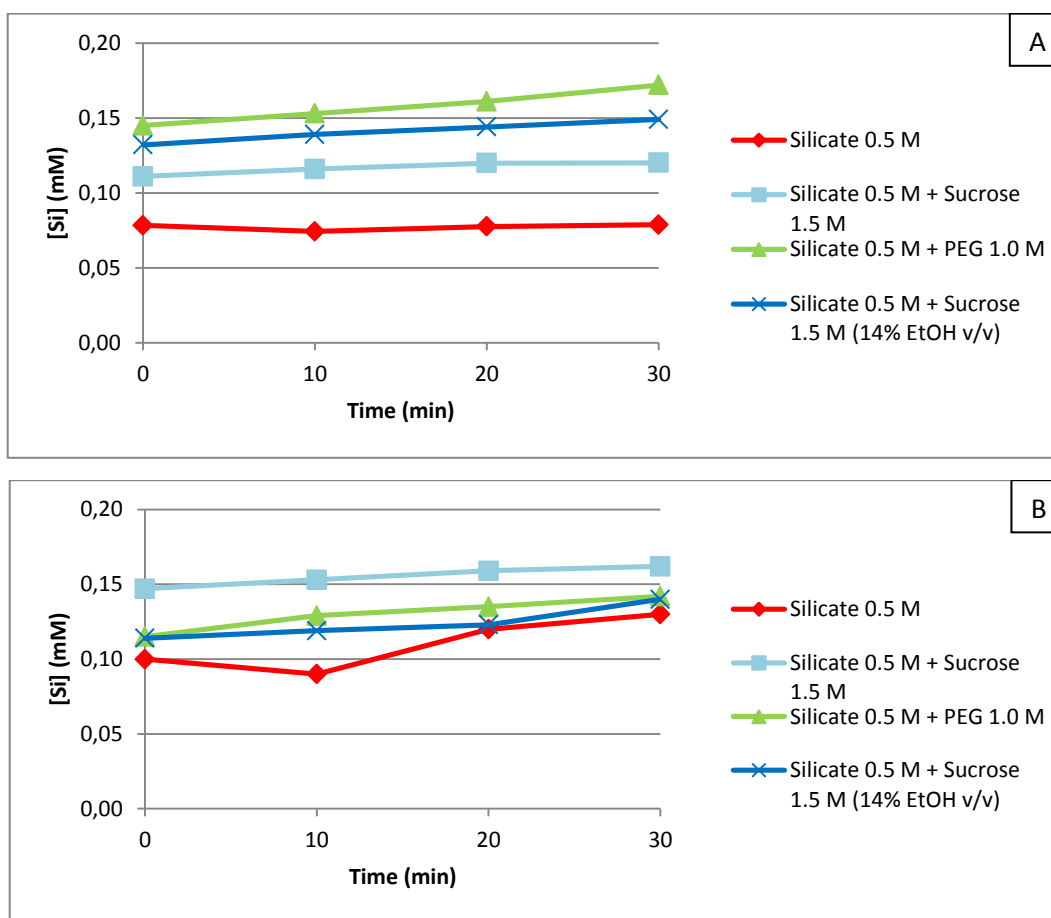


Figure 30 – Soluble silicon content in the silicate suspensions with the different stabilizers at pH 2.5 (A) and pH 3.5 (B).

3.4.2. Dissolution Assay

While the molybdate assay discussed in 3.4 provided some insight of how further dilution would affect the synthesised silicate suspensions overtime, the conditions in which the tests were made, differed too much from the conditions the suspensions would be exposed to, during digestion. Therefore, these results were not appropriate to make

assumptions about the bioavailability of the materials, which is one of the most important factors in the manufacturing of a supplement. Also, since one of the main factors that influence the molybdate analysis performance is the pH at which the silico-molybdate complex is formed, it would not be possible to establish a relation between pH 3.5 and 2.5.

In the next part of the work it was used a continuous flow *in vitro* dialysis model, that aimed to mimic the process of digestion. It consisted of two phases, one gastric stage, at pH 1.25, and one duodenal, at pH 7.0. This would provide a good first estimate of the bioavailability of the synthesised materials, without having to consider host related influences. First, it was necessary to find a suitable positive control and, since there are already some silicate supplements on the counters, it would be interesting to see how the synthesised silicate suspension would perform in comparison. Biosil seemed like the most appropriate choice, since it is also a supplement with some degree of polymerization, and there are already some studies on its bioavailability, that show that Biosil is much more bioavailable than other silicate polymerized type supplements. Also, in a particular study with the same type of dissolution assay [57], it was confirmed that the correlation between the analysed samples *in vitro*, was the same to that *in vivo*. The dissolution assay was performed first with three different concentrations of Biosil, to confirm if the amount of silicate that passed through the dialysis bag was concentration dependent. In Appendix D it is possible to see the results of this test, which confirmed that Biosil bioavailability was concentration dependent, so for the next studies it was used diluted Biosil, so that its concentration matched that of our samples.

In Figure 31 and 32 it is possible to observe the results, for the dissolution assay, of the synthesised materials, at pH 2.5 and pH 3.5, respectively, and also of the diluted Biosil. At pH 2.5 is possible to observe a pattern for all the materials tested, the total silicon content, in the mixture surrounding the dialysis bag, increases for the first 6 hours, reaching a more steady state after and until the 24 hours. However, this initial increase is more dramatic for the synthesised silicate suspensions, when compared to Biosil, particularly in the case of the silicate suspensions stabilised with PEG. Looking at the graph it is clear that the PEGylated suspensions delivered the best results, reaching concentrations of released silicon above 3.50 mM, and maintaining those from the 4 hours onwards, while the maximum achieved by Biosil, at the 24 hours mark, was 2.44 mM. At pH 3.5 it is possible to observe the same increasing pattern, as in pH 2.5, however the

difference between the synthesised suspensions and Biosil is not as pronounced, still in general they delivered slightly better results throughout the process, being the best results achieved, with the suspensions stabilised with PEG, and the suspensions stabilised with sucrose in UHP water and ethanol. At pH 3.5 none of the materials tested achieved a concentration of released silicon as higher as at pH 2.5, all staying below 2.5 mM. So the synthesised materials seem to be more bioavailable when synthesised at pH 2.5, rather than 3.5, even though at the assay starting point the samples are all at pH 1.25, this might be because the suspensions at pH 3.5 have a greater degree of polymerization to start with. In comparison to Biosil, the synthesised suspensions performed very well, at both pH's, none of them showing worst results than a supplement that is one of the staples of the silicate supplement market, staying only behind MMST, which is monomeric silica, and therefore not comparable.

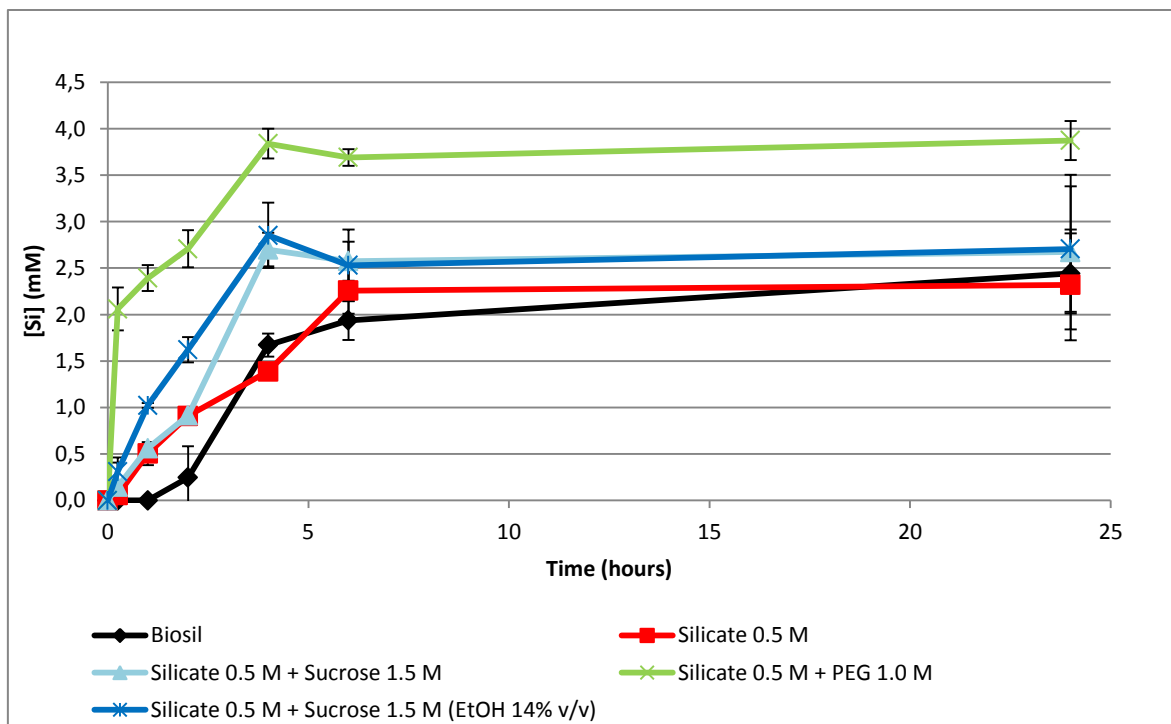


Figure 31 - Total silicon content in the mixture surrounding the dialysis bag, as a function of time, at pH 2.5

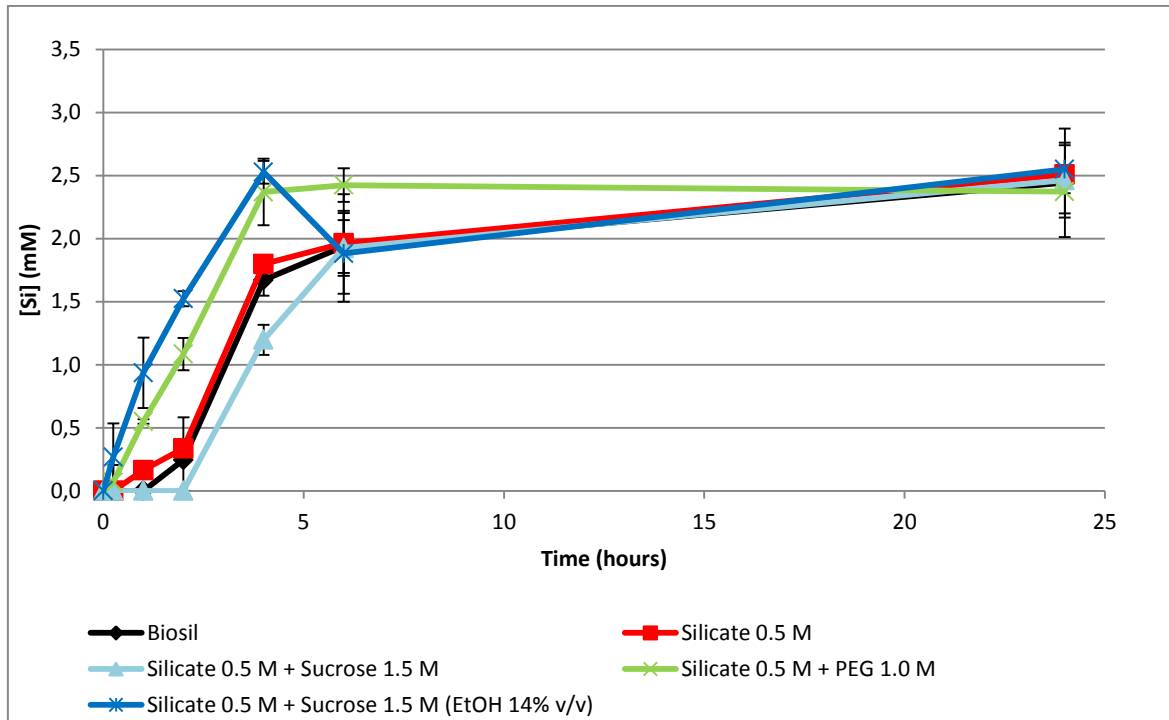


Figure 32 – Total silicon content in the mixture surrounding the dialysis bag, as a function of time at pH 3.5 (B).

Those results, however, stand for total silicon, and even though decent concentrations were achieved, if the silicate released had a high degree of polymerization, it would not be readily absorbed at the intestinal lumen. To assess this issue the mixture was also sampled for analysis with 3 kD filters, which stands for a size of less than 1 nm, so whatever goes through the sieve could be considered soluble. In Figure 33 and 34 are displayed the results achieved with the 3 kD filters, at pH 2.5 and 3.5, respectively, for the synthesised materials and diluted Biosil. Analysing the graphs it is possible to observe that there are no data until the 4 hours time point, this is because, when centrifuging the samples, only negligible content was ultra-filterable. This seems to be related to the change from pH 1.25 to pH 7.00 after two hours, suggesting that, at low concentrations, silica is more soluble under near-neutral conditions (intestinal conditions), compared with mildly acidic conditions (i.e. gastric conditions) [57]. This, however, would not affect bioavailability, if the absorption of silicon happens in the initial portion of the small intestine. After the 4 hours, at both pHs, the concentration of soluble silicon is very close to 100%, out of the total silicate released to the mixture surrounding the dialysis bag, for all the materials tested, including Biosil.

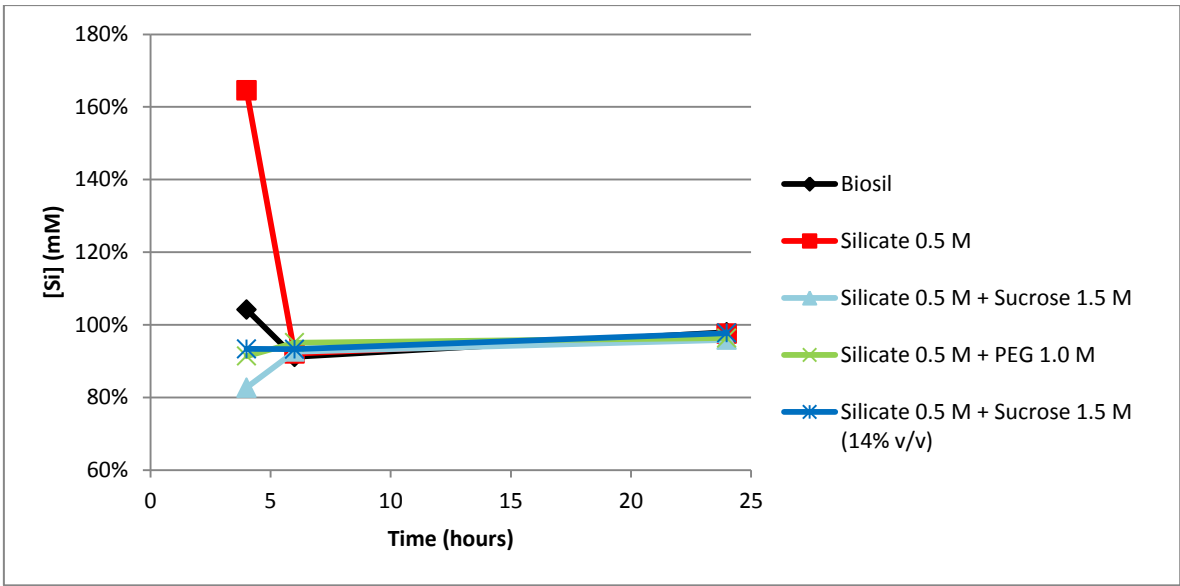


Figure 33 - Soluble silicon content in the mixture surrounding the dialysis bag, as a function of time, at pH 2.5.

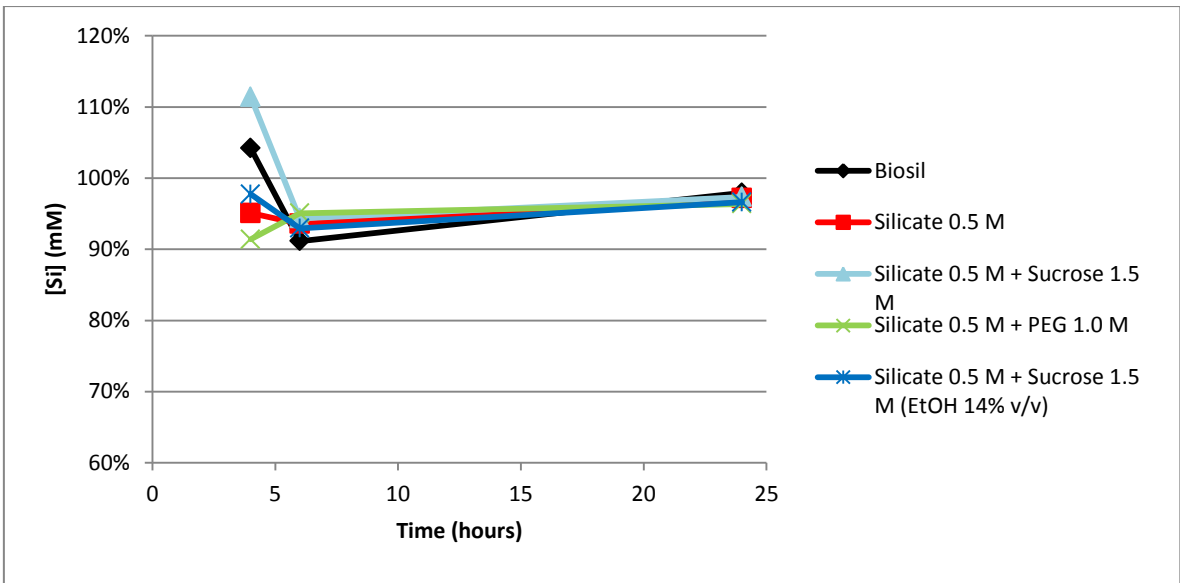


Figure 34 – Soluble silicon content in the mixture surrounding the dialysis bag, as a function of time, at pH 3.5.

Even though the content of the filtered samples could be considered soluble, so only monomeric silica, or very small polymers, would go through, the amount of exclusively monomeric silica was assessed through the molybdate assay. Since the molybdate assay is affected by pH and works better at acidic medium [165], the samples acquired after the two hours, at which the pH of the mixture in the surrounding solution is

adjusted to pH 7.0, were acidified to pH 1.25. This would allow comparison with the samples acquired before, and at the two hours, however, it could potentially affect the concentration of soluble silicon in the acidified samples, so the data after the two hours is not completely reliable. Still, given the short time that the samples are left to react, after the pH adjustment, approximately 10 minutes, it is likely that the data is near accurate. Analysing the graphs (Figure 35 for pH 2.5; Figure 36 for pH 3.5), at both pHs, the values are very close to the total content of silicon acquired through ICP. This would suggest that, if the synthesised materials behaved, *in vivo*, in a similar way as they did *in vitro*, they would provide a content of soluble silicon of about the maximum that is possible to exist in the gut, since the solubility limit of silica, at intestinal conditions, is about 2-3 mM [57]. Similar to what was observed in previous results, out of all the materials tested, the best result was delivered by the silicate suspension stabilised with PEG, at pH 2.5, reaching, at the 24 hours mark a concentration of soluble silicate of approximately 3.0 mM. The only synthesised material that falls short is the silicate suspension with no stabilizer, delivering its best result at pH 2.5, with a silicon concentration of approximately 1.5 mM, while at pH 3.5 it never rises above 1.0 mM. In Appendix E it is possible to see the graphs of each tested material, comparing the results acquired through ICP, both total and ultra-filtered silicon, with the results acquired with the molybdate assay.

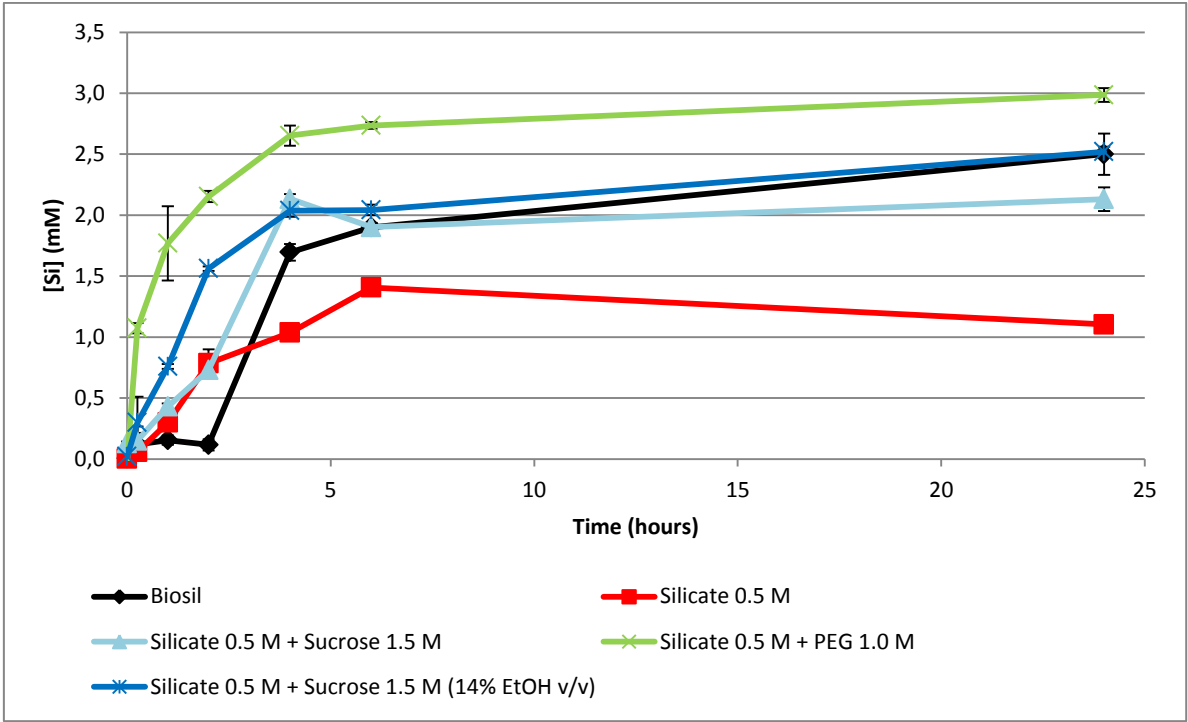


Figure 35 - Monomeric silicon concentration in the mixture surrounding the dialysis bag (acquired through the molybdate assay), as a function of time, at pH 2.5.

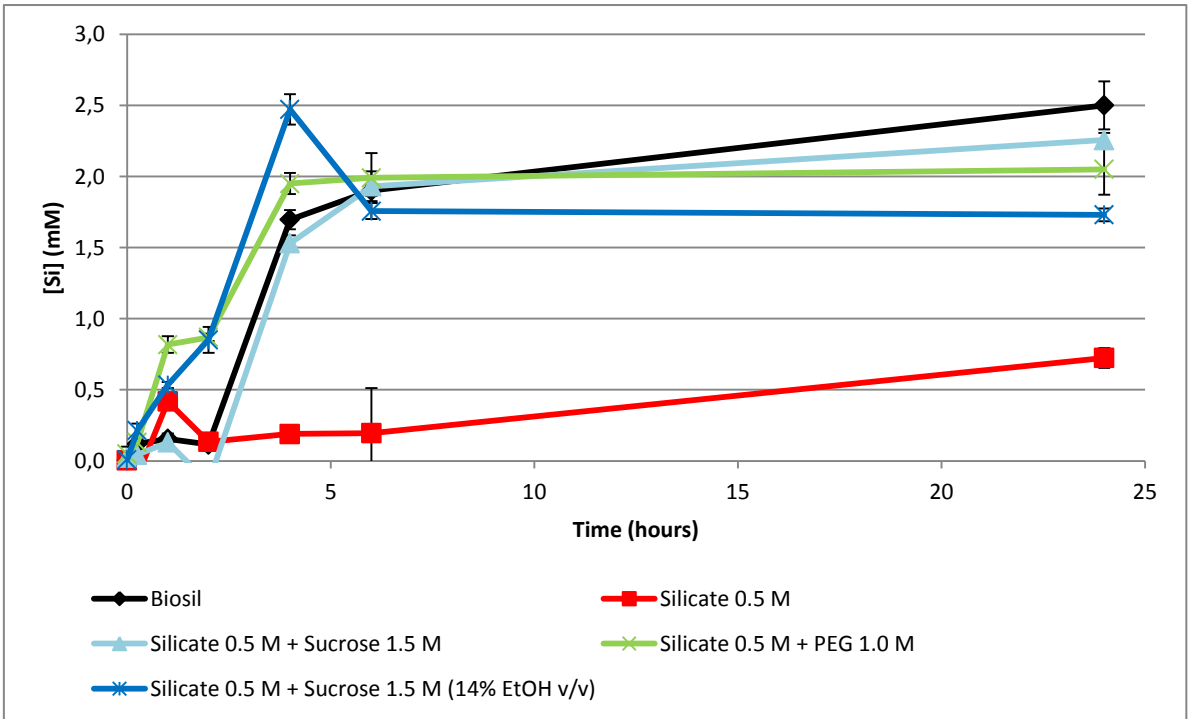


Figure 36 - Monomeric silicon content in the mixture surrounding the dialysis bag (acquired through the molybdate assay), as a function of time, at pH 3.5.

Conclusion and Future Work

4. Conclusion and Future Work

Currently there are already a few silicon supplements available in the market, however, most of them have some clear flaws, like high degree of polymerization, which will impair absorption in the gut, or the need of high daily doses, to achieve the desired silicon intake. This work was focused on the development of a new silicon supplement that may overcome some of those problems. The main strategy for this was the synthesis of colloid silicate suspensions, while attempting to prevent further polymerization of the nanoparticles through the use of surface stabilizers.

From all the systems tested and characterised, the silicate suspensions stabilised with PEG, in UHP water, and the suspensions stabilised with sucrose, in UHP water and 14% ethanol (v/v), were the ones who better improved stability overall. This was particularly evident at lower pH (pH 2.5 and lower), at which both synthesized materials reached peaks of more than 60 days stable, while the non-stabilised silicate suspension maximum was 15 days. This improvement in stability, although not completely clear, seems to be due to steric hindrance alone, in the case of the PEG stabilised suspension, while in the case of sucrose, besides the steric hindrance, the ethanol in the medium also contributed greatly to the stability. For further characterization, pH 2.5 and 3.5 were chosen, since both would be acceptable for supplement manufacturing. The synthesised nanoparticles presented desirable properties, such as a very small size (< 2 nm), and signs of some degree of depolymerisation upon dissolution, since both would be favourable for monomer formation and, therefore, increase absorption in the intestine.

When compared to an already available silicon supplement, Biosil, in a dissolution assay mimicking digestion, all the suspensions tested, performed either similar or better, being the best result achieved with the PEG stabilised silicate suspension, synthesized at pH 2.5. It had a total silicon release of more than 3.5 mM, while the soluble fraction was of approximately 3.0 mM, which is roughly the maximum possible amount of soluble silicon, at intestinal conditions. Therefore, if the suspension performed *in vivo*, the same as *in vitro*, it would have a higher bioavailability than for example Biosil, which is the most bioavailable supplement of the ones in the nanoparticulate range.

Nonetheless, although some improvement in stability and suggestion of high bioavailability was achieved, none of the suspensions were stable long enough to what

would be a reasonable shelf life for a supplement, so further changes to the process are required. Different compounds should be tested, and based on the results of this work, it would be logical to test other polymers, like PLGA, since it is one of the most successfully developed biodegradable polymers. Also, other possibilities would be to add ethanol to the medium with other stabilizers besides sucrose, or even to add small amounts of different salts, without making the suspension unstable. To further characterize, and better understand the role of the stabilizers in the suspensions, one of the techniques that could be used is SAXS, since it does not need a crystalline sample and they can be both liquid and solid, and NMR would also be a suitable technique to assess the structure of the synthesised materials. Further on, in an advanced stage, when the ideal system is achieved, the formula of the supplement would have to be tested for toxicity in human cells, first through cellular assays, then in animals and lastly in different groups of human subjects. Finally, if the tested supplement showed no detrimental side effects, bioavailability *in vivo* would have to be assessed, to see if it matched the results *in vitro*.

All in all, even though the perfect system, for a new silicon supplement, was not finalised in this work, it was successful in pointing to what might be the right direction to follow next, and, also, not least important, in ruling out, as possible stabilizers, a series of compounds. As Thomas Edison would say, I have not failed, I have successfully discovered some ways that do not work.

This page intentionally left blank.

Bibliography

6. Bibliography

1. Lewis, Richard J., Sr., *Hawley's condensed chemical dictionary (15th edition)*.
2. Cusanovich, Michael A., *The chemistry of silica (iler, ralph k.)*. Journal of Chemical Education, 1980. 57(11)
3. Carlisle, E. M., *Invivo requirement for silicon in articular-cartilage and connective-tissue formation in chick*. Journal of Nutrition, 1976. 106(4)
4. Jugdaohsingh, R., *Silicon and bone health*. Journal of Nutrition Health & Aging, 2007. 11(2)
5. Jugdaohsingh, R., M. R. Calomme, K. Robinson, F. Nielsen, S. H. C. Anderson, P. D'Haese, P. Geusens, N. Loveridge, R. P. H. Thompson, and J. J. Powell, *Increased longitudinal growth in rats on a silicon-depleted diet*. Bone, 2008. 43(3)
6. Calomme, M., J. Sindambiwe, P. Cos, C. Vyncke, P. Geusens, and D. Vanden Berghe, *Effect of choline stabilized orthosilicic acid on bone density in ovariectomized rats*. Journal of Bone and Mineral Research, 2004. 19
7. Jugdaohsingh, R., K. L. Tucker, N. Qiao, L. A. Cupples, D. P. Kiel, and J. J. Powell, *Dietary silicon intake is positively associated with bone mineral density in men and premenopausal women of the framingham offspring cohort*. Journal of Bone and Mineral Research, 2004. 19(2)
8. Dickinson, A., L. Bonci, N. Boyon, and J. C. Franco, *Dietitians use and recommend dietary supplements: Report of a survey*. Nutrition Journal, 2012. 11
9. Marra, M. V. and A. P. Boyar, *Position of the american dietetic association: Nutrient supplementation*. Journal of the American Dietetic Association, 2009. 109(12)
10. Medeiros, Denis M, *Dietary reference intakes: The essential guide to nutrient requirements*. The American Journal of Clinical Nutrition, 2007. 85(3)
11. Annenkov, V. V., E. N. Danilovtseva, Y. V. Likhoshway, S. V. Patwardhan, and C. C. Perry, *Controlled stabilisation of silicic acid below ph 9 using poly(1-vinylimidazole)*. Journal of Materials Chemistry, 2008. 18(5)
12. *The colloid chemistry of silica*. Advances in chemistry, 1994. 234(234)
13. Kauffman, George B., *Inorganic reactions and structure (gould, edwin s.)*. Journal of Chemical Education, 1962. 39(12)
14. *Index of /mingeo2010/aulas praticas/tema 2 - mineralogia/imagens cristalografia*. 24-Feb-2010 [cited 2012 28-11]; Available from: <http://geomuseu.ist.utl.pt/MINGEO2010/Aulas%20praticas/TEMA%202%20%20Mineralogia/Imagens%20Cristalografia/>
15. Bellia, J. P., J. D. Birchall, and N. B. Roberts, *Beer: A dietary source of silicon*. The Lancet, 1994. 343(8891)
16. Everett, D. H., *Symbols and terminology for physicochemical quantities and units*. International Union of Pure and Applied Chemistry, 1971
17. Derjaguin, B. V., *Theory of stability of colloids and thin films*. 1989

18. S. D. Kinrade, K. J. Maa, A. S. Schach, T. A. Sloan and C. T. G. Knight, C. T. G., 1999. *J. Chem. Soc., Dalton Trans*(3149)
19. Kinrade, S. D., E. W. Deguns, A. M. E. Gillson, and C. T. G. Knight, *Complexes of pentaoxo and hexaoxo silicon with furanoidic vicinal cis-diols in aqueous solution*. Dalton Transactions, 2003(19)
20. Jugdaohsingh, R., S. D. Kinrade, and J. J. Powell, *Is there a biochemical role for silicon?* Metal ions in biology and medicine, 2008. 10
21. Jugdaohsingh, R., S. H. C. Anderson, K. L. Tucker, H. Elliott, D. P. Kiel, R. P. H. Thompson, and J. J. Powell, *Dietary silicon intake and absorption*. American Journal of Clinical Nutrition, 2002. 75(5)
22. Schwarz, K. and D. B. Milne, *Growth-promoting effects of silicon in rats*. Nature, 1972. 239(5371)
23. Macdonald, H. M., A. E. Hardcastle, R. Jugdaohsingh, D. M. Reid, and J. J. Powell, *Dietary silicon intake is associated with bone mineral density in premenopausal women and postmenopausal women taking hrt*. Journal of Bone and Mineral Research, 2005. 20(9)
24. Keeting, Philip E., Merry Jo Oursler, Karl E. Wiegand, Susan K. Bonde, Thomas C. Spelsberg, and B. Lawrence Riggs, *Zeolite a increases proliferation, differentiation, and transforming growth factor β production in normal adult human osteoblast-like cells in vitro*. Journal of Bone and Mineral Research, 1992. 7(11)
25. Xynos, Ioannis D., Alasdair J. Edgar, Lee D. K. Buttery, Larry L. Hench, and Julia M. Polak, *Gene-expression profiling of human osteoblasts following treatment with the ionic products of bioglass® 45s5 dissolution*. Journal of Biomedical Materials Research, 2001. 55(2)
26. Carlisle, E. M., *Silicon as an essential trace-element in animal nutrition*. Ciba Foundation Symposia, 1986. 121
27. Arumugam, M. Q., D. C. Ireland, R. A. Brooks, N. Rushton, and W. Bonfield, *The effect orthosilicic acid on collagen type i, alkaline phosphatase and osteocalcin mrna expression in human bone-derived osteoblasts in vitro*. Bioceramics 18, pts 1 and 2, 2006. 309-311
28. Reffitt, D. M., N. Ogston, R. Jugdaohsingh, H. F. J. Cheung, B. A. J. Evans, R. P. H. Thompson, J. J. Powell, and G. N. Hampson, *Orthosilicic acid stimulates collagen type I synthesis and osteoblastic differentiation in human osteoblast-like cells in vitro*. Bone, 2003. 32(2)
29. Herreros, F. O. C., M. L. Cintra, R. L. Adam, A. Machado Moraes, and Konradin Metzger, *Remodeling of the human dermis after application of salicylate silanol*. Archives of Dermatological Research, 2007. 299(1)
30. Seaborn, C. D. and F. H. Nielsen, *Dietary silicon and arginine affect mineral element composition of rat femur and vertebra*. Biological Trace Element Research, 2002. 89(3)

31. Kokubo, T., H. M. Kim, M. Kawashita, and T. Nakamura, *Process of calcification on artificial materials*. Zeitschrift fuer Kardiologie, 2001. 90(Supplement 3)
32. Kubo, K., N. Tsukasa, M. Uehara, Y. Izumi, M. Ogino, M. Kitano, and T. Sueda, *Calcium and silicon from bioactive glass concerned with formation of nodules in periodontal-ligament fibroblasts in vitro*. Journal of Oral Rehabilitation, 1997. 24(1)
33. Porter, A. E., C. M. Botelho, M. A. Lopes, J. D. Santos, S. M. Best, and W. Bonfield, *Ultrastructural comparison of dissolution and apatite precipitation on hydroxyapatite and silicon-substituted hydroxyapatite in vitro and in vivo*. Journal of Biomedical Materials Research Part A, 2004. 69A(4)
34. Calomme, M. R. and D. A. VandenBerghe, *Supplementation of calves with stabilized orthosilicic acid - effect on the si, ca, mg, and p concentrations in serum and the collagen concentration in skin and cartilage*. Biological Trace Element Research, 1997. 56(2)
35. Birchall, J. D., *The essentiality of silicon in biology*. Chemical Society Reviews, 1995. 24(5)
36. Meiri, H., E. Banin, M. Roll, and A. Rousseau, *Toxic effects of aluminum on nerve-cells and synaptic transmission*. Progress in Neurobiology, 1993. 40(1)
37. Macdonald, Timothy L. and R. Bruce Martin, *Aluminum ion in biological systems*. Trends in Biochemical Sciences, 1988. 13(1)
38. Saltman, P. D. and L. G. Strause, *The role of trace minerals in osteoporosis*. Journal of the American College of Nutrition, 1993. 12(4)
39. Reid, D. M. and S. A. New, *Nutritional influences on bone mass*. Proceedings of the Nutrition Society, 1997. 56(3)
40. Jensen, Christopher, Leah Holloway, Gladys Block, Gene Spiller, Ginny Gildengorin, Erica Gunderson, Gail Butterfield, and Robert Marcus, *Long-term effects of nutrient intervention on markers of bone remodeling and calciotropic hormones in late-postmenopausal women*. The American Journal of Clinical Nutrition, 2002. 75(6)
41. Nordin, B. E. Christopher, Allan G. Need, Barry E. Chatterton, Michael Horowitz, and Howard A. Morris, *The relative contributions of age and years since menopause to postmenopausal bone loss*. Journal of Clinical Endocrinology & Metabolism, 1990. 70(1)
42. Zhou, H., A. Iida-Klein, S. S. Lu, M. Ducayen-Knowles, L. R. Levine, D. W. Dempster, and R. Lindsay, *Anabolic action of parathyroid hormone on cortical and cancellous bone differs between axial and appendicular skeletal sites in mice*. Bone, 2003. 32(5)
43. Eisinger, J and D Clairet, *Effects of silicon, fluoride, etidronate and magnesium on bone mineral density: A retrospective study*. 1993. 6(3)
44. Seaborn, C. D. and F. H. Nielsen, *Silicon deprivation decreases collagen formation in wounds and bone, and ornithine transaminase enzyme activity in liver*. Biological Trace Element Research, 2002. 89(3)

45. Calomme, M. R., P. Cos, P. C. D'Haese, R. Vingerhoets, L. V. Lamberts, M. E. De Broe, C. Van Hoorebeke, and D. A. Vanden Berghe, *Absorption of silicon in healthy subjects*. Metal ions in biology and medicine, 1998. 5
46. Bisse, E., T. Epting, A. Beil, G. Lindinger, H. Lang, and H. Wieland, *Reference values for serum silicon in adults*. Analytical Biochemistry, 2005. 337(1)
47. Jugdaohsingh, Ravin, David M Reffitt, Claire Oldham, J Phillip Day, L Keith Fifield, Richard PH Thompson, and Jonathan J Powell, *Oligomeric but not monomeric silica prevents aluminum absorption in humans*. The American Journal of Clinical Nutrition, 2000. 71(4)
48. Van Dyck, K., R. Van Cauwenbergh, H. Robberecht, and H. Deelstra, *Bioavailability of silicon from food and food supplements*. Fresenius Journal of Analytical Chemistry, 1999. 363(5-6)
49. Bellia, J. P., J. D. Birchall, and N. B. Roberts, *Beer - a dietary source of silicon*. Lancet, 1994. 343(8891)
50. Pennington, J. A. T., *Silicon in foods and diets*. Food Additives and Contaminants, 1991. 8(1)
51. Reffitt, D. M., R. Jugdaohsingh, R. P. H. Thompson, and J. J. Powell, *Silicic acid: Its gastrointestinal uptake and urinary excretion in man and effects on aluminium excretion*. Journal of Inorganic Biochemistry, 1999. 76(2)
52. Carlisle, *Silicon*. Biochemistry of the essential ultratrace elements 1984(3)
53. Bowen, H. J. M. and A. Peggs, *Determination of the silicon content of food*. Journal of the Science of Food and Agriculture, 1984. 35(11)
54. Dobbie, J. W. and M. J. B. Smith, *Urinary and serum silicon in normal and uremic individuals*. Ciba Foundation Symposia, 1986. 121
55. Cefali, E. A., J. C. Nolan, W. R. McConnell, and D. L. Walters, *Pharmacokinetic study of zeolite-a, sodium aluminosilicate, magnesium-silicate, and aluminum hydroxide in dogs*. Pharmaceutical Research, 1995. 12(2)
56. Yokoi, H and S Enomoto, *Effect of degree of polymerization of silicic acid on the gastrointestinal absorption of silicate in rats*. 1979. 27(8)
57. Sripanyakorn, S., R. Jugdaohsingh, W. Dissayabutr, S. H. C. Anderson, R. P. H. Thompson, and J. J. Powell, *The comparative absorption of silicon from different foods and food supplements*. British Journal of Nutrition, 2009. 102(6)
58. Allain, P., A. Cailleux, Y. Mauras, and J. C. Renier, *Study of silicon digestive absorption after oral ingestion of an organo silicon complex in man*. Therapie, 1983. 38(2)
59. Domingo, J. L., M. Gomez, and M. T. Colomina, *Oral silicon supplementation: An effective therapy for preventing oral aluminum absorption and retention in mammals*. Nutrition Reviews, 2011. 69(1)
60. Villa, R. T., B. Bonbonatti, L. Nakanishi, V. O. Rachel, C. Salviano, M. R. Vellasco, and V. Bedin, *Oral supplementation of silicon and its impact on quality of hair*. Journal of Investigative Dermatology, 2012. 132

61. Barel, A., M. Calomme, A. Timchenko, K. De Paepe, N. Demeester, V. Rogiers, P. Clarys, and D. Vanden Berghe, *Effect of oral intake of choline-stabilized orthosilicic acid on skin, nails and hair in women with photodamaged skin*. Archives of Dermatological Research, 2005. 297(4)
62. Schiano, A., F. Eisinger, P. Detolle, A. M. Laponche, B. Brisou, and J. Eisinger, *Silicium, bone tissue and immunity*. Revue Du Rhumatisme, 1979. 46(7-9)
63. Eisinger, J. and D. Clairet, *Effects of silicon, fluoride, etidronate and magnesium on bone mineral density: A retrospective study*. Magnesium Research, 1993. 6(3)
64. Calomme, M. R., P. Wijnen, J. B. Sindambiwe, P. Cos, J. Mertens, P. Geusens, and D. A. Vanden Berghe, *Effect of choline stabilized orthosilicic acid on bone density in chicks*. Calcified Tissue International, 2002. 70(4)
65. Spector, T. D., M. R. Calomme, S. H. Anderson, G. Clement, L. Bevan, N. Demeester, R. Swaminathan, R. Jugdaohsingh, D. A. Vanden Berghe, and J. J. Powell, *Choline-stabilized orthosilicic acid supplementation as an adjunct to calcium/vitamin d3 stimulates markers of bone formation in osteopenic females: A randomized, placebo-controlled trial*. BMC Musculoskeletal Disorders, 2008. 9
66. Barel, A., M. Calomme, A. Timchenko, K. De Paepe, N. Demeester, V. Rogiers, P. Clarys, and D. Vanden Berghe, *Effect of oral intake of choline-stabilized orthosilicic acid on skin, nails and hair in women with photodamaged skin (vol 297, 147, 2005)*. Archives of Dermatological Research, 2006. 297(10)
67. Authority, European Food Safety, *Monomethylsilanetriol added for nutritional purposes to food supplements*. The EFSA Journal, 2009. 950
68. Gioia, Lodovico Di and Marlène Jacquemont, *A process for producing water enriched with natural orthosilicic acid*. 2010.
69. Feynman, Richard, *There's plenty of room at the bottom (reprint from the speech given at the annual meeting of the west coast section of the american physical society)*. Engineering and Science, 1960. 23
70. Leary, J. F., *Nanotechnology: What is it and why is small so big?* Canadian Journal of Ophthalmology-Journal Canadien D Ophtalmologie, 2010. 45(5)
71. Lloyd, Jonathan R, James M Byrne, and Victoria S Coker, *Biotechnological synthesis of functional nanomaterials*. Current Opinion in Biotechnology, 2011. 22
72. Ju-Nam, Yon and Jamie R. Lead, *Manufactured nanoparticles: An overview of their chemistry, interactions and potential environmental implications*. Science of the Total Environment, 2008. 400(1-3)
73. Niemeyer, C. M., *Nanoparticles, proteins, and nucleic acids: Biotechnology meets materials science*. Angewandte Chemie-International Edition, 2001. 40(22)
74. Gao, Guang-Yao, Ying Chen, and X. Peter Zhang, *General synthesis of meso-amidoporphyrins via palladium-catalyzed amidation*. ChemInform, 2004. 35(40)
75. Drexler KE, Peterson C, Pergamit G., *Unbounding the future: The nanotechnology revolution*. 1991

76. Daniel, Marie-Christine and Didier Astruc, *Gold nanoparticles: Assembly, supramolecular chemistry, quantum-size-related properties, and applications toward biology, catalysis, and nanotechnology*. Chemical Reviews, 2003. 104(1)
77. Deepak, Thassu, Pathak Yashwant, and Deleers Michel, *Nanoparticulate drug-delivery systems*. Nanoparticulate drug delivery systems, 2007
78. Poole, Charles P., Frank J. Jones, and Frank J. Owens, *Introduction to nanotechnology*. 2003
79. Stark, Wendelin J., *Nanoparticles in biological systems*. Angewandte Chemie International Edition, 2011. 50(6)
80. Wuelfing, W. P., A. C. Templeton, J. F. Hicks, and R. W. Murray, *Taylor dispersion measurements of monolayer protected clusters: A physicochemical determination of nanoparticle size*. Analytical Chemistry, 1999. 71(18)
81. Hwang, Y., J. K. Lee, Y. M. Jeong, S. I. Cheong, Y. C. Ahn, and S. H. Kim, *Production and dispersion stability of nanoparticles in nanofluids*. Powder Technology, 2008. 186(2)
82. Sayes, Christie M. and David B. Warheit, *Characterization of nanomaterials for toxicity assessment*. WIREs Nanomed Nanobiotechnol 2009. 1
83. Christina Raab, Myrtil Simkó, André Gzásó, Ulrich Fiedeler, Michael Nentwich. *What are synthetic nanoparticles?* 2011; Available from: http://www.arhiv.mkgp.gov.si/fileadmin/mkgp.gov.si/pageuploads/EFSA/nov11/collected_dossiers_E.pdf.
84. Rotello, V.M., *Nanoparticles: Building blocks for nanotechnology*. 2003
85. Gong, Ping, Huimin Li, Xiaoxiao He, Kemin Wang, Jianbing Hu, Weihong Tan, Shouchun Zhang, and Xiaohai Yang, *Preparation and antibacterial activity of fe₃o₄@ag nanoparticles*. Nanotechnology, 2007. 18
86. Bärsh, Dr.-Ing. Niko. *Nanoparticle blog*. Available from: <http://nanoparticle-blog.com/>.
87. Kreuter, Jörg, *Nanoparticle-based drug delivery systems*. Journal of Controlled Release, 1991. 16(1–2)
88. Jacobson, Gunilla B, Rajesh Shinde, Christopher H Contag, and Richard N Zare, *Sustained release of drugs dispersed in polymer nanoparticles*. Angewandte Chemie, 2008. 120(41)
89. M. Vallet-Reg, F. Balas, D. Arcos, *Angew. Chem.* 2007
90. Kabanov, Alexander V and Serguei V Vinogradov, *Nanogeles als pharmazeutische trägersysteme: Winzige netzwerke mit großen möglichkeiten*. Angewandte Chemie, 2009. 121(30)
91. Musumeci, T., C. A. Ventura, I. Giannone, B. Ruozi, L. Montenegro, R. Pignatello, and G. Puglisi, *Plga nanoparticles for sustained release of docetaxel*. International Journal of Pharmaceutics, 2006. 325(1–2)
92. Lee, Jae-Hyun, Kyuri Lee, Seung Ho Moon, Yuhan Lee, Tae Gwan Park, and Jinwoo Cheon, *All-in-one target-cell-specific magnetic nanoparticles for*

- simultaneous molecular imaging and sirna delivery*. *Angewandte Chemie*, 2009. 121(23)
93. Volodkin, Dmitry V, Andre G Skirtach, and Helmuth Möhwald, *Near-ir remote release from assemblies of liposomes and nanoparticles*. *Angewandte Chemie*, 2009. 121(10)
 94. Scarberry, Kenneth E., Erin B. Dickerson, John F. McDonald, and Z. John Zhang, *Magnetic nanoparticle-peptide conjugates for in vitro and in vivo targeting and extraction of cancer cells*. *Journal of the American Chemical Society*, 2008. 130(31)
 95. Kettering, M., J. Winter, M. Zeisberger, C. Alexiou, S. Bremer-Streck, C. Bergemann, W. A. Kaiser, and I. Hilger, *Magnetisch basierte steigerung der nanopartikelaufnahme in tumorzellen: Kombination von magnetisch induzierter zellmarkierung und magnetischer wärmebehandlung*. *Fortschr Röntgenstr*, 2006. 178(12)
 96. Sondi, Ivan and Branka Salopek-Sondi, *Silver nanoparticles as antimicrobial agent: A case study on e. Coli as a model for gram-negative bacteria*. *Journal of Colloid and Interface Science*, 2004. 275(1)
 97. Nowack, Bernd and Thomas D. Bucheli, *Occurrence, behavior and effects of nanoparticles in the environment*. *Environmental Pollution*, 2007. 150(1)
 98. Jose Ruben, Morones, Elechiguerra Jose Luis, Camacho Alejandra, Holt Katherine, B. Kouri Juan, Ramírez Jose Tapia, and Yacaman Miguel Jose, *The bactericidal effect of silver nanoparticles*. *Nanotechnology*, 2005. 16(10)
 99. Chen, X. and H. J. Schluesener, *Nanosilver: A nanoparticle in medical application*. *Toxicology Letters*, 2008. 176(1)
 100. Conde, Joao, Goncalo Doria, and Pedro Baptista, *Noble metal nanoparticles applications in cancer*. *Journal of drug delivery*. 2012
 101. Taton, T. A., C. A. Mirkin, and R. L. Letsinger, *Scanometric DNA array detection with nanoparticle probes*. *Science*, 2000. 289(5485)
 102. Pathak, S., S. K. Choi, N. Arnheim, and M. E. Thompson, *Hydroxylated quantum dots as luminescent probes for in situ hybridization*. *Journal of the American Chemical Society*, 2001. 123(17)
 103. Wu, X. Y., H. J. Liu, J. Q. Liu, K. N. Haley, J. A. Treadway, J. P. Larson, N. F. Ge, F. Peale, and M. P. Bruchez, *Immunofluorescent labeling of cancer marker her2 and other cellular targets with semiconductor quantum dots*. *Nature Biotechnology*, 2003. 21(1)
 104. Liu, Wen-Tso, *Nanoparticles and their biological and environmental applications*. *Journal of Bioscience and Bioengineering*, 2006. 102(1)
 105. Das, S. K., A. R. Das, and A. K. Guha, *Gold nanoparticles: Microbial synthesis and application in water hygiene management*. *Langmuir*, 2009. 25(14)
 106. Moraru, C. I., C. P. Panchapakesan, Q. R. Huang, P. Takhistov, S. Liu, and J. L. Kokini, *Nanotechnology: A new frontier in food science*. *Food Technology*, 2003. 57(12)

107. *The relevance for food safety of applications of nanotechnology in the food and feed industries*. Food Safety Authority of Ireland, 2008
108. Powell, J. J., N. Faria, E. Thomas-McKay, and L. C. Pele, *Origin and fate of dietary nanoparticles and microparticles in the gastrointestinal tract*. Journal of Autoimmunity, 2010. 34(3)
109. Kalgaonkar, S. and B. Lonnerdal, *Receptor-mediated uptake of ferritin-bound iron by human intestinal caco-2 cells*. Journal of Nutritional Biochemistry, 2009. 20(4)
110. Seifert, J. and W. Sass, *Intestinal-absorption of macromolecules and small particles*. Digestive Diseases, 1990. 8(3)
111. Beier, R. and A. Gebert, *Kinetics of particle uptake in the domes of peyer's patches*. American Journal of Physiology-Gastrointestinal and Liver Physiology, 1998. 275(1)
112. Bockmann, J., H. Lahl, T. Eckhert, and B. Unterhalt, *Blood levels of titanium before and after oral administration of titanium dioxide*. Pharmazie, 2000. 55(2)
113. Volkheimer, G., *Passage of particles through the wall of the gastro intestinal tract*. Environmental Health Perspectives, 1974. 9
114. Hillyer, J. F. and R. M. Albrecht, *Gastrointestinal persorption and tissue distribution of differently sized colloidal gold nanoparticles*. Journal of Pharmaceutical Sciences, 2001. 90(12)
115. Powell, J. J., M. W. Whitehead, S. Lee, and R. P. H. Thompson, *Mechanisms of gastrointestinal absorption - dietary minerals and the influence of beverage ingestion*. Food Chemistry, 1994. 51(4)
116. Moyes, S. M., S. H. Smyth, A. Shipman, S. Long, J. F. Morris, and K. E. Carr, *Parameters influencing intestinal epithelial permeability and microparticle uptake in vitro*. International Journal of Pharmaceutics, 2007. 337(1-2)
117. AshaRani, P. V., G. L. K. Mun, M. P. Hande, and S. Valiyaveetil, *Cytotoxicity and genotoxicity of silver nanoparticles in human cells*. Acs Nano, 2009. 3(2)
118. Richter, S. *Nanoparticles in food supplements – a fast and reliable method based on an international standard*. Available from: http://www.emc2012.org.uk//documents/Abstracts/Abstracts/EMC2012_0103.pdf.
119. Brunner, Tobias J., Peter Wick, Pius Manser, Philipp Spohn, Robert N. Grass, Ludwig K. Limbach, Arie Bruinink, and Wendelin J. Stark, *In vitro cytotoxicity of oxide nanoparticles: Comparison to asbestos, silica, and the effect of particle solubility†*. Environmental Science & Technology, 2006. 40(14)
120. Auffan, Mélanie, Jérôme Rose, Mark R. Wiesner, and Jean-Yves Bottero, *Chemical stability of metallic nanoparticles: A parameter controlling their potential cellular toxicity in vitro*. Environmental Pollution, 2009. 157(4)
121. Teow, Y., P. V. Asharani, M. P. Hande, and S. Valiyaveetil, *Health impact and safety of engineered nanomaterials*. Chemical Communications, 2011. 47(25)
122. Goodman, C. M., C. D. McCusker, T. Yilmaz, and V. M. Rotello, *Toxicity of gold nanoparticles functionalized with cationic and anionic side chains*. Bioconjugate Chemistry, 2004. 15(4)

123. Pavesi, L., L. Dal Negro, C. Mazzoleni, G. Franzo, and F. Priolo, *Optical gain in silicon nanocrystals*. Nature, 2000. 408(6811)
124. Ding, Zhifeng, Bernadette M. Quinn, Santosh K. Haram, Lindsay E. Pell, Brian A. Korgel, and Allen J. Bard, *Electrochemistry and electrogenerated chemiluminescence from silicon nanocrystal quantum dots*. Science, 2002. 296(5571)
125. Kang, Z. H., Y. Liu, and S. T. Lee, *Small-sized silicon nanoparticles: New nanolights and nanocatalysts*. Nanoscale, 2011. 3(3)
126. Canham, L. T., *Silicon quantum wire array fabrication by electrochemical and chemical dissolution of wafers*. Applied Physics Letters, 1990. 57(10)
127. Stewart, M. P. and J. M. Buriak, *Chemical and biological applications of porous silicon technology*. Advanced Materials, 2000. 12(12)
128. Y. Wei, L. M. Fan and L. R. Chen, *Chromatographia*. 1997
129. Mathew, Joice P. and M. Srinivasan, *Silica-supported polymer-palladium complexes as catalysts for the reduction of nitro and azo groups*. Polymer International, 1992. 29(3)
130. García, Monserrat, Werner E. van Zyl, Mattijs G. J. ten Cate, Jan W. Stouwdam, Henk Verweij, Makarand S. Pimplapure, and Günter Weickert, *Novel preparation of hybrid polypropylene/silica nanocomposites in a slurry-phase polymerization reactor*. Industrial & Engineering Chemistry Research, 2003. 42(16)
131. Stafford, C. M., A. Y. Fadeev, T. P. Russell, and T. J. McCarthy, *Controlled adsorption of end-functionalized polystyrene to silicon-supported tris(trimethylsiloxy)silyl monolayers*. Langmuir, 2001. 17(21)
132. Yu, Yang-Yen and Wen-Chang Chen, *Transparent organic-inorganic hybrid thin films prepared from acrylic polymer and aqueous monodispersed colloidal silica*. Materials Chemistry and Physics, 2003. 82(2)
133. Arquier, D., G. Calleja, G. Cerveau, and R. J. P. Corriu, *A new solution route for the synthesis of silicon nanoparticles presenting different surface substituents*. Comptes Rendus Chimie, 2007. 10(9)
134. Tan, W. H., K. M. Wang, X. X. He, X. J. Zhao, T. Drake, L. Wang, and R. P. Bagwe, *Bionanotechnology based on silica nanoparticles*. Medicinal Research Reviews, 2004. 24(5)
135. Shekunov, B. Y., P. Chattopadhyay, H. H. Y. Tong, and A. H. L. Chow, *Particle size analysis in pharmaceuticals: Principles, methods and applications*. Pharmaceutical Research, 2007. 24(2)
136. Berne, B.J.; Pecora, R, *Dynamic light scattering*. 2000
137. W. Brown, T. Nicolai, *Dynamic light scattering*. 1993
138. Alexander, Marcela and Douglas G. Dalgleish, *Dynamic light scattering techniques and their applications in food science*. Food Biophysics, 2006. 1(1)
139. *Malvern instruments technical note, dynamic light scattering : An introduction in 30 minutes*.

140. *Dynamic light scattering*. 2012 28-10-2012; Available from: http://en.wikipedia.org/wiki/Dynamic_light_scattering.
141. *Colloidal dynamics tutorial, the zeta potential*. Electroacoustics Tutorials, 1999
142. Malvern, *Malvern instruments technical note, zeta potential: An introduction in 30 minutes*.
143. Hauptkorn, S., J. Pavel, and H. Seltner, *Determination of silicon in biological samples by icp-oes after non-oxidative decomposition under alkaline conditions*. Fresenius Journal of Analytical Chemistry, 2001. 370(2-3)
144. Manning, Thomas J. and William R. Grow, *Inductively coupled plasma - atomic emission spectrometry*. The Chemical Educator, 1997. 2(1)
145. (UCD), Kevin Vo. *Spectrophotometry* 2011; Available from: <file:///E:/Tese/Artigos%2013/Spectrophotometry.htm>.
146. *Spectrophotometry absorption measurements & their application to quantitative analysis*. Chemistry 111 Lab: Intro to Spectrophotometry 2005 2-12-2012]; Available from: http://employees.oneonta.edu/kotzjc/LAB/Spec_intro.pdf.
147. Kwan, Kermit, *The role of penetrant structure on the transport and mechanical properties of a thermoset adhesive*. 1998
148. Pillai, Karthikeyan Chyan Oliver Ming-Ren. *Ftir-atr characterization of hydrogel, polymer films, protein immobilization and benzotriazole adsorption on copper surface*. 2007; Available from: <http://digital.library.unt.edu/permalink/meta-dc-5132>.
149. Halasz, I., M. Agarwal, R. B. Li, and N. Miller, *What can vibrational spectroscopy tell about the structure of dissolved sodium silicates?* Microporous and Mesoporous Materials, 2010. 135(1-3)
150. Howell, John M., *Alkaline ingestions*. Annals of Emergency Medicine, 1986. 15(7)
151. nutrition, US FDA - Center for food safety and applied. *Approximate ph of foods and food products* 23/10/2008; Available from: <http://www.foodscience.caes.uga.edu/extension/documents/fdaapproximatephoffoodslacf-phs.pdf>.
152. Lambert, J. B., G. Lu, S. R. Singer, and V. M. Kolb, *Silicate complexes of sugars in aqueous solution*. Journal of the American Chemical Society, 2004. 126(31)
153. Zhang, L. H., L. J. J. Catalan, R. J. Balec, A. C. Larsen, H. H. Esmaili, and S. D. Kinrade, *Effects of saccharide set retarders on the hydration of ordinary portland cement and pure tricalcium silicate*. Journal of the American Ceramic Society, 2010. 93(1)
154. Kinrade, S. D., R. J. Hamilton, A. S. Schach, and C. T. G. Knight, *Aqueous hypervalent silicon complexes with aliphatic sugar acids*. Journal of the Chemical Society-Dalton Transactions, 2001(7)
155. Manson, J., D. Kumar, B. J. Meenan, and D. Dixon, *Polyethylene glycol functionalized gold nanoparticles: The influence of capping density on stability in various media*. Gold Bulletin, 2011. 44(2)

156. Zhu, Y. F., Y. Fang, L. Borchardt, and S. Kaskel, *Pegylated hollow mesoporous silica nanoparticles as potential drug delivery vehicles*. *Microporous and Mesoporous Materials*, 2011. 141(1-3)
157. *Polyethylene glycol (peg) and pegylation of proteins*. Protein Methods Library; Available from: <http://www.piercenet.com/browse.cfm?fldID=12D97D8D-5056-8A76-4E95-9EA0D0B54BDB>.
158. Zhang, Z. K., A. E. Berns, S. Willbold, and J. Buitenhuis, *Synthesis of poly(ethylene glycol) (peg)-grafted colloidal silica particles with improved stability in aqueous solvents*. *Journal of Colloid and Interface Science*, 2007. 310(2)
159. Ghosh, S. K., S. Deguchi, S. A. Mukai, and K. Tsujii, *Supercritical ethanol - a fascinating dispersion medium for silica nanoparticles*. *Journal of Physical Chemistry B*, 2007. 111(28)
160. Cursiefen, C. and A. Bergua, *Acute bilateral blindness caused by accidental methanol intoxication during fire "eating"*. *British Journal of Ophthalmology*, 2002. 86(9)
161. Music, S., N. Filipovic-Vincekovic, and L. Sekovanic, *Precipitation of amorphous sio2 particles and their properties*. *Brazilian Journal of Chemical Engineering*, 2011. 28(1)
162. Max, J. J. and C. Chapados, *Sucrose hydrates in aqueous solution by ir spectroscopy*. *Journal of Physical Chemistry A*, 2001. 105(47)
163. Garrigues, J. M., M. Akssira, F. J. Rambla, S. Garrigues, and M. de la Guardia, *Direct atr-ftir determination of sucrose in beet rest*. *Talanta*, 2000. 51(2)
164. Rozenberg, M., A. Loewenschuss, and Y. Marcus, *Ir spectra and hydration of short-chain polyethyleneglycols*. *Spectrochimica Acta Part a-Molecular and Biomolecular Spectroscopy*, 1998. 54(12)
165. *Silica*. Handbook of environmental analysis, 1997

Appendix

This page intentionally left blank.

Appendix A – Compounds Tested As Stabilizers

Table A. 1 – Table of all the compounds tested as possible stabilizers and respective system characteristics.

	Stabilizer 1	[Stabilizer 1] M	Stabilizer 2	[Stabilizer 2] M	Stabilizer 3	[Stabilizer 3] M	Acid	Base	pH _f	Number of days stable
Silicate 0.5 M	Sucrose	0.50					HCl	NaOH	3.50	8
		1.00				10				
		1.50				17				
	Sucrose	1.50	Calcium	0.050			HCl	NaOH	3.50	2
				0.10		2				
				0.25		2				
	Sucrose	1.50	Calcium	0.10			HCl	Na ₂ CO ₃	3.50	18
										18
	Maltose	0.50					HCl	NaOH	3.50	12
		1.00				12				
		1.50				16				
	SDS	0.40					HCl	NaOH	3.50	<1
	Polyacrylic Acid	0.50					HCl	NaOH	3.50	4
		1.00				8				
	PEG	0.50					HCl	NaOH	3.50	11
		1.00				16				
Sucrose	1.50					Citric Acid	NaOH	3.50	7	
Gallic Acid	0.06					HCl	NaOH	3.50	1	
Polypropylene Glycol	1.50					HCl	NaOH	3.50	6	
Ethylene Glycol		6								

² Precipitation occurs as soon as NaOH is added.

Silicate 0.5 M	Sucrose	1.50	Calcium	0.20			HCl	Na ₂ CO ₃	3.50	18
				0.20						13
	Sucrose	1.50		0.5						18
				0.5						15
			Copper	0.2						4
				0.5						6
	Sucrose	1.50	Calcium	0.25			HCl	Na ₂ CO ₃	<1	16
				0.5						12
				1						12
				2						³
	Sucrose	1.50	Ethanol				HCl	NaOH	3.50	14
	Carnitine	0.05					HCl	NaOH	3.50	1
		0.10				1				
		0.50				<1				
	Sucrose	1.50	Calcium	0.25	Gluconate	0.125	HCl		3.50	1
						0.25				1
	Sucrose	1.50				0.25				1
						0.25				1
	Sucrose	1.50	Gluconate	0.125			HCl		3.80	1
				0.25						1
Sucrose	1.50	Calcium	0.25	Citrate	0.125	HCl		3.50	1	
					0.25				1	
Sucrose	1.50				0.25				1	
					0.25				1	
Silicate 1.0 M	Sucrose	1,00				HCl	NaOH	3.50	3	
		2,00							6	
		3,00							7	
	Maltose	1,00							3	

³ Calcium did not dissolve.

Appendix B – ATR-FTIR Spectrums

Background – UHP Water

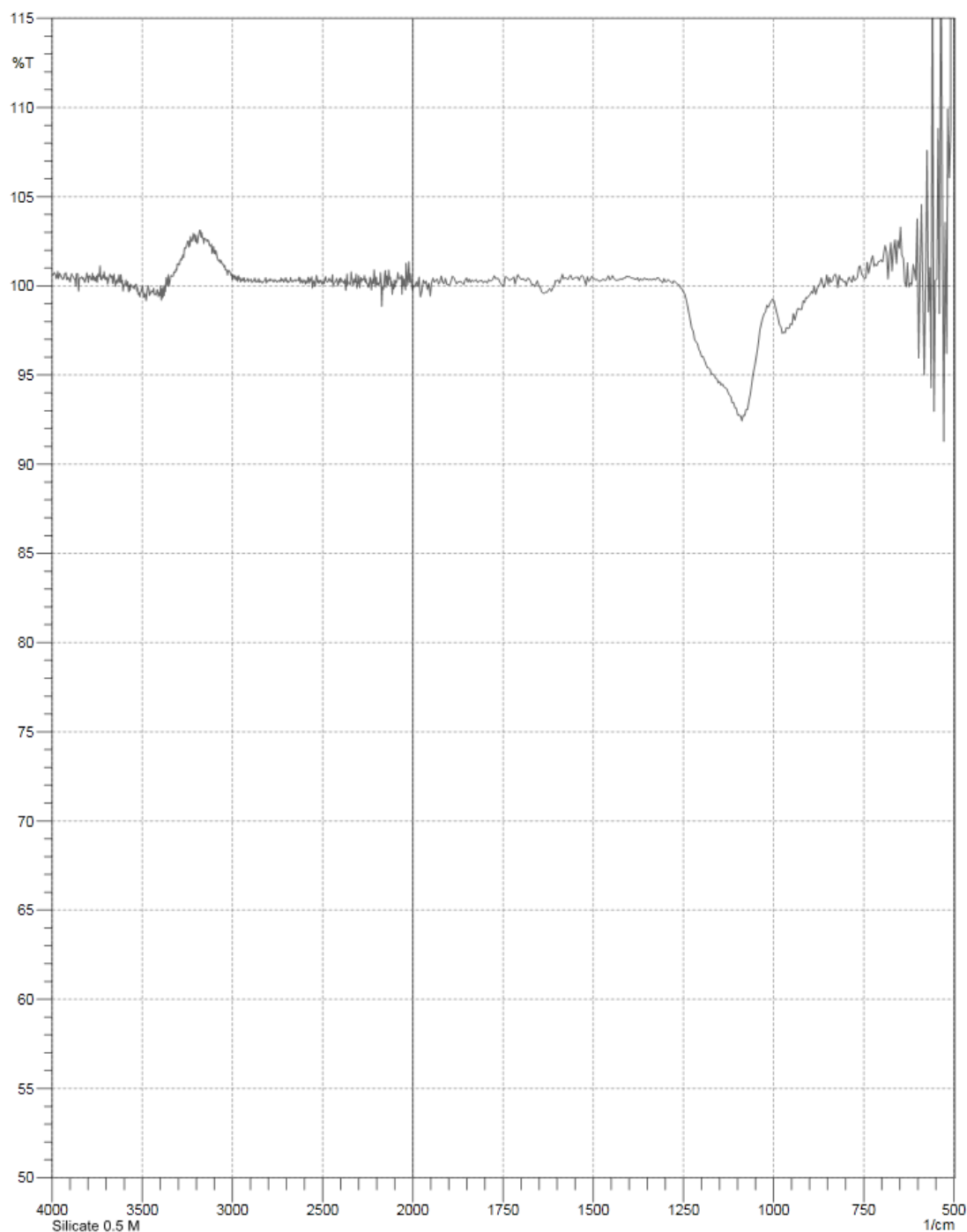


Figure B. 1 – ATR-FTIR spectra of the non-stabilised silicate suspension, at pH 3.5, using water as background.

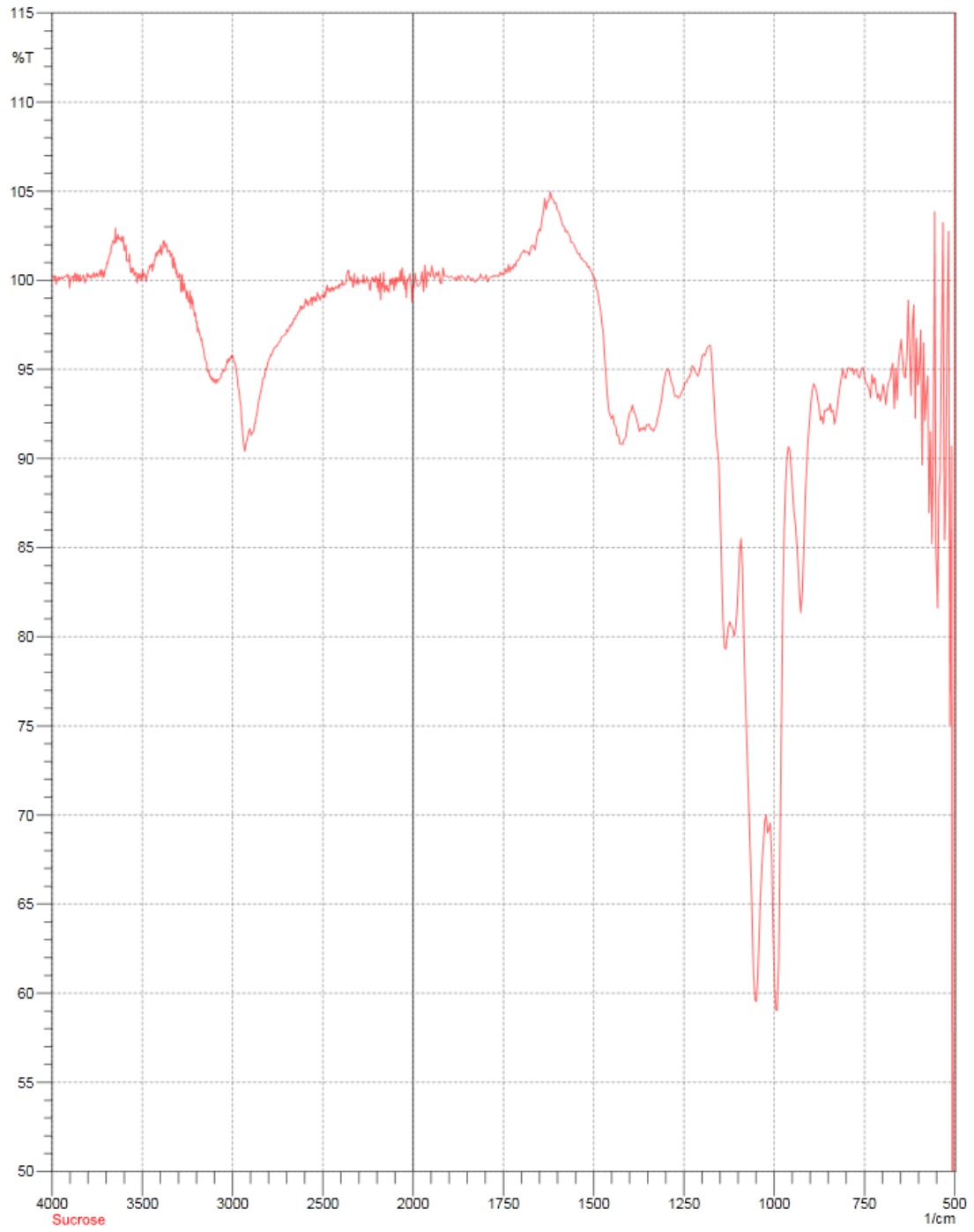


Figure B. 2 – ATR-FTIR spectra of a sucrose solution, at pH 3.5, using water as background.

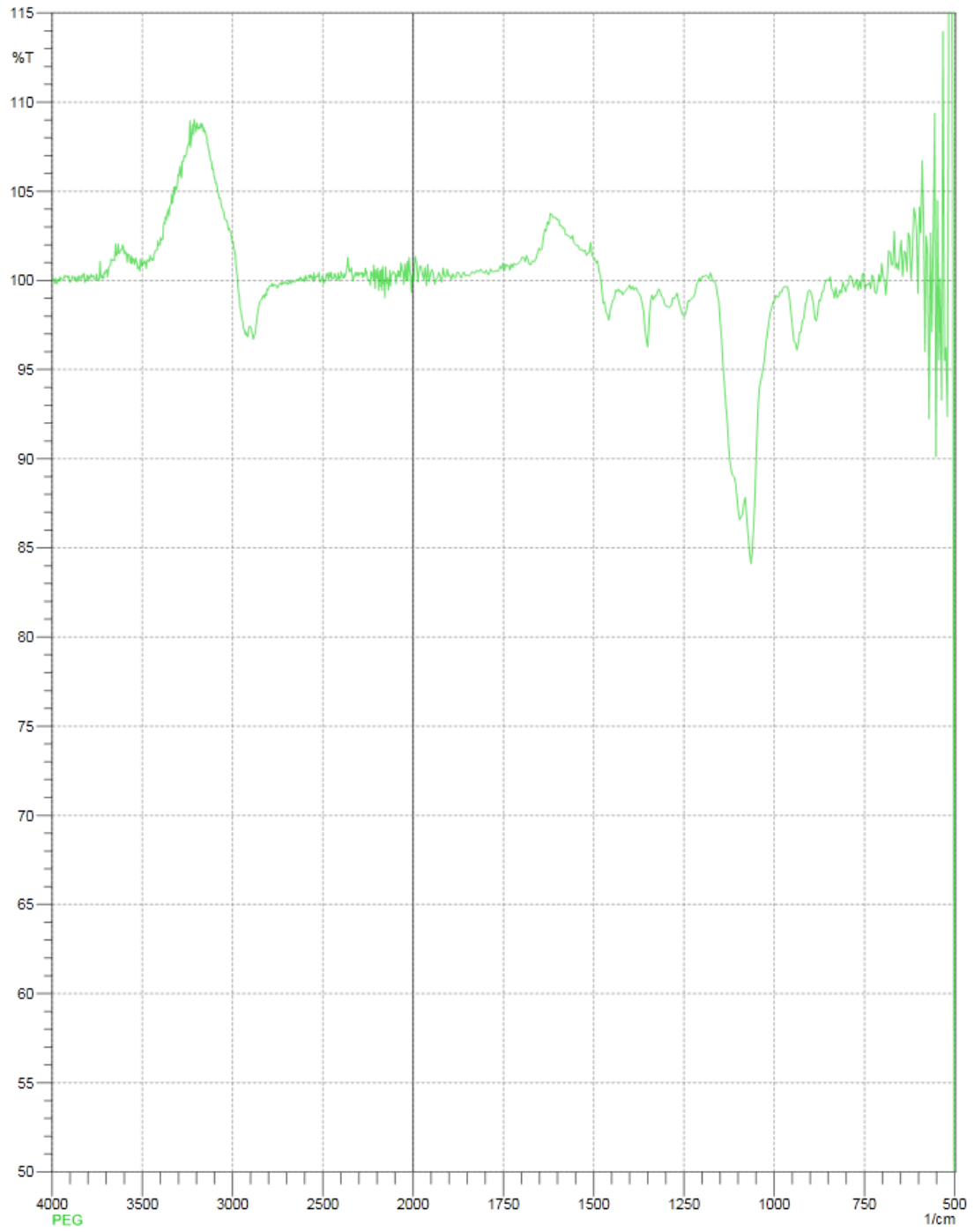


Figure B. 3 - ATR-FTIR spectra of a PEG solution, at pH 3.5, using water as background.

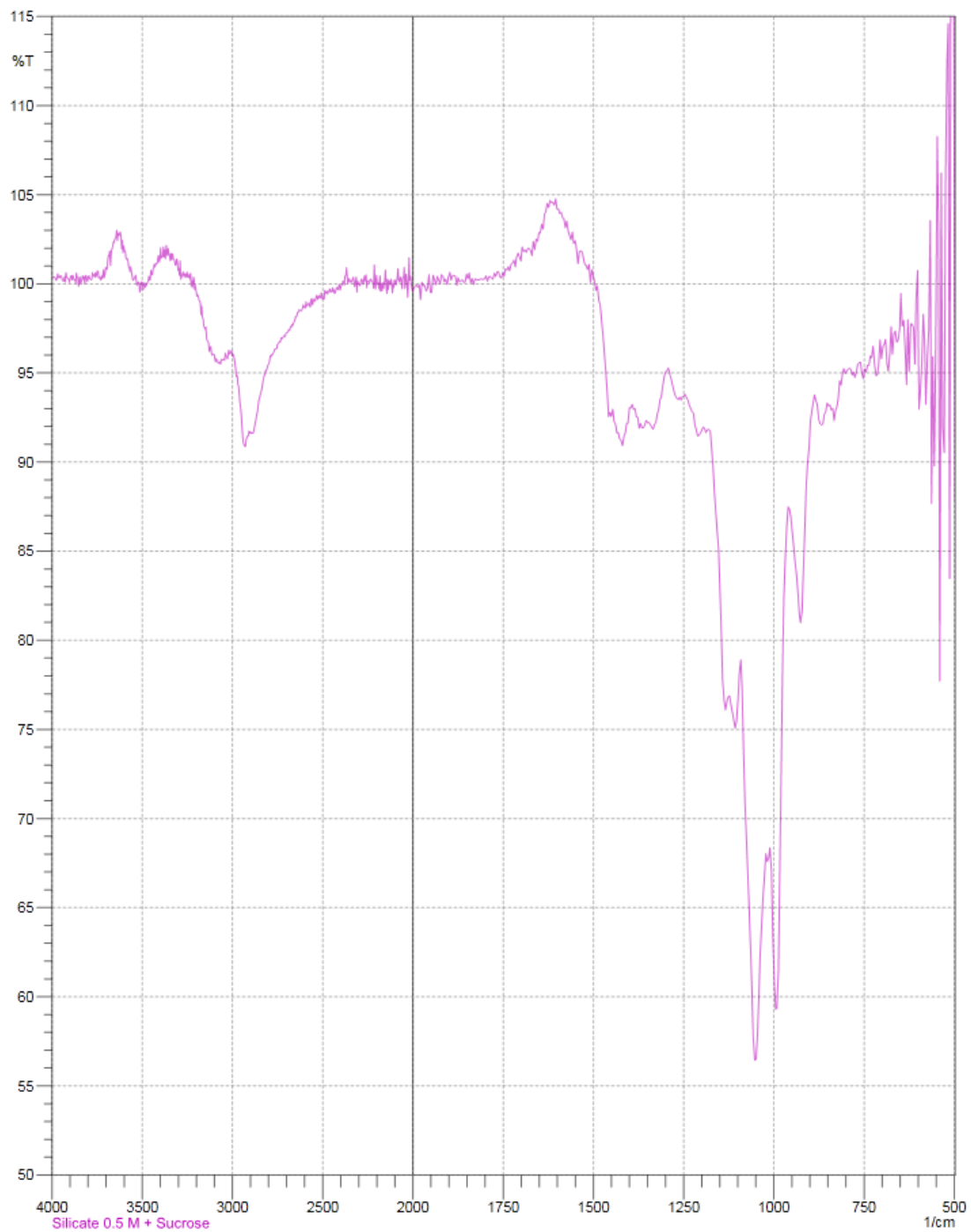


Figure B. 4 – ATR-FTIR spectra of the sucrose stabilised silicate suspension, at pH 3.5, using water as background.

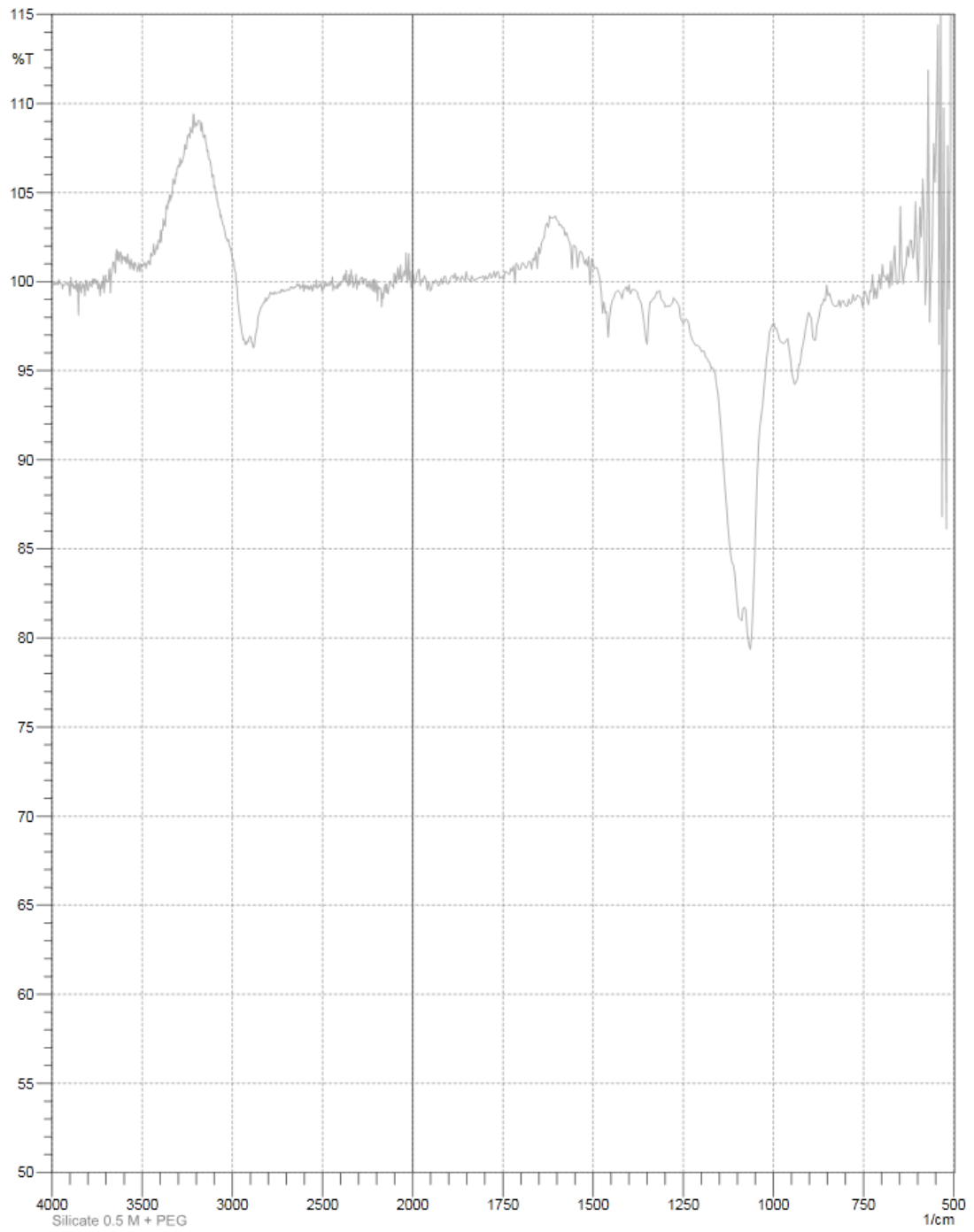


Figure B. 5 – ATR-FTIR spectra of the PEG stabilised silicate suspension, at pH 3.5, using water as background.

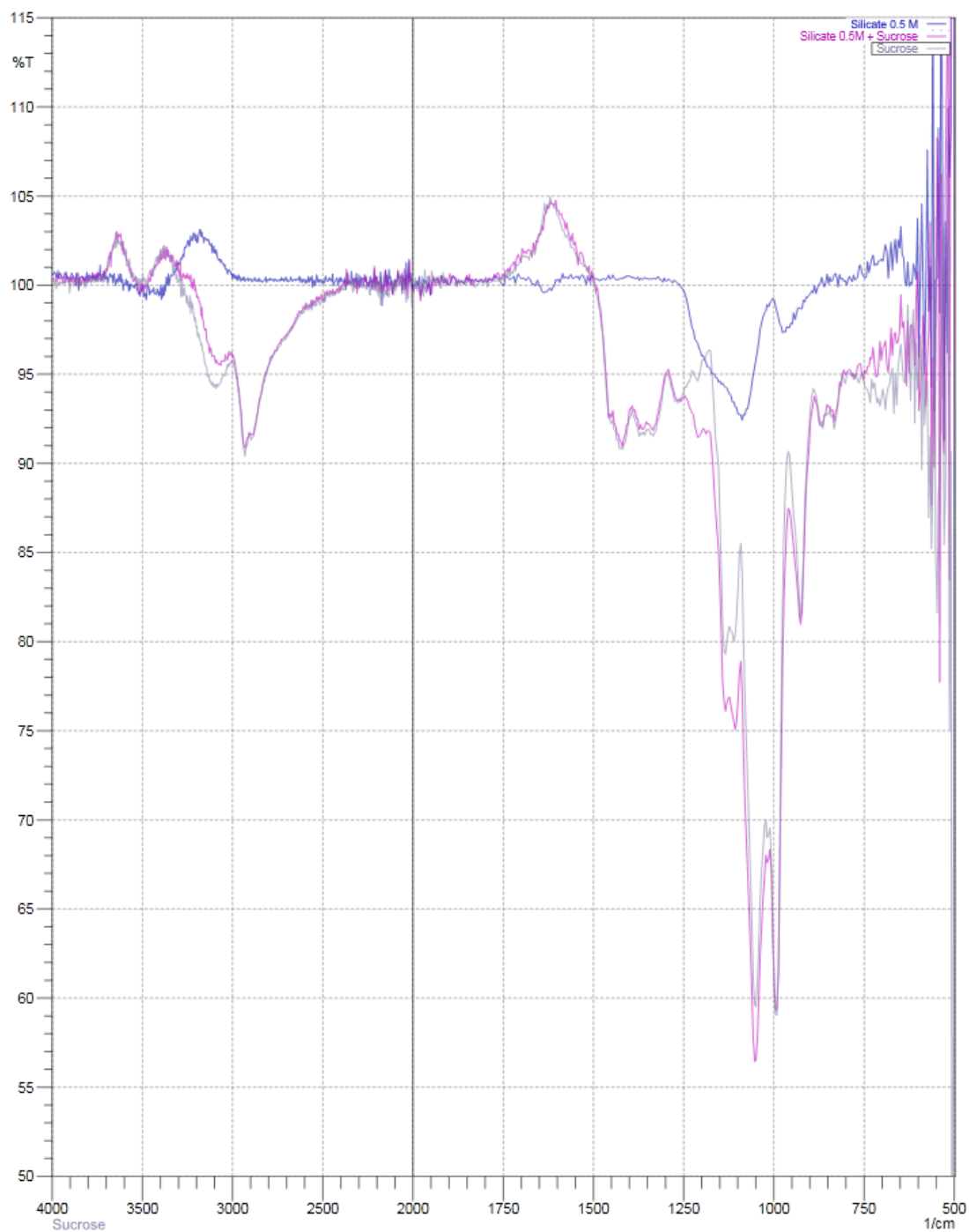


Figure B. 6 – Overlay of the ATR-FTIR spectrums of the non-stabilised silicate suspensions, the sucrose solution and the sucrose stabilised silicate suspension, all at pH 3.5, using water as background.

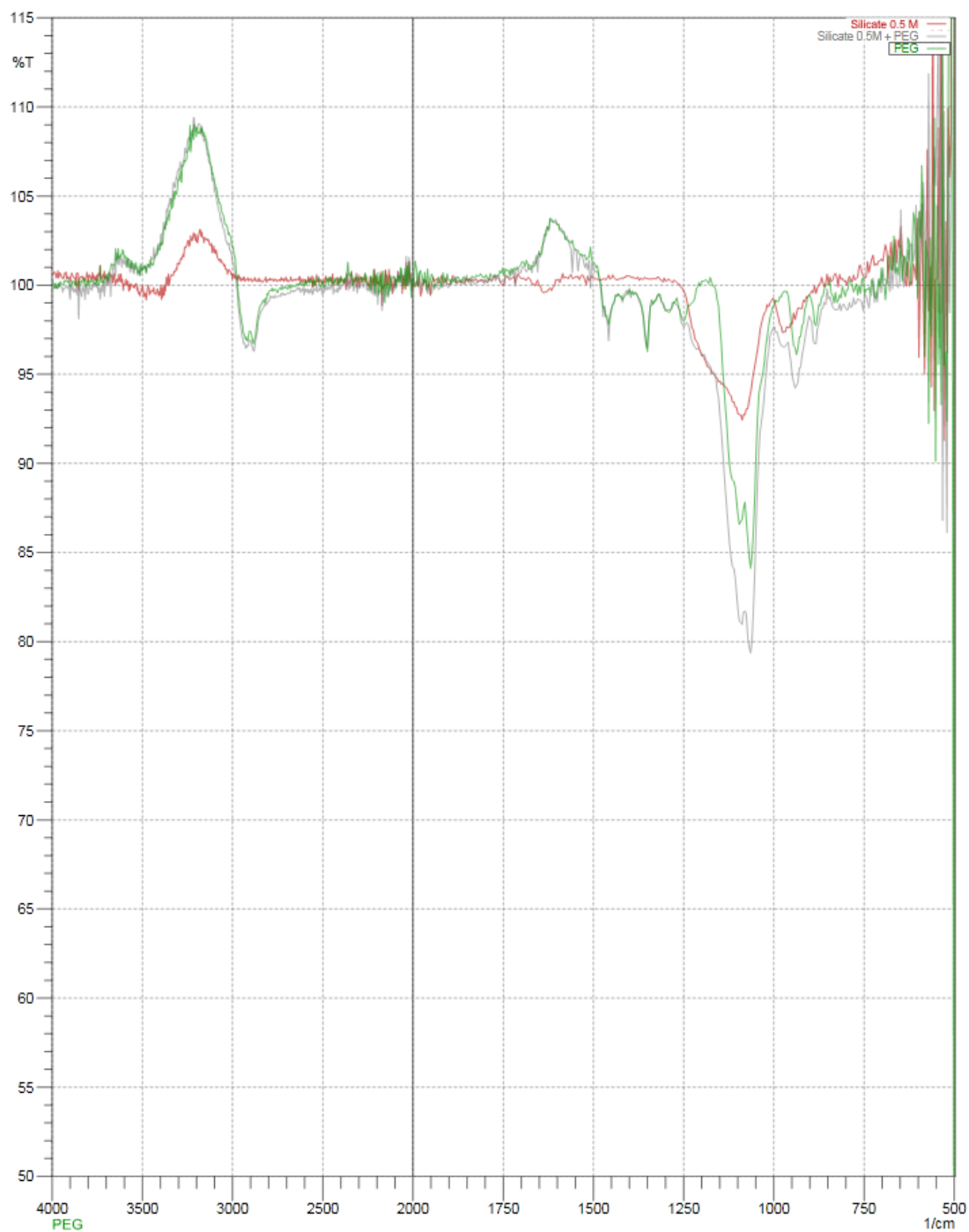


Figure B. 7 – Overlay of the ATR-FTIR spectrums of the non-stabilised silicate suspensions, the PEG solution and the PEG stabilised silicate suspension, all at pH 3.5, using water as background.

Background – Air

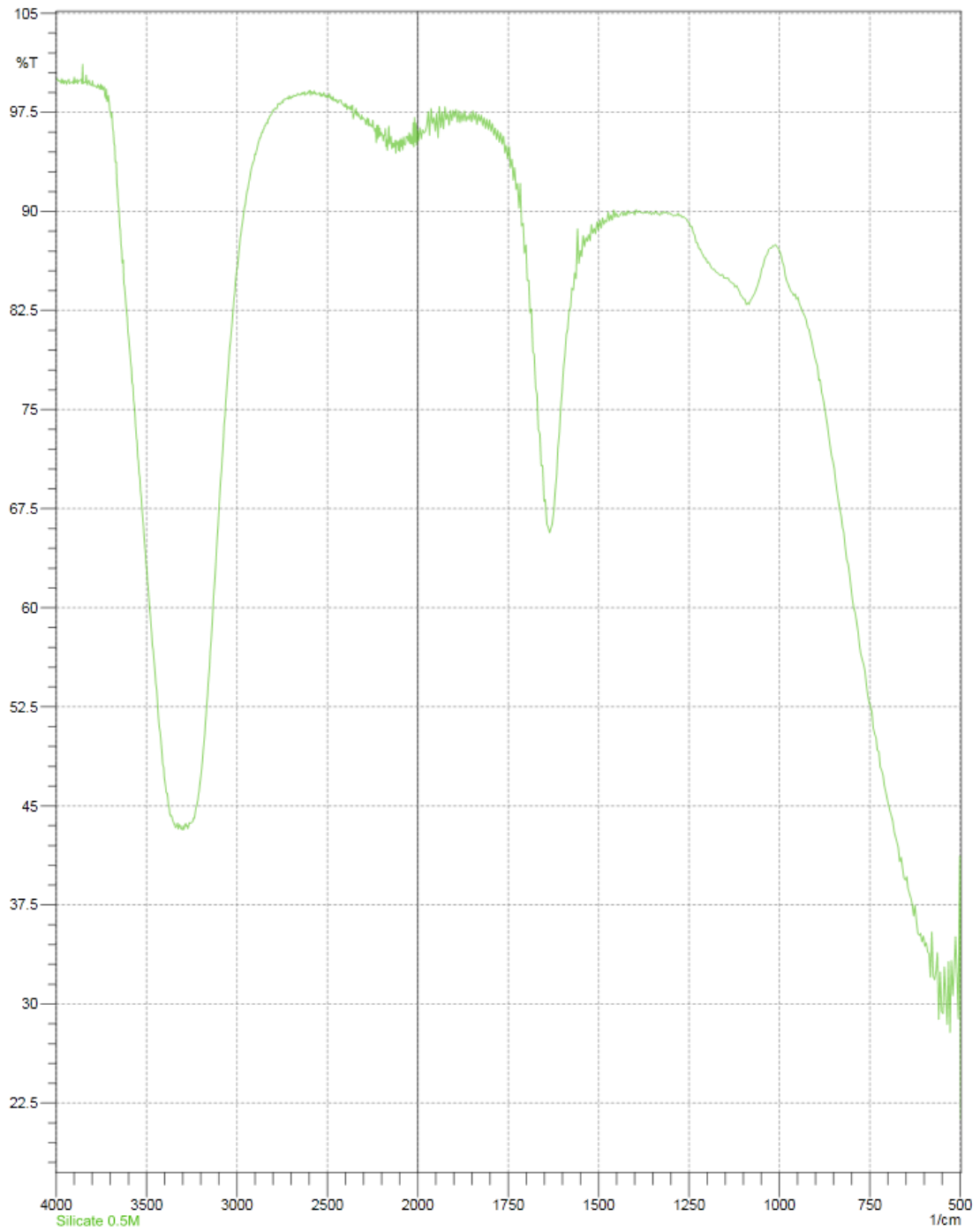


Figure B. 8 – ATR-FTIR spectra of the non-stabilised silicate suspension, at pH 3.5, using water as background.

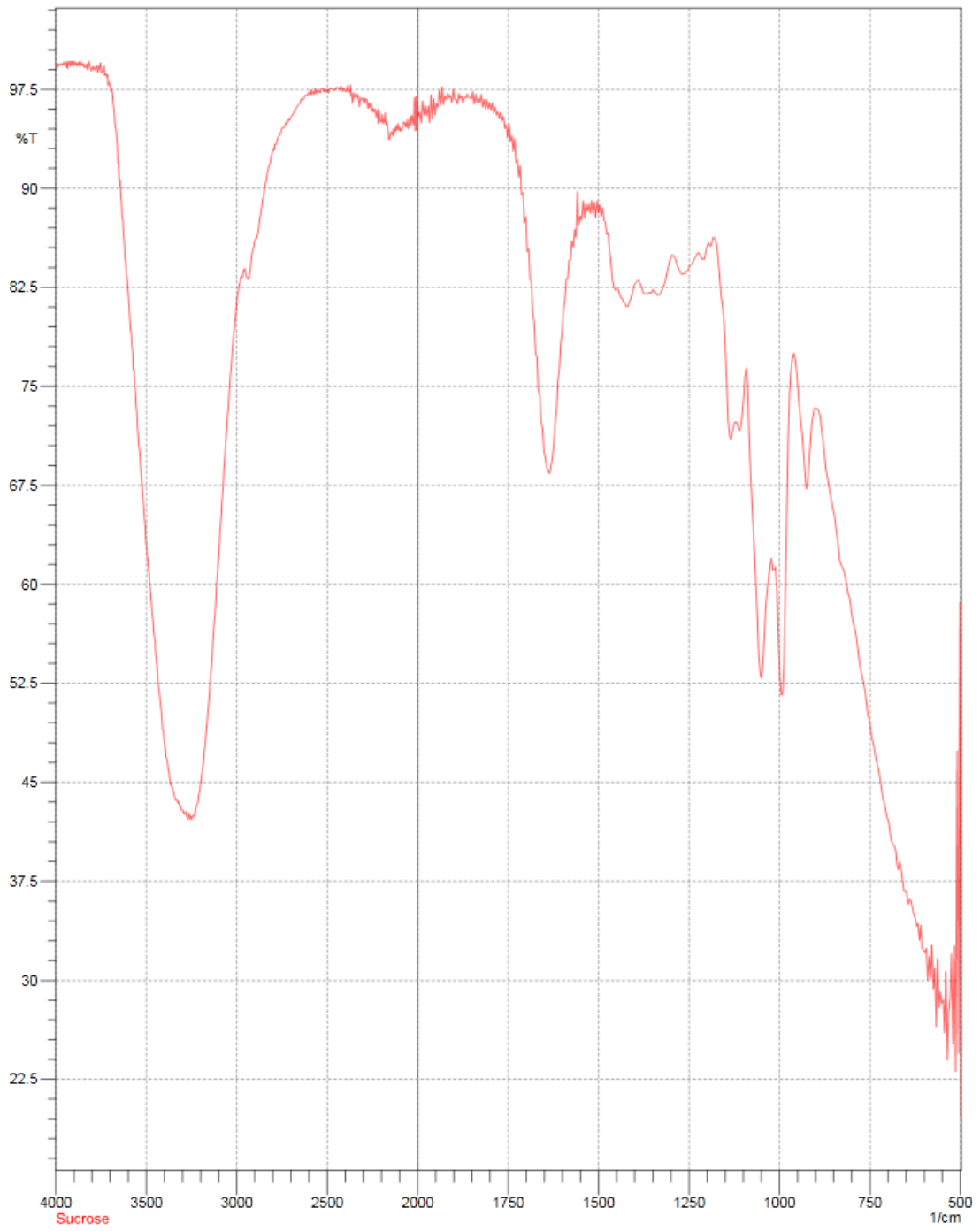


Figure B. 9 – ATR-FTIR spectra of a sucrose solution, at pH 3.5, using air as background.

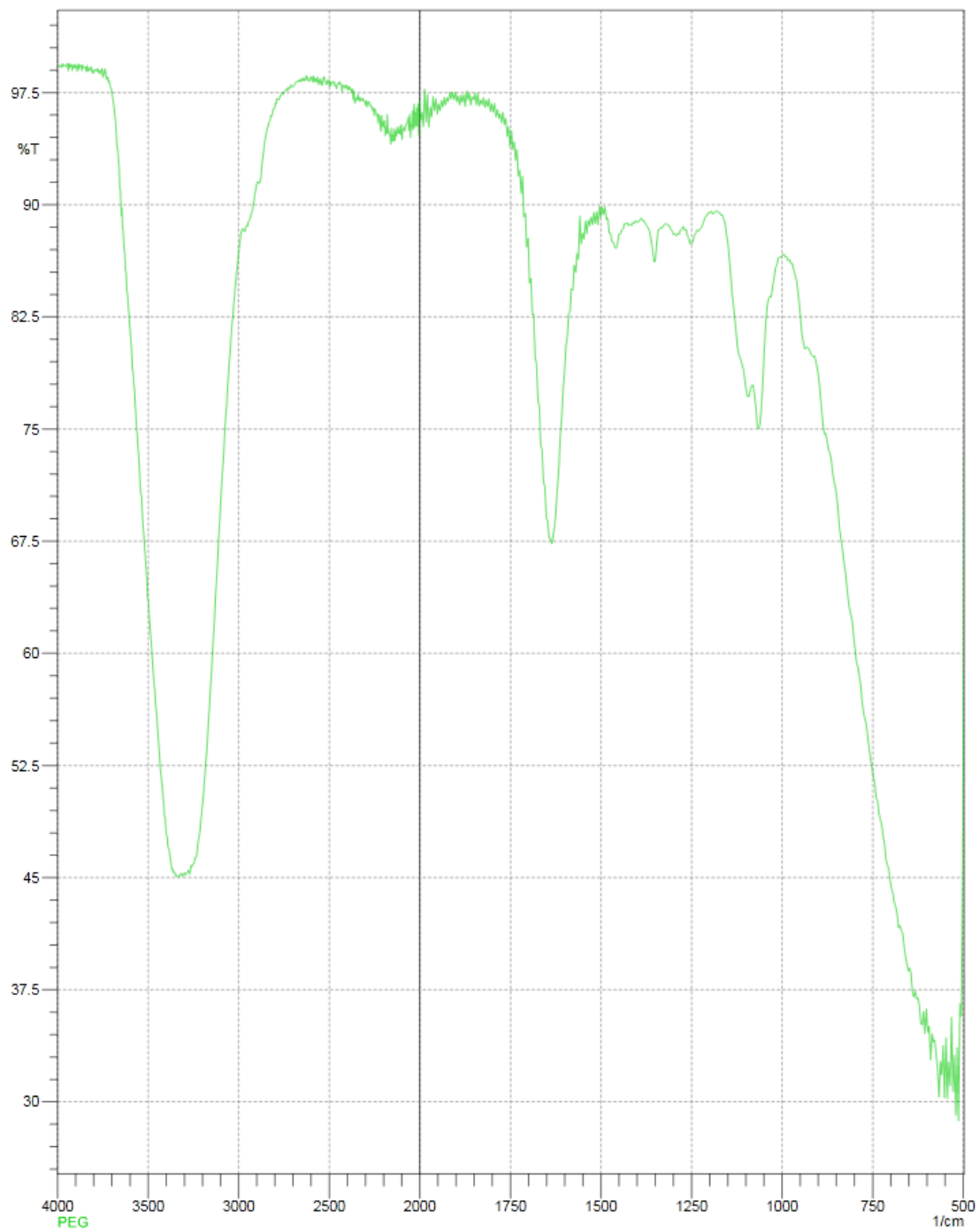


Figure B. 10 - ATR-FTIR spectra of a PEG solution, at pH 3.5, using air as background.

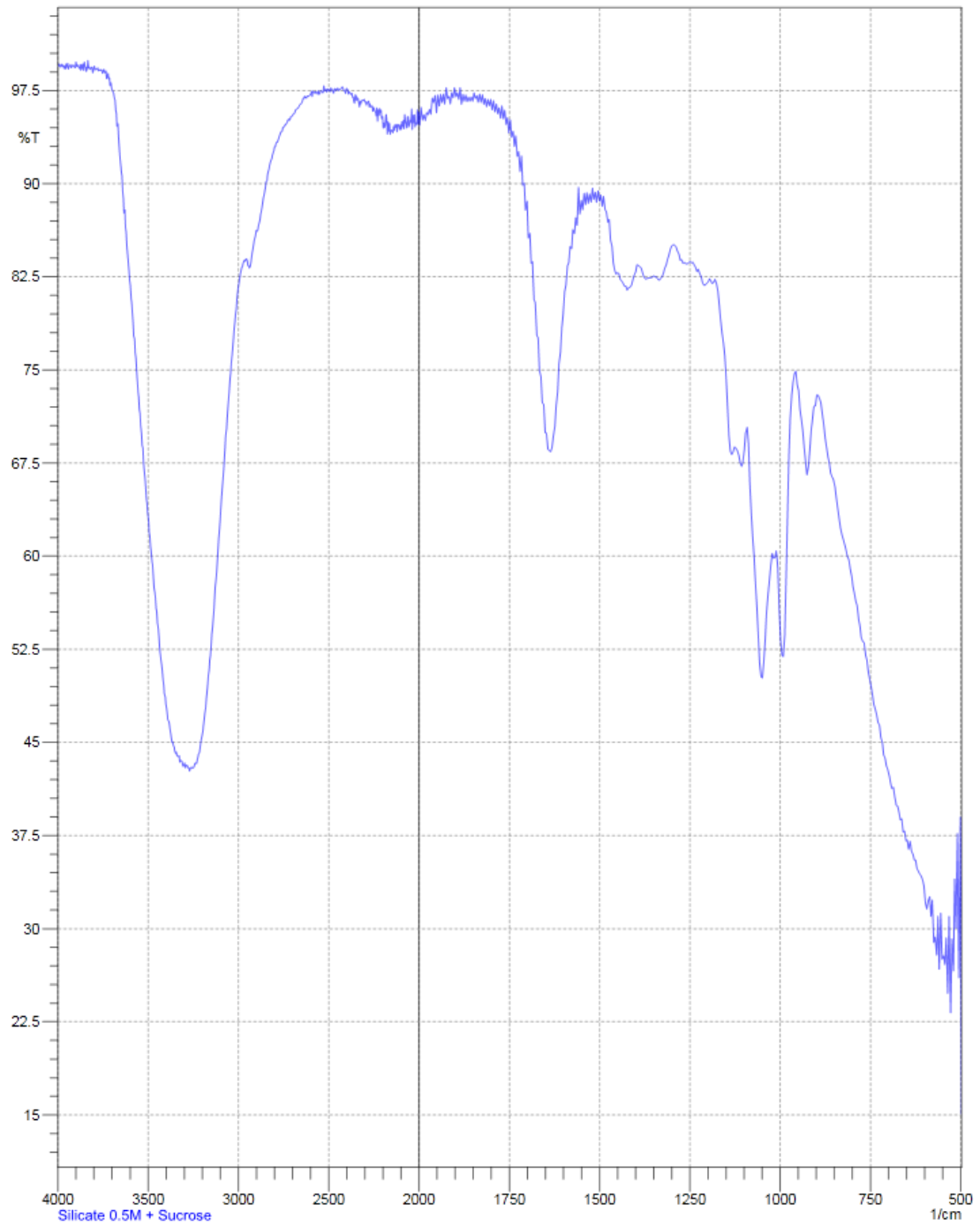


Figure B. 11 – ATR-FTIR spectra of the sucrose stabilised silicate suspension, at pH 3.5, using air as background.

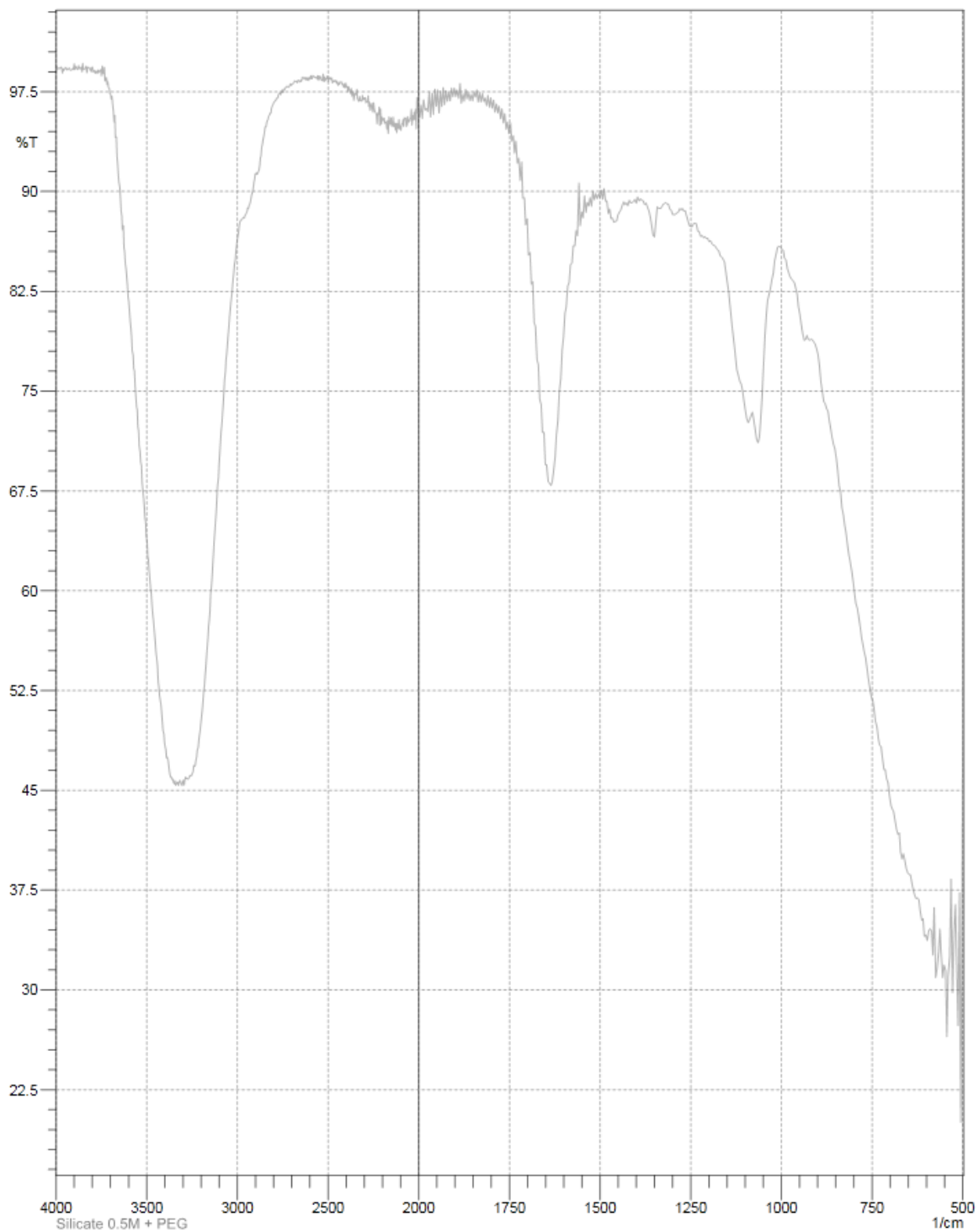


Figure B. 12 – ATR-FTIR spectra of the PEG stabilised silicate suspension, at pH 3.5, using air as background.

Background – Medium

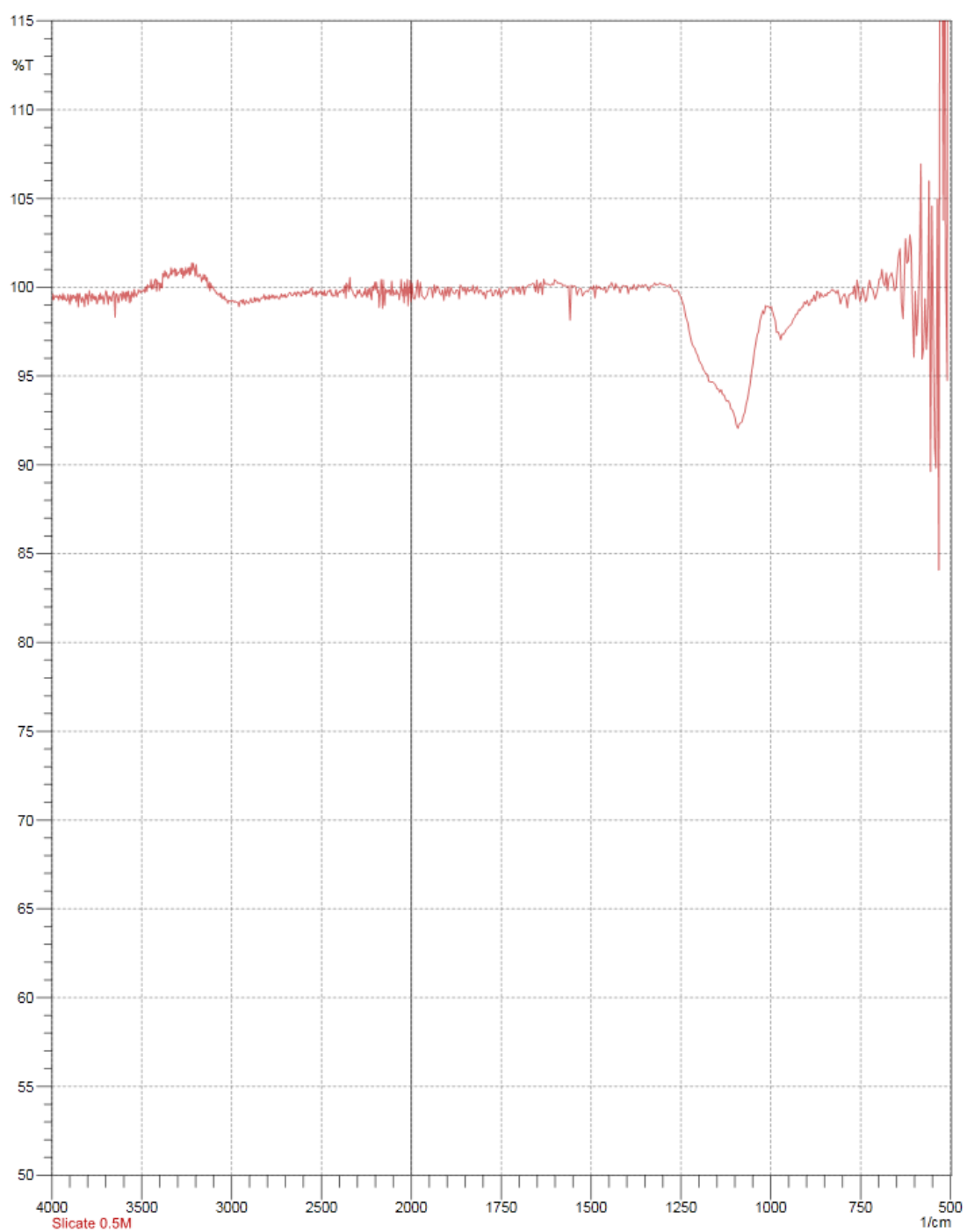


Figure B. 13 – ATR-FTIR spectra of the non-stabilised silicate suspension, at pH 3.5, using, as background, the same medium as the silicate suspensions, minus the silicate and stabilizer.

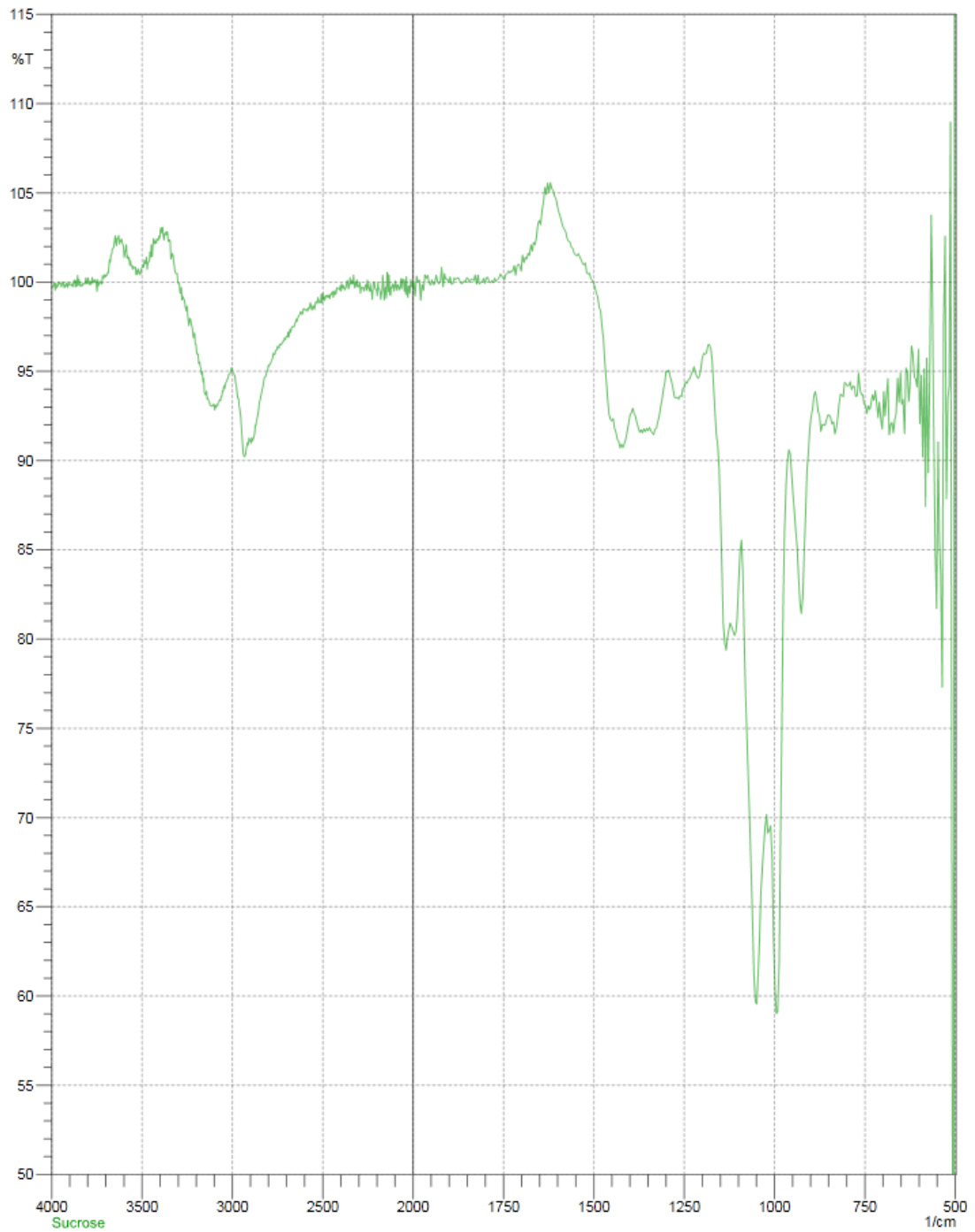


Figure B. 14 – ATR-FTIR spectra of a sucrose solution, at pH 3.5, using, as background, the same medium as the silicate suspensions, minus the silicate and stabilizer.

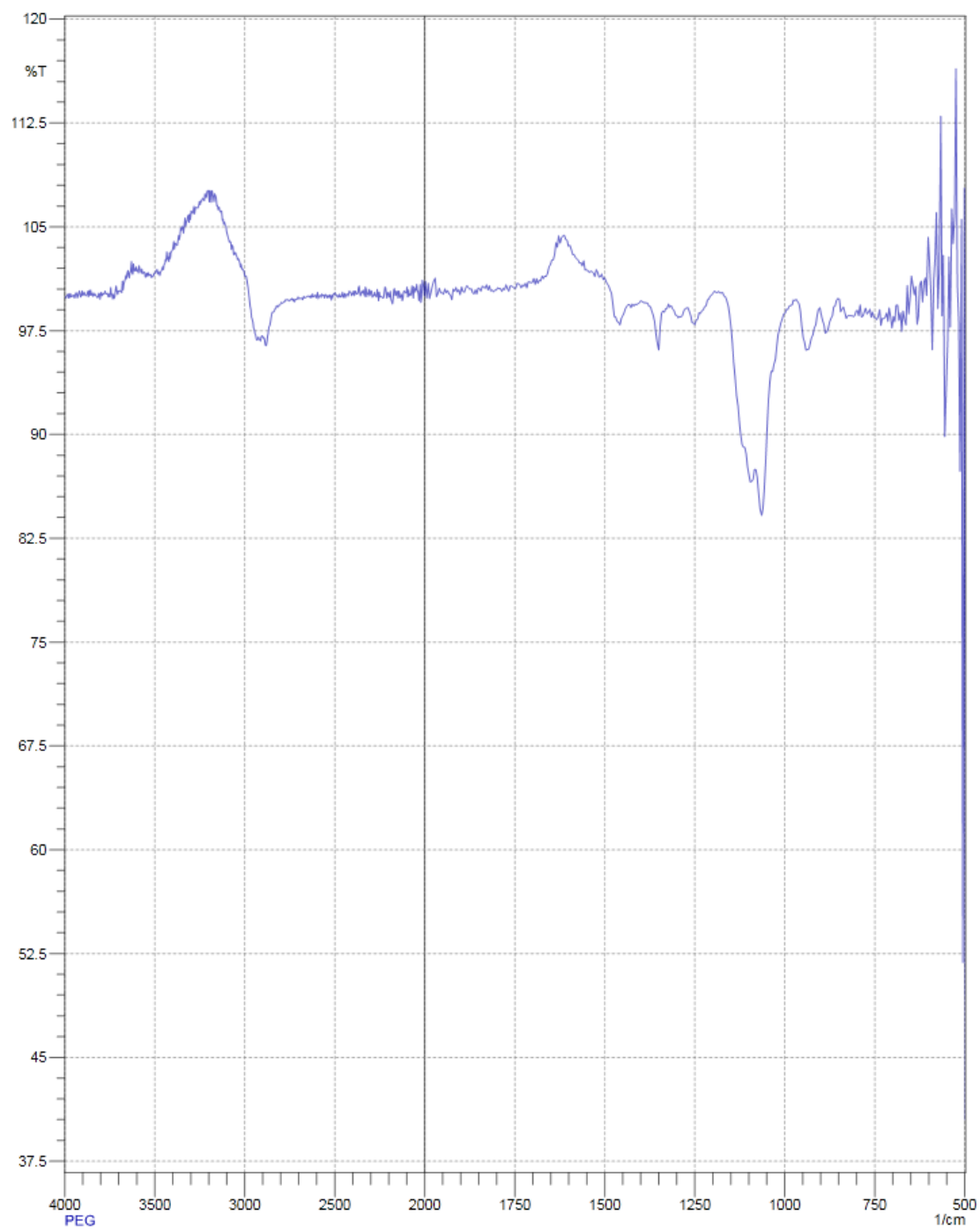


Figure B. 15 – ATR-FTIR spectra of a PEG solution, at pH 3.5, using, as background, the same medium as the silicate suspensions, minus the silicate and stabilizer.

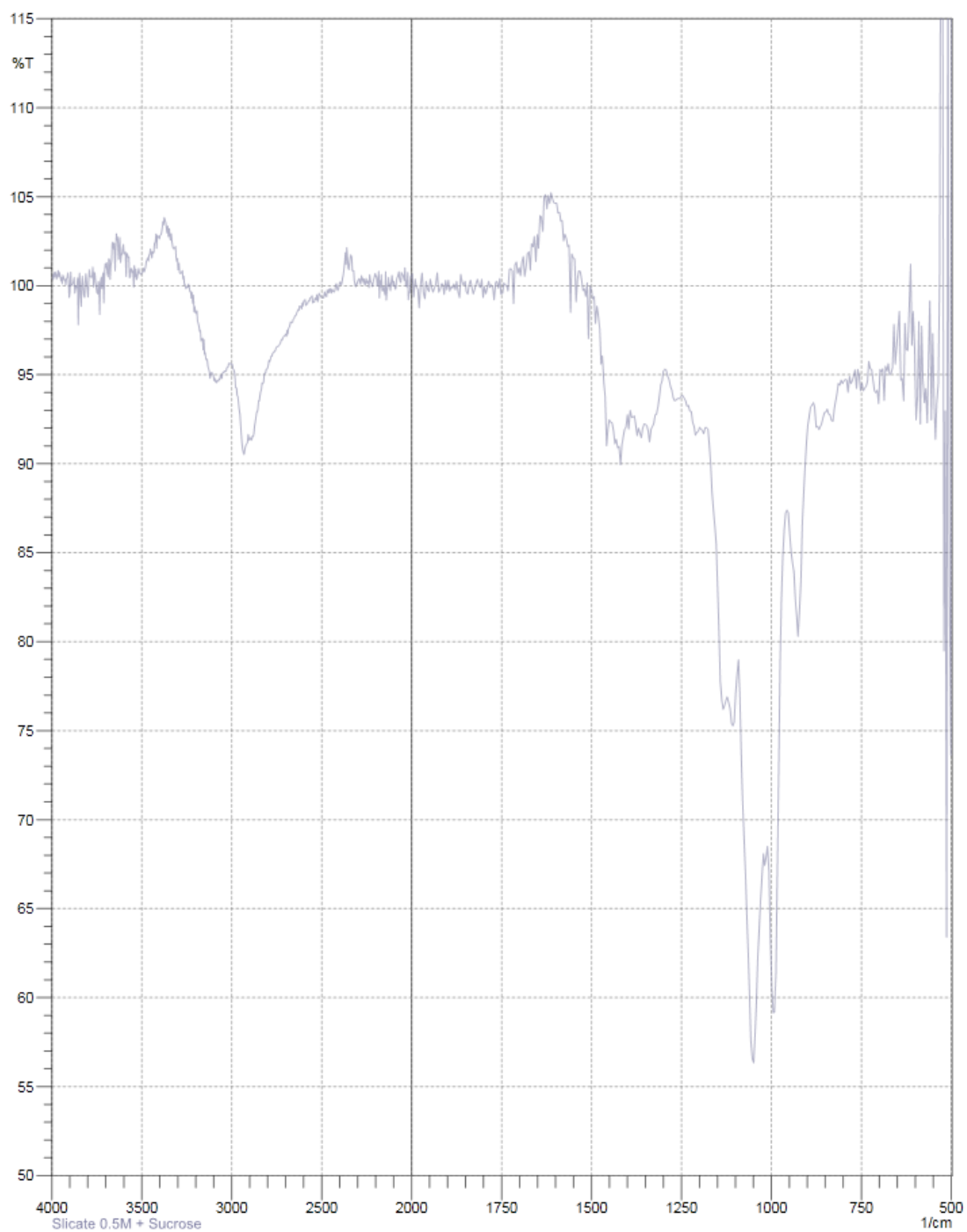


Figure B. 16 – ATR-FTIR spectra of the sucrose stabilised silicate suspension, at pH 3.5, using, as background, the same medium as the silicate suspensions, minus the silicate and stabilizer.

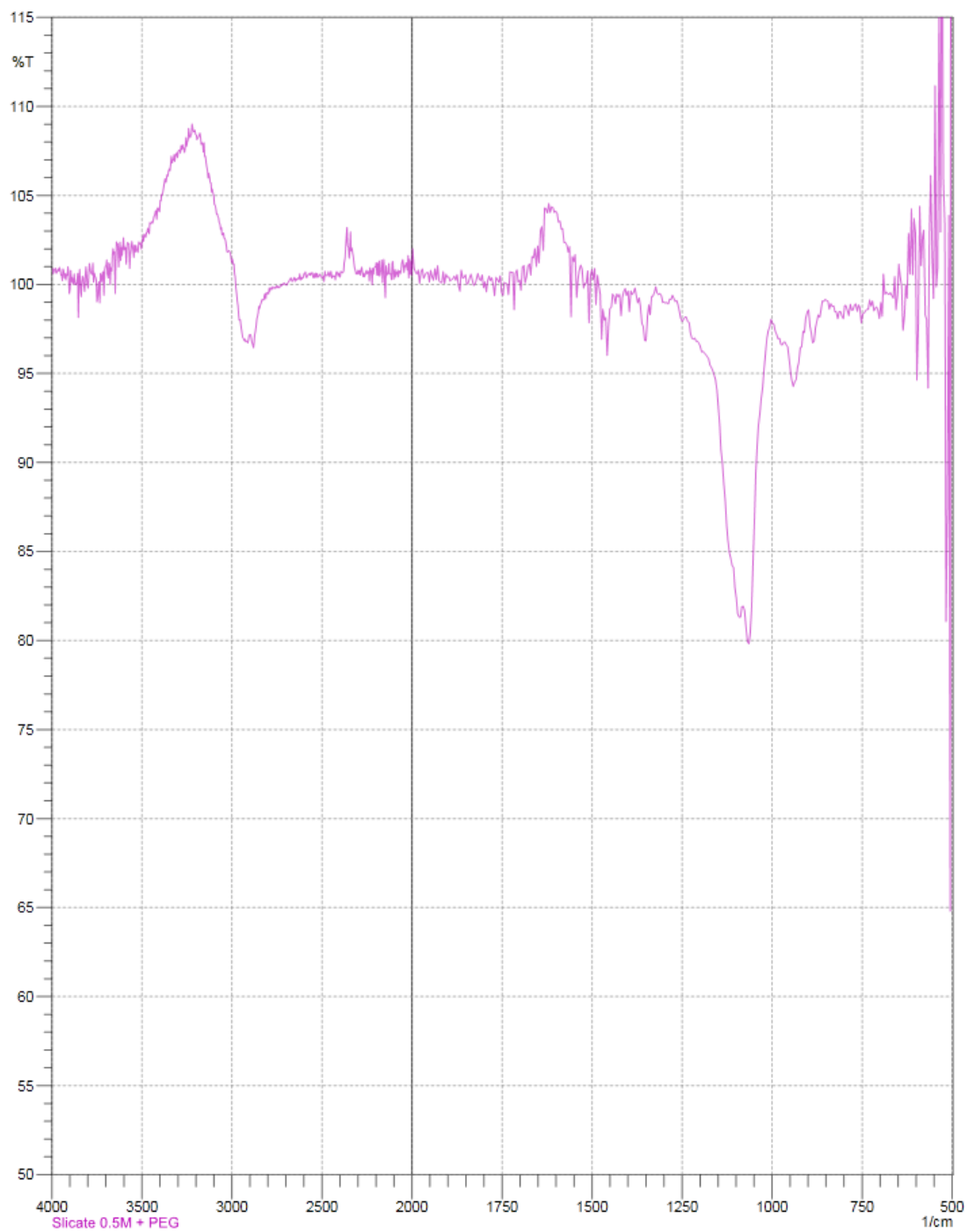


Figure B. 17 – ATR-FTIR spectra of the PEG stabilised silicate suspension, at pH 3.5, using, as background, the same medium as the silicate suspensions, minus the silicate and stabilizer.

This page intentionally left blank.

Appendix C – Fraction Analysis of Silicate Suspensions (EtOH 40% v/v)

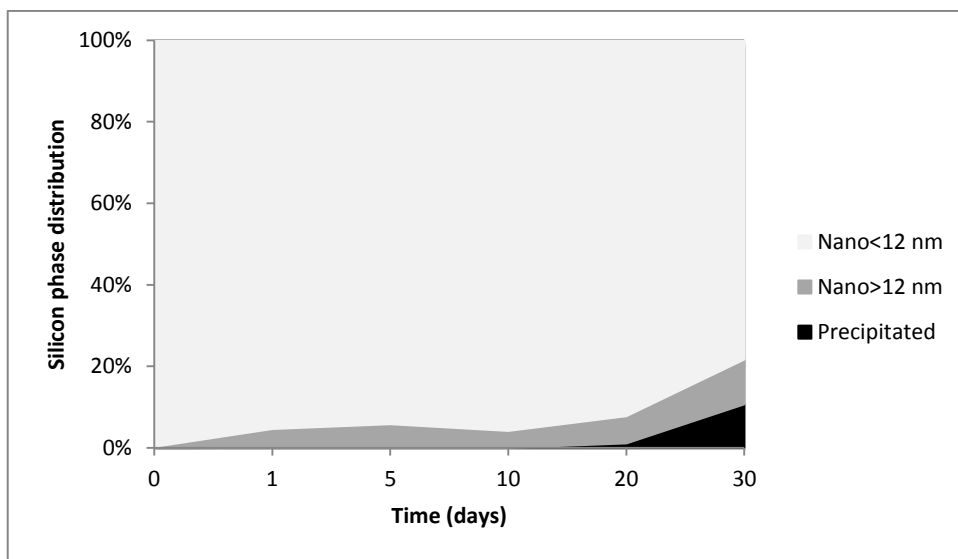


Figure C. 1 – Silicon phase distribution overtime of the sucrose stabilised silicate suspensions (14% EtOH v/v), at pH 2.5.

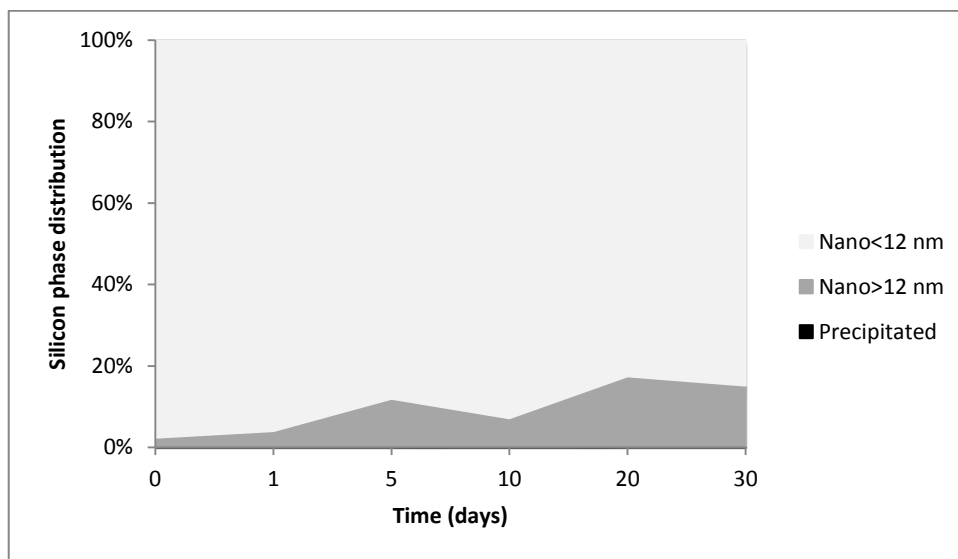


Figure C. 2 – Silicon phase distribution overtime of the sucrose stabilised silicate suspensions (14% EtOH v/v), at pH 3.5.

This page intentionally left blank.

Appendix D – Dissolution Assay Results for Biosil

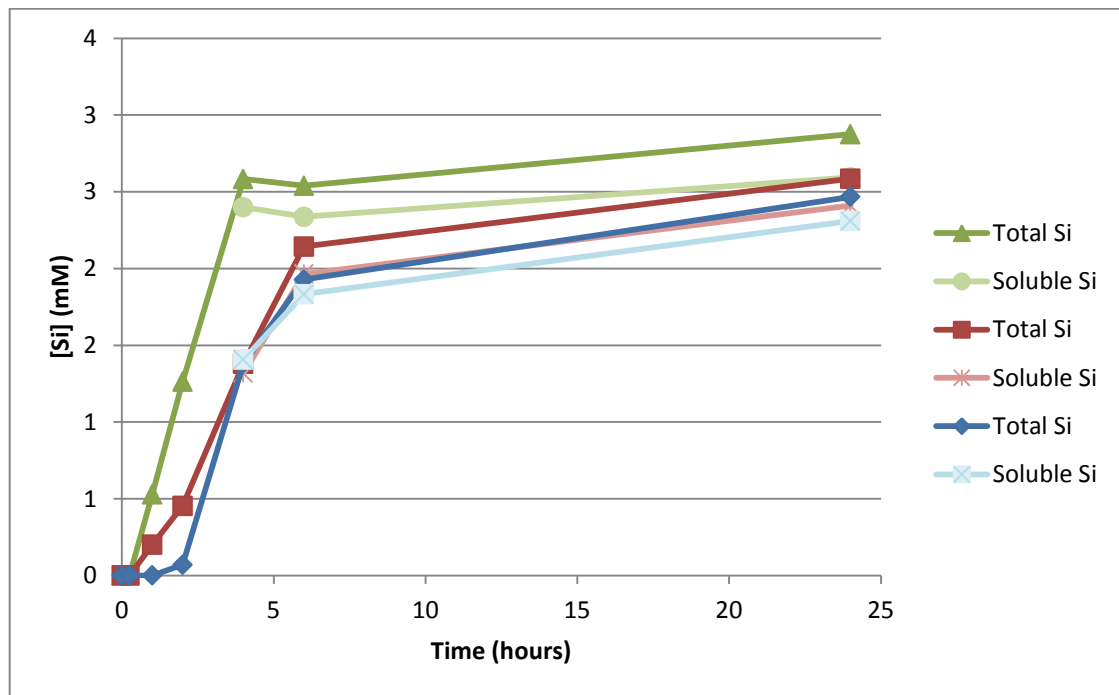


Figure D. 1 – Total and soluble silicon fractions for different concentrations of Biosil tested, with the dissolution assay, those being, 70 mM (green), 35 mM (red) and 17.5 mM (blue).

This page intentionally left blank.

Appendix E – Overlay of the ICP and Molybdate Dissolution Assay Results

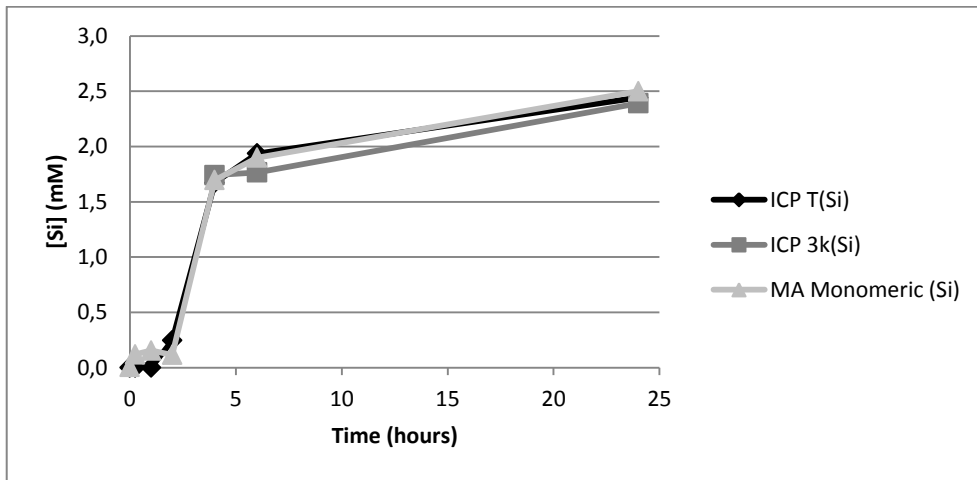


Figure E. 1 – Overlay of the results acquired in the dissolution assay, for Biosil, with ICP and the molybdate assay.

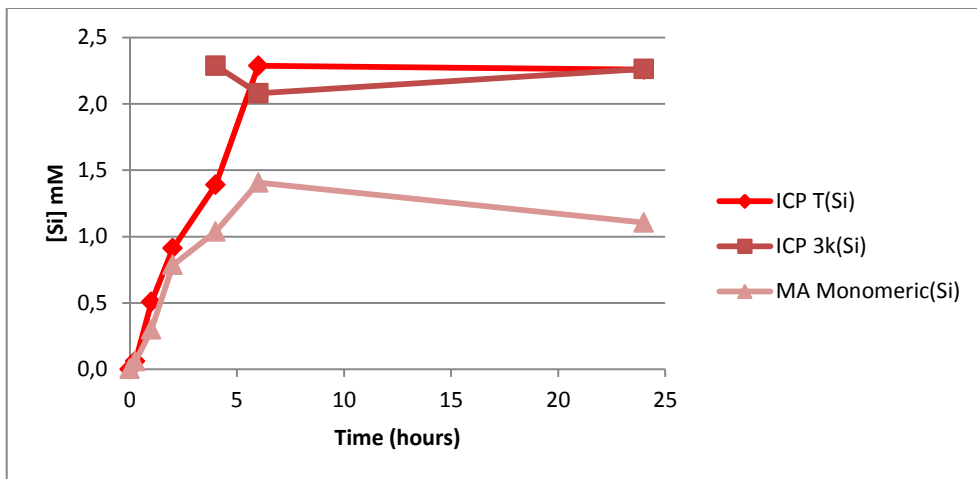


Figure E. 2 – Overlay of the results acquired in the dissolution assay, for the non-stabilised silicate suspensions, at pH 2.5, with ICP and the molybdate assay.

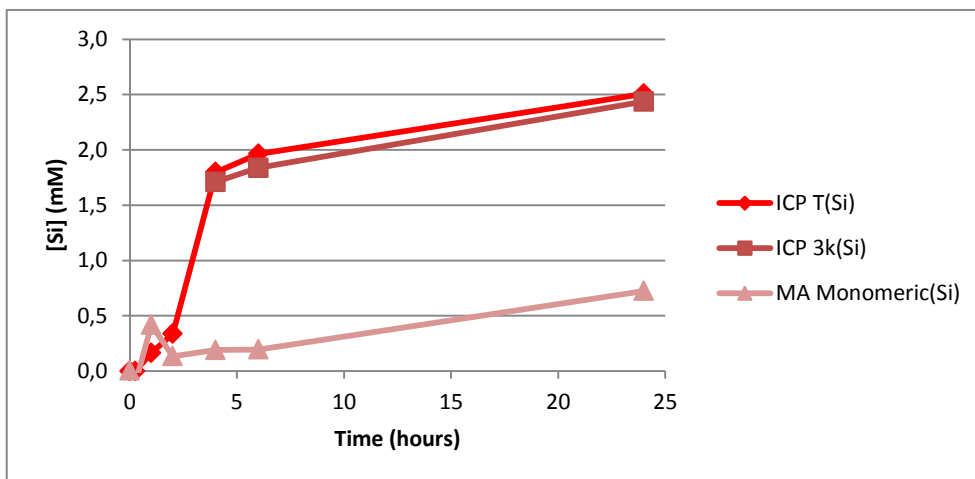


Figure E. 3 – Overlay of the results acquired in the dissolution assay, for the non-stabilised silicate suspensions, at pH 3.5, with ICP and the molybdate assay.

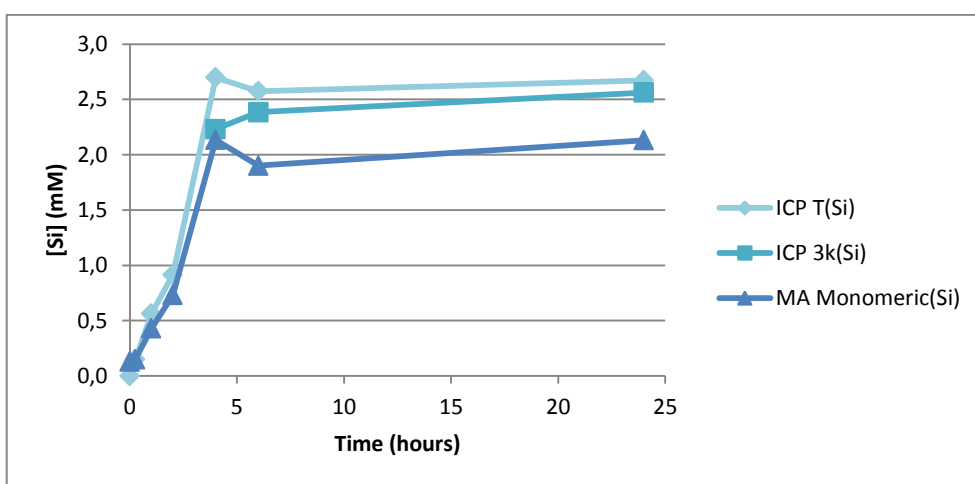


Figure E. 4 – Overlay of the results acquired in the dissolution assay, for the sucrose stabilised silicate suspensions, at pH 2.5, with ICP and the molybdate assay.

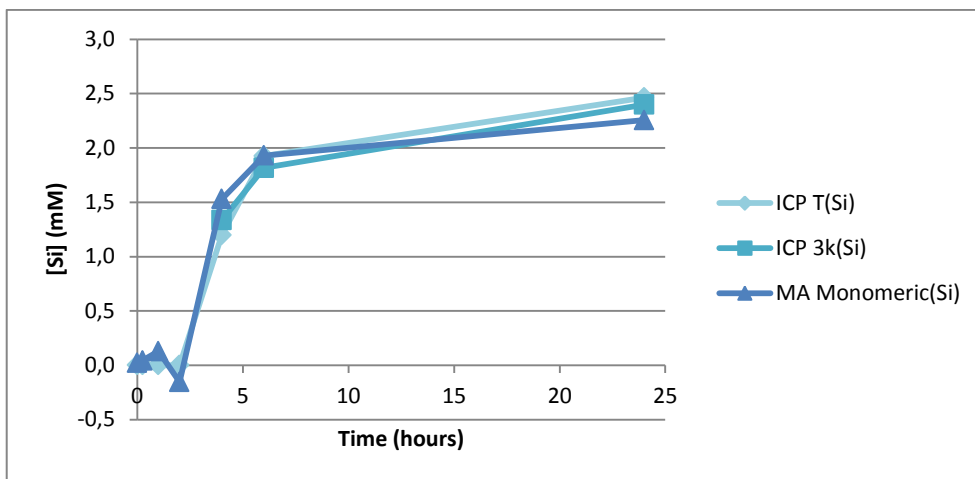


Figure E. 5 – Overlay of the results acquired in the dissolution assay, for the sucrose stabilised silicate suspensions, at pH 3.5, with ICP and the molybdate assay.

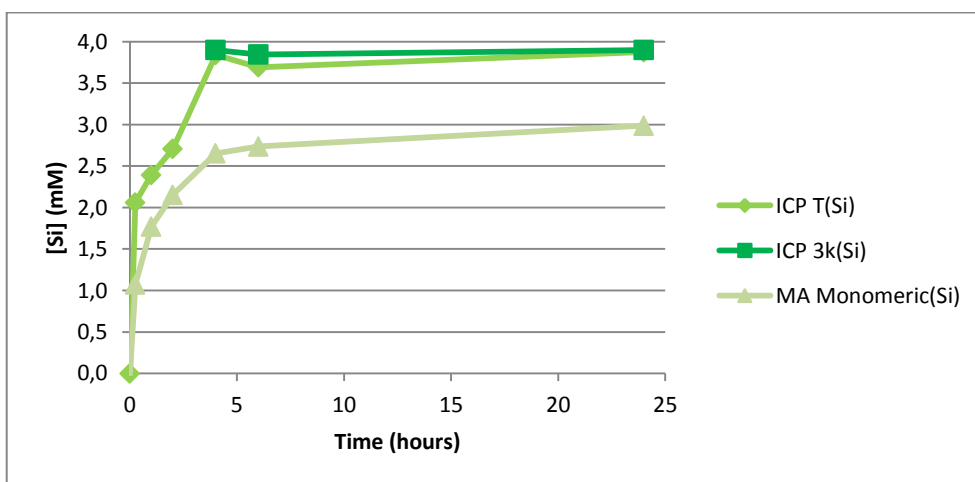


Figure E. 6 – Overlay of the results acquired in the dissolution assay, for the PEG stabilised silicate suspensions, at pH 2.5, with ICP and the molybdate assay.

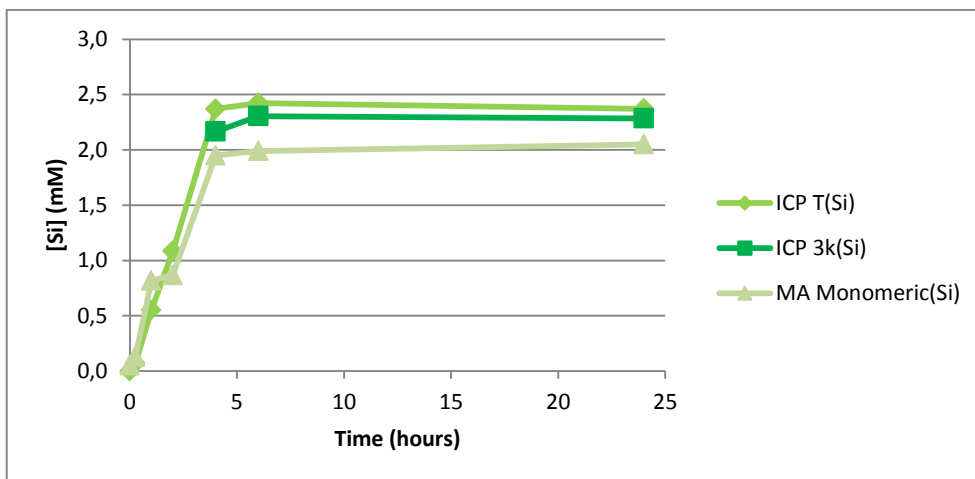


Figure E. 7 – Overlay of the results acquired in the dissolution assay, for the PEG stabilised silicate suspensions, at pH 3.5, with ICP and the molybdate assay.

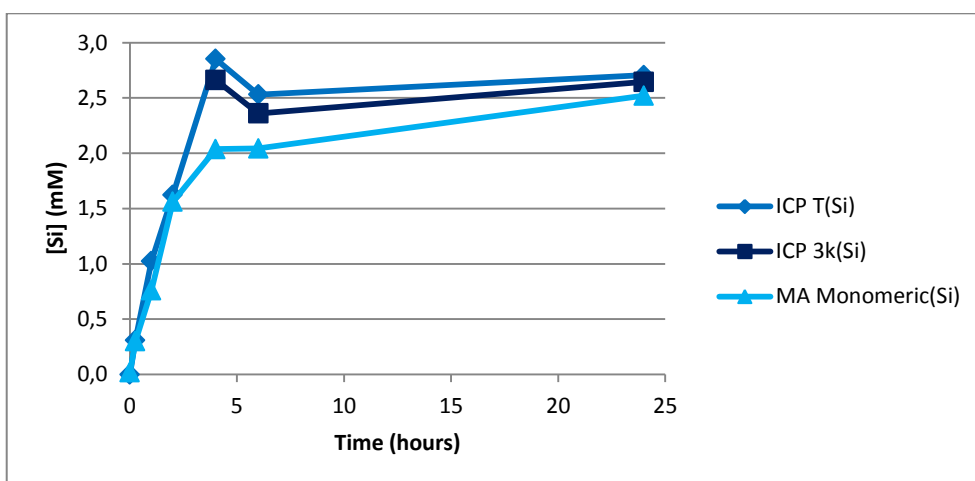


Figure E. 8 – Overlay of the results acquired in the dissolution assay, for the sucrose stabilised silicate suspensions, with 14% EtOH (v/v), at pH 2.5, with ICP and the molybdate assay.

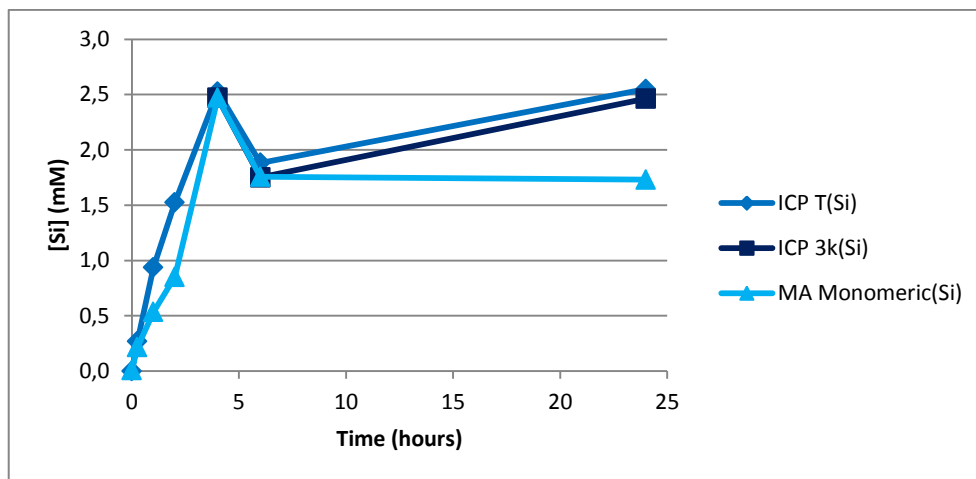


Figure E. 9 – Overlay of the results acquired in the dissolution assay, for the sucrose stabilised silicate suspensions, with 14% EtOH (v/v), at pH 3.5, with ICP and the molybdate assay.